Thesis for doctoral degree (PhD)

2014

Development of the oocyst wall in *Eimeria maxima* and biochemical analysis of gametocyte wall forming bodies

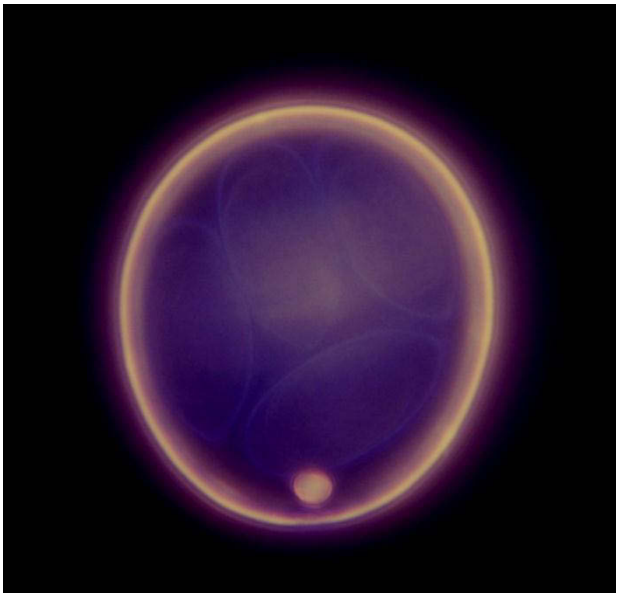

Sonja Frölich

ithreeinstitute
infection · immunity · innovation

UNIVERSITY OF TECHNOLOGY SYDNEY

To my family

CERTIFICATE OF ORIGINAL AUTHORSHIP

I certify that the work in this thesis has not previously been submitted for a degree nor has it been submitted as part of requirements for a degree except as fully acknowledged within the text.

I also certify that the thesis has been written by me. Any help that I have received in my research work and the preparation of the thesis itself has been acknowledged. In addition, I certify that all information sources and literature used are indicated in the thesis.

Signature of Student:

Date:

Acknowledgements

It would not be possible to write this thesis without the support from my family, guidance of my supervisor and help from my friends.

Above all, I would like to thank my family for their personal support and great patience at all times. My parents, sister and partner have given me their unequivocal support throughout, as always, for which mere expression of thanks likewise does not suffice.

This thesis would have not been possible without the guidance, caring and patience of my principal supervisor and friend, Professor Michael Wallach, not to mention his patient correcting of my writing and financially supporting my research. The good advice, support and friendship of my secondary supervisors, Dr. Lisa Sedger and Associate Professor Stella Valenzuela, had been invaluable on both academic and a personal level, for which I am extremely grateful.

I am most grateful to Dr. Michael Johnson, who was always willing to help with microscopy and give his best suggestions. I would like to thank Jacqueline Farhat and Annisha Shahparee for all their help. It would have been a lonely lab without them. Many thanks to Associate Professor Jan Slapeta at (USYD), Miss Joyce To (UTS), Dr. Matthew Padula (UTS), Dr. Valerie Wasinger (UNSW) and Dr. Richard Whurer (UWS) for helping me with tissue sections, microscopy and proteomics. My research would have not been possible without them.

I would like to thank Professor Rolf Entzeroth and Professor Tomley for hosting me while visiting their laboratories in Dresden and London and for giving me opportunities to work with their groups. I also thank them for their encouragement, insightful comments, and hard questions.

Amongst my fellow postgraduate students in the Science Faculty, the effort made by Erin Gloag, Heba Al Khamici, Raquel Alvarado, Charmain Castel, Michael Strauss, Maria Lund, Jane Mun Ng, Alex Gale, Rita Rappa, Ben Raymond and Joel Barrat in promoting a stimulating and welcoming social environment will stand as an example to

those that succeed them. I would also like to thank my friends at Stanford Medical School in America and Technische Universiat in Dresden for their support and encouragement throughout.

I am also grateful to the team at the Ernst Animal Facility at UTS, Fiona Read and Lalit Overlunde, for their help with raising and taking care of our chickens.

Last, but by no means least, I would like to acknowledge the financial support of the Australian Government and the Science Faculty at UTS, particularly in the award of a Postgraduate Research Stipend (APA) and numerous travel grants that provided necessary financial support for this project.

For any errors or inadequacies that may remain in this work, the responsibility is entirely my own.

Table of Contents

List of Figures

List of Tables

Abstract

Eimeria is a cyst-forming intracellular parasite that causes the economically important disease, coccidiosis, in intensely reared broiler chickens worldwide. The ability of the Eimeria parasite to replicate very rapidly and to synthesize an impenetrable, highly resistant oocyst wall, allows it to build up to very large numbers in the litter of broiler flocks. The molecular machinery involved in the assembly of the oocyst wall is housed in the two types of wall forming bodies (WFB1 and WFB2) of the sexual stage parasites (macrogametocytes).

The current project aimed to expand our understanding of the fundamental mechanisms involved in oocyst wall formation by: (1) characterising the morphological changes involved in oocyst wall assembly during parasite development; (2) developing a method to isolate gametocyte WFBs in order to characterise their molecular composition; and (3) studying the nature and characterizing the mechanisms of nutrient acquisition in developing *E. maxima* gametocytes *in vitro.*

Extracted macrogametocytes were stained using cytochemical and immune-labelling methods, and morphological changes of the developing zygote characterised by bright-field, scanning electron and 3D confocal microscopy. Additionally, the WFBs of macrogametocytes were enriched by subcellular fractionation and fractions containing these organelles were analysed by microscopy, western blot and label-free quantitative shotgun proteomics. Data from these studies has shown that gametocytes and early stage oocysts contain surface pores and are capable of actively taking up and internalizing nano beads via endocytosis. In addition, microscopic analyses shows that *E. maxima* is selective in compartmentalizing neutral lipids to the type 1, and glycoproteins to the type 2 wall forming bodies during gametocytogenesis.

Furthermore, it became possible to visualise both neutral lipids and glycoproteins during outer and inner oocyst wall formation. Thus, a model of outer oocyst wall formation was proposed and suggests that neutral lipids found in the WFB1s are translocated to the parasite's surface where they deposit their cargo via exocytosis. The

released molecules fuse with the parasite's limiting membrane for incorporation into the neutral lipid rich outer oocyst wall.

Finally, biochemical and proteomic methods were employed to identify and analyse vesicular trafficking proteins and other putative regulators of endocytosis and transport. The results reported here reveal valuable insights into the mechanisms by which the parasite is able to acquire nutrients essential for development, transport organelles and at the same time synthesise the impervious oocyst wall.

List of papers

I. Frölich S., Entzeroth R., Wallach M., 2012, Comparison of protective immune responses to apicomplexan parasites. Journal of Parasitology Research 2012, 852591. doi:10.1155/2012/852591*

II. Frölich S., Johnson M., Robinson M., Entzeroth R., Wallach M., 2013, The spatial organization and extraction of the wall forming bodies of *Eimeria maxima*. Parasitology 140, 876 - 887. doi: 10.1017/S0031182012002247*

III. Frölich S., Wasinger V., Padula M., Wallach M., 2013, Endocytosis and intracellular trafficking in *Eimeria maxima* sexual stages. Plos ONE, manuscript number: PONE-D-13-49560.*

IV. Frölich S., Shahparee A., Wasinger V., Wallach M., 2013, In vivo localisation of antibodies raised against Eimeria maxima wall forming bodies. (accepted for publication in Parasitology, PAR-2014-0054.R2)

V. Frölich S., Farhat J., Wallach M., 2013, Designing strategies for the control of coccidiosis in chickens on poultry farms using modern diagnostic tools. Reports in Parasitology 2013, 2013:3, 1 – 10. doi: http:// dx.doi.org/10.2147/RIP.S32811

*Papers reprinted with permission from Publishers

List of conferences

I. Frölich S., Johnson M., Sharman P., Katrib M., Smith N. and Wallach M., 2010, Development of *Eimeria maxima* gametocytes and isolation of wall forming bodies. Oral presentation delivered at the 27th Annual Scientific Research Meeting, co-hosted by the University of Technology, Sydney, The University of Sydney, The Kolling Institute and the Royal North Shore Hospital, Sydney, NSW, November, 2010.

II. Frölich S., Robinson M., Johnson M., Sharman P., Katrib M., Smith N., Wallach M., 2011, Development of *Eimeria maxima* gametocytes and isolation of the wall forming bodies. Oral presentation delivered at the Australian Society of Parasitology Annual Conference, Pullman Reef Casino Hotel, Cairns, Queensland, July, 2011.

III. Frölich S., Johnson M., Wallach M., 2011, The role of neutral lipids in gametocytogenesis and oocyst wall formation of *Eimeria maxima.* Oral presentation delivered at the 28th Annual Scientific Research Meeting, co-hosted by the University of Technology, Sydney, The University of Sydney, The Kolling Institute and the Royal North Shore Hospital, Sydney, NSW, November, 2011.

IV. Frölich S., Robinson M., Johnson M., Entzeroth R., Wallach M., 2012, The spatial organisation and extraction of the wall forming bodies of *Eimeria maxima.* Poster presentation delivered at the Biology of Host-Parasite Interactions Conference, Salve Regina University Newport, RI, USA, June, 2012.

V. Frölich S., Robinson M., Johnson M., Entzeroth R., and Wallach M., 2012, The spatial organisation and extraction of the wall forming bodies of *Eimeria maxima.* Oral presentation delivered at the 2nd International Symposium On Protozoal Infections in Poultry, at the University of Veterinary Medicine Veterinärplatz 11210-Vienna, Austria, July, 2012.

VI. Shahparee A., Frölich S., Wallach M., 2012, *In vitro* localization of antibodies against *Eimeria maxima* Wall Forming Bodies. Poster presentation delivered at the 29th Annual Scientific Research Meeting, co-hosted by the University of Technology, Sydney, The University of Sydney, The Kolling Institute and the Royal North Shore Hospital, Sydney, NSW, November, 2012.

VII. Frölich S., Shahparee A., Wasinger V., Wallach M., 2013, Endocytosis and intracellular trafficking of wall forming bodies in Eimeria maxima gametocytes. Oral presentation delivered at the New Horizons Conference, the 30th Combined Health Science Conference, co-hosted by the University of Technology, Sydney, The University of Sydney, The Kolling Institute and the Royal North Shore Hospital, Sydney, NSW, November 2013.

VIII. Frölich S., Wasinger V., Padula M., Wallach M., 2014, Intracellular trafficking of wall forming bodies in Eimeria maxima gametocytes. Oral presentation delivered at the Biology of Host-Parasite Interactions Conference, Salve Regina University Newport, RI, USA, June, 2014.

IX. Frölich S., Wasinger V., Padula M., Wallach M., 2014, Intracellular trafficking of wall forming bodies in Eimeria maxima gametocytes. Oral presentation delivered at the Biology of Host-Parasite Interactions Conference, Salve Regina University Newport, RI, USA, June, 2014.

X. Frölich S., Wasinger V., Padula M., Wallach M., 2014, Effects of cytoskeletal inhibitors on the uptake of carboxylated polystyrene nanoparticles and the development of sexual stages of *Eimeria maxima.* Oral presentation delivered at the Australian Society of Parasitology Annual Conference, Australian National University, Canberra, ACT, July, 2014.

Awards and prizes

The Australian Postgraduate Award, 2011

Department of Industry, Innovation Science, Research and Tertiary Education

Australian Government

Postgraduate Research Student Conference Travel Award, 2010-2012

Faculty of Science, University of Technology, Sydney

1st place Young Investigator Travel Award, 2011

28th RNSH-UTS-USYD-KIMR Scientific Research Meeting

Dean's Award for Academic Excellence, 2011

Faculty of Science, University of Technology, Sydney

Vice Chancellor's Postgraduate Research Student Conference Travel Award, 2012

Faculty of Science, University of Technology, Sydney

Technion Society of Australia Travel Scholarship, 2013

Student entrepreneurship, Technion Israel Institute of Technology

BSA	Bovine Serum Albumin
bp	Base pair
Da	Dalton
DAPI	4', 6-diamidino-2-phenylindole
DNA	Deoxyribonucleic Acid
EtOH	Ethanol
FITC	Fluoresceine isothiocyanate
h	Hour
HN	Host nucleus
IFA	Immunofluorescent microscopy
IW	Inner oocyst wall
kDa	Kilodalton
L	Litre
L	Lipid body
M	Moles
Min	Minute
Mg	Milligram
ML	Millilitre
mM	millimoles per litre
N	Nucleus
Nu	Nucleolus
OW	Outer oocyst wall
p.i.	Post infection
PG	Polysaccharide granule
PBS	Phosphate buffered saline
s	Second
SDS	Sodium-dodecyl-sulphate
TBS	Tris buffered saline
V	Veil, the outermost layer of the oocyst wall
VFBs	Veil forming bodies
WFB1	Wall forming body Type 1

WFB2	Wall forming body Type 2
µg	Microgram
µl	Microlitre

Chapter One

Paper I: General background to apicomplexan parasites and host-parasite relationship

Declaration

I declare that the following publication included in this thesis in lieu of a chapter meets the following:

- More than 50% of the content in the following publication included in this chapter has been planned, executed and prepared for publication by me
- The work presented here has been peer-reviewed and accepted for publication
- I have obtained approval to include the publication in this thesis from the Publisher
- The initial draft of the work has been written by me and any subsequent changes in response to co-authors and editors reviews was performed by me
- The publication is not subject to any obligations or contractual agreements with a third party that would constrain its inclusion in the thesis.

Publication title: Comparison of Protective Immune Responses to Apicomplexan Parasites

Authors: Sonja Frölich, Rolf Entzeroth and Michael Wallach

Candidate's contribution (%): above 50 %

Journal name: Journal of Parasitology Research

Volume/ page numbers: Volume 2012 (2012), Article ID 852591, 11 pages

Status: Published 27 June 2011

I declare that the publication above meets the requirements to be included in the thesis.

Candidate's name: Candidate's signature: Date (dd/mm/yy):

Members of the phylum Apicomplexa, which includes the species Plasmodium, *Eimeria*, *Toxoplasma*, and Babesia amongst others, are the most successful intracellular pathogens known to humankind. The widespread acquisition of antimicrobial resistance to most drugs used to date has sparked a great deal of research and commercial interest in the development of vaccines as alternative control strategies. A few antigens from the asexual and sexual stages of apicomplexan development have been identified and their genes characterised; however, the fine cellular and molecular details of the effector mechanisms crucial for parasite inhibition and stimulation of protective immunity are still not entirely understood. This paper provides an overview of what is currently known about the protective immune response against the various types of apicomplexan parasites and focuses mainly on the similarities of these pathogens and their host interaction. Finally, the evolutionary relationships of these parasites and their hosts, as well as the modulation of immune functions that are critical in determining the outcome of the infection by these pathogenic organisms, are discussed.

1.1 General introduction to apicomplexan parasites

Parasitic protozoans of the phylum Apicomplexa are the most prevalent and successful pathogens known to humankind. Today, half of the world's population is at risk of malaria caused by four Plasmodium species (Guerra et al., 2006), and more than 50 billion livestock reared for food production suffer from debilitating intestinal diseases caused by many species of *Eimeria*, Theileria, and Babesia, amongst others (Tomley and Shirley, 2009). *Eimeria* is the cause of coccidiosis in chickens, a parasite that infects the intestinal mucosa of the infected bird leading to severe weight loss and even death of the host. Cryptosporidiosis is caused by Cryptosporidium species and, like *Eimeria*, is transmitted by accidental ingestion of highly resistant and environmentally stable oocysts that contaminate the food and water. The disease is marked by self-limiting diarrhoea in immunocompetent individuals, but in immunocompromised patients, the disease can be fatal. Babesia is related to the malaria parasite in that it infects the reticulocytes of the infected cow and causes severe pathology and can cause death as well. *Toxoplasma* is the cause of toxoplasmosis in humans, a disease characterized by mild flu-like symptoms in healthy hosts. However, immunocompromised individuals, such as HIV/AIDS patients and organ transplant

recipients, often suffer from ocular toxoplasmosis or even encephalitis. Theileria, an important cattle parasite transmitted by ticks, is characterized by anaemia and high mortality rate especially in pregnant cows.

Plasmodium infects red blood cells and is the cause of malaria in humans as well as in several other vertebrate and bird species. Nearly one million human deaths are attributed to malaria each year, meaning that every 30 seconds a child dies of this disease in Africa. This high toll in human and animal life and wellbeing has been further exacerbated by the inappropriate use of antimicrobial compounds over the years. Thus, widespread resistance to most (if not all) drugs used to date makes control of these parasites extremely difficult (Coombs and Muller, 2002; Shirley et al., 2005). The novel artemisinin-based therapies are considered to be the new hope for malaria control and have proved to be successful in interrupting the maturation of the infectious stages (oocysts) in the related parasite, *Eimeria*, thereby reducing or blocking the transmission and spread of the parasite (Allen et al., 1998; Allen et al., 1997; del Cacho et al., 2010). However, there are fears that overuse of these novel compounds will also facilitate the selection of even more potent strains.

Over the past three decades, a number of putative protective antigens from several members of the phylum has attracted a great deal of research and commercial interest in the hope to develop vaccines and alleviate the burden on public health and world economy imposed by this class of parasites (Bhopale, 2003; de Graaf et al., 1999; de Waal and Combrink, 2006; Graves and Gelband, 2003, 2006a, b, c; Miura et al., 2007; Williams, 2002). The first antiprotozoan subunit vaccine developed to date, CoxAbic, which contains antigens isolated from the sexual stages of development of *Eimeria* is a proof of principle for transmission-blocking immunity and an example of a strategy that has been proved successful in helping to tackle one of these important apicomplexan diseases (Smith et al., 1994a; Smith et al., 1994b; Smith et al., 1994c; Wallach et al., 1995; Wallach et al., 2008).

Despite the enormous efforts to characterise the apicomplexan immunostimulatory antigens and genes encoding them, the fine cellular and molecular details of the effector mechanisms crucial for parasite inhibition and stimulation of protective immunity are still not fully understood. It is hoped that unravelling the proteomes and genome sequences of these protozoan pathogens will facilitate our understanding of the

mechanisms involved in the infectious process and lead to the design of new effective control strategies (Belli et al., 2005).

Early studies concerning the developmental biology and immunology of the Apicomplexans have provided valuable insights into the immune mechanisms responsible for the inhibition of parasite growth and development and in the establishment of host resistance to infection (Clark and Allison, 1974b; Danforth, 1983; Hammond, 1973; Rose, 1971, 1972, 1987; Rose and Hesketh, 1976). Efforts by research laboratories across the globe have demonstrated that, in order to control the infection, both the innate and adaptive arms of the immune system are crucial for resistance and cross-protection (Artavanis-Tsakonas et al., 2003). This paper provides an overview of Apicomplexan biology and focuses on the protective immune response against the various types of apicomplexan parasites, from *Eimeria* to Plasmodium including *Toxoplasma*, Cryptosporidium, Theileria, and Babesia. It also addresses the evolutionary relationship of these parasites and their hosts and the modulation of the host immune response that are critical in determining the outcome of an infection.

1.2 Apicomplexan life cycle and parasite-host relationship

The apicomplexan life cycle includes both asexual multiplication (schizogony, merogony) and sexual reproduction (gametogony) [25, 29, 30] (Hammond, 1973; Mehlhorn, 1971; Smith et al., 2002). While some members of the phylum require an intermediate host and a variety of cell types to complete their developmental life cycle (i.e., Plasmodium, Babesia, Theileria, *Toxoplasma*), others lead a monoxenous life style with the asexual and sexual stages of development restricted to specific tissues of a single host (i.e., *Eimeria* and Cryptosporidium species). Thus, the possibility of culturing asexual stages in vitro (Tomley, 1997), as well as the feasibility of isolating relatively large numbers of sexual forms (gametocytes), has granted *Eimeria* species a status of an attractive and a relatively simple model for investigating parasite-host interactions, as well as applying transmission-blocking immunity (Pugatsch et al., 1989; Wallach, 1997).

Apicomplexan parasites affect all classes of vertebrates, including fish, amphibians, reptiles, birds and mammals. The apparently long coevolutionary history of the

apicomplexans means that targeting the metabolic reactions and pathways of the parasite also harms the host, making the identification of therapeutic targets extremely difficult. Recent advancements in molecular biology have shed new light into the coevolutionary history of the apicomplexa and their hosts. This is based on the finding that the branching of the evolutionary tree of at least some of these parasites coincided with the evolution of the vertebrate host (Templeton, 2007). In addition, it was found that several enzymes involved in a variety of metabolic pathways are highly conserved between the parasite and its host. Furthermore, comparative studies of whole genome nucleotide sequences in several members of the phylum have revealed that surface proteins, unlike the house-keeping proteins and enzymes, have evolved rapidly over the past 500 million years due to functional and immune selective pressure (Janouskovec et al., 2010; McFadden and van Dooren, 2004; Sato, 2011; Templeton, 2007). This is especially evident in the molecules comprising the apical complex, the invasion machinery mediating physical recognition, cytoadherence, and penetration of the host, which are parasite specific.

The successful invasion of the host cell by the apicomplexan parasite is dependent upon the sequential secretion of proteins and other molecules from the rhoptries, micronemes, and dense granules and results in the formation of the parasitophorous vacuole (PV) (i.e., *Toxoplasma*, Cryptosporidium, Plasmodium, and *Eimeria* spp.). This in turn provides access to intracellular nutrients and protection from the host's immune system (Soldati et al., 2004). Although the PV shields the parasite from the host defences, at the same time it restricts access to nutrients in the host's cytoplasm. Thus, the Apicomplexa has adopted different tactics to circumvent this problem, including biochemical modification of the PV making it permeable to essential nutrients. In contrast, some parasites, such as Theileria spp., do not form the PV and proliferate freely in the cytoplasm with direct access to host nutrients (Dobbelaere and Heussler, 1999; Dobbelaere and Rottenberg, 2003; Shiels et al., 2006).

Lateral gene transfer, best known for its role in antibiotic resistance in bacteria, has been proposed as a mechanism by which these opportunistic organisms acquire new genes that confer parasite fitness (Janouskovec et al., 2010; McFadden and van Dooren, 2004; Sato, 2011). For example, the apical complex, actin-myosin-powered motor, evolved as a result of the nuclear transfer of genes acquired during the secondary endosymbiotic

event. It is believed that origin of the apicoplast can be attributed to endosymbiotic partnership in which the plastid-containing eukaryote was engulfed by a second eukaryotic cell. In addition, sexual replication appears to be another contributing factor to the diverse functions of the apicomplexan surface proteins and the adaptations to genera-specific niches (Ferguson et al., 2008; West et al., 2003; West et al., 2000). Therefore, it is not surprising that Plasmodium and Babesia species share evolutionarily conserved mechanisms of erythrocyte invasion (Clark and Allison, 1974a). Moreover, transmembrane proteins (thrombospondin-related anonymous proteins—TRAP) bridging the apical complex to the host cell in Plasmodium, *Eimeria*, and *Toxoplasma* also share a high degree of homology (Cowman and Crabb, 2006; Moreira et al., 2008; Soldati et al., 2004; Witcombe et al., 2003), suggesting that Apicomplexa use the same molecular machinery to invade a wide variety of cells.

A great deal of research has also been carried out to study the role of surface antigens in parasite growth, development, and survival. Passive transfer of polyclonal and monoclonal antibodies raised to asexual stage surface antigens of T. gondii are capable of conferring resistance against lethal challenge with this parasite (Brinkmann et al., 1993; Sharma et al., 1984). Similarly, *Eimeria* and Plasmodium antisporozoite and antimerozoite antibodies that recognize surface antigens, namely, glycosyl-phosphatidylinositol- (GPI-) anchored antigens in *E. tenella* (EtSAG1) and P. falciparum (MSP1), respectively, are able to induce a strong inhibitory response and provide protection against infection (Dent et al., 2005; Witcombe et al., 2004). In addition, the antigens found on the surface of sporozoites have been implicated in the recognition and invasion of the hepatocytes in malaria and, therefore, represent promising targets for vaccine developers (Graves and Gelband, 2006b; Moreira et al., 2008; Sturm et al., 2006; Sturm and Heussler, 2007) (a detailed description of apicomplexan invasion and egress has been reviewed recently by Westwood and colleagues with a special emphasis on elements of the apical complex and their potential role as vaccine targets (Morgan et al., 2007)). Thus, both asexual-stage surface proteins and the molecules associated with the apical complex have been proposed as potential candidates for vaccine development.

Another conserved feature of the phylum is the transmissible, environmentally durable oocyst/cyst, the zygote stage of the Coccidia (i.e., *Toxoplasma*, *Eimeria*, Cryptosporidium, and Neospora species) (Mai et al., 2009; Mehlhorn, 1971). It is intriguing that asexual reproduction in *Eimeria* is tightly regulated, and although signals initiating the start of sexual reproduction have not yet been identified, the 2nd, 3rd, and 4th generation merozoites (depending upon which *Eimeria* species infects the host chicken) differentiate into male (micro-) and female (macro-) gametes in a synchronised manner. The trademark of apicomplexan gametogenesis is the synthesis of numerous lipid bodies and polysaccharide granules, believed to be acquired from the host cell, serving as an energy source for the developing zygote. Moreover, increased DNA synthesis and RNA transcription to produce multinucleated microgametocytes and heightened protein synthesis in the macrogametocytes to produce wall forming bodies (WFBs) are characteristics of sexual stage development at the molecular level (Ferguson et al., 2003; Ferguson et al., 1977; Ferguson et al., 1975; Fried et al., 1992; Pittilo and Ball, 1979). *Eimeria*, Cryptosporidium, and *Toxoplasma* spp. gametogenesis is completed by the formation of environmentally resilient oocysts in the mucosae lining the gastrointestinal tract of chickens, humans, and cats, respectively. The oocysts are then excreted with the faeces where they mature (sporulate) becoming infectious. Cryptosporidium is slightly different from *Eimeria* and *Toxoplasma* in that the Cryptosporidium oocysts can also release sporozoites in the gut which are capable of infecting new epithelial cells (i.e., autoreinfection). In all three cases, transmission is primarily by the accidental ingestion of sporulated oocysts.

Unlike the intestinal parasites described above, gametogenesis of Plasmodium and Babesia spp. is completed in the gut of their arthropod hosts. During development, after fertilization of macrogametes by the microgametes and invasion of the gut by the ookinete, the zygotes encase themselves in a protective single-layered cyst wall to form an oocyst. Flagellated sporozoites then exit the oocyst and migrate from the midgut to the salivary gland of their arthropod host. From there, they are injected into the blood and subcutaneous tissue of the next vertebrate host the arthropod bites.

1.3 Naturally acquired immunity to apicomplexan parasites is exclusively dependent upon cell-mediated immunity

Studies to elucidate the mechanism(s) of the protective immune response to apicomplexan parasites have been limited mainly due to the lack of being able to carry out such studies in the definitive host such as cattle or human beings. Thus, much of our understanding of the protective immune response to apicomplexan infections has been derived from murine models which can be genetically modified (Meeusen et al., 1984a; Rose, 1987). Generally speaking, parasite replication in the host eventually leads to host cell lysis and parasite egress. It is now widely accepted that cells of the innate immune system and the molecules they produce and/or secrete are important controlling factors of parasite infectivity and in limiting the extent of parasitemia (Akiba et al., 1991; Artavanis-Tsakonas et al., 2003; Laurent et al., 1998; Laurent et al., 1999; Nelson et al., 2008). It is not clear exactly how these molecules, particularly in the case of parasites infecting host erythrocytes (i.e., Plasmodium and Babesia spp.), interfere with parasite development. What does appear to be the case is that this inhibition is accomplished by the production of gamma interferon (IFN-γ),by natural killer cells (NK), and tumour necrosis factor alpha (TNF-α), nitric oxide (NO) and reactive oxygen species (ROS) by macrophages [62–64]. Despite the fact that the mechanisms by which IFN-γ mediates protection are not completely understood, studies using IFN-γ and iNOS knock-out mice infected with T. gondii indicated that activation of p47 guanosine triphosphatases (GTPases) leads to degradation of the PV in infected cells (Molestina et al., 2003).

While the immune response in healthy hosts is often but not always able to control parasite replication and limit the disease, immunocompromised individuals fail to stop parasite growth, and clinical disease develops in nearly all cases. This is especially evident in toxoplasmosis where immunocompetent hosts control parasite replication causing tachyzoites (the rapidly replicating asexual stages) to migrate to muscle and brain tissues where they differentiate into bradyzoite cysts (the slow-replicating form) and persist throughout the host's life. Although the tissue cysts can become reactivated periodically, most healthy hosts never develop clinical disease. In contrast, immunocompromised patients, such as those suffering from AIDS, remain chronically infected, whereby reactivation of the tissue cysts can lead to toxoplasmic encephalitis with severe pathological consequences.

The ability to clear acute and chronic infections with the Apicomplexa seems to correlate with host CD4+ T-cell levels (Igarashi et al., 1999; Lang et al., 2006). Thus,

studies involving athymic animals have shown that T cells play a crucial role in the infectious process (Igarashi et al., 1999; Igarashi et al., 1994; Matsubara et al., 1993).

The population of T cells coexpressing αβ markers appears to be important for host defence against apicomplexan infections (Lillehoj and Trout, 1994, 1996; Trout and Lillehoj, 1996). Thus, it was demonstrated that TCRα-deficient mice developed severe disease when compared to controls (Trout and Lillehoj, 1993, 1995, 1996). Furthermore, mice lacking major histocompatibility complex class II expression (i.e., CD4+ T-cell deficient) appeared more susceptible to apicomplexan infections (Igarashi et al., 1999; Igarashi et al., 1994).

CD8+ T cells also appear to play a role in parasite growth and dissemination because they provide sporozoite transport from their initial infection site, as is the case for *Eimeria* and *Toxoplasma* infections (Lang et al., 2006; Lillehoj and Trout, 1996). During the course of primary infection with *Eimeria*, CD8+ T cells appear to play a role in parasite growth and dissemination because they provide sporozoite transport from their initial infection site to the crypt cells. On the other hand, reports have also shown that increased numbers of CD8+ T cells in the crypt epithelium act as cytotoxic killer cells facilitating the clearance of the parasite-infected cells (Trout and Lillehoj, 1993, 1995, 1996). Furthermore, studies in infected chickens have shown that the contribution of both CD4+ and CD8+ T-cell populations differs according to the infective species used. Nevertheless, during avian coccidiosis and babesiosis, CD4+ T-cell subsets were found to be elevated in animals following challenge infections. An intriguing question arises from all of these observations: why are some species or strains of parasites extremely "immunogenic" and induce protective immunity, while others seem to be invisible to the immune system?

Studies on naturally acquired immunity to malaria have shown that adequate protective immunity to P. falciparum, the etiological agent of the most severe malaria in humans, usually required repeated infections. Thus, protection against this particular strain appeared to be acquired more slowly than against the less pathogenic P. vivax or P. malariae (Artavanis-Tsakonas and Riley, 2002). Moreover, numerous studies have shown that immunity appeared to be species specific and did not confer protection against challenge with heterologous species. However, it was reported that heavy exposure to parasites induces the development of antigenic memory (Jeffery, 1966).

Although the molecular and cellular mechanisms driving the onset of protective host immunity against malaria or any other pathogenic protozoan are not entirely understood, it is believed that susceptibility to infection is driven by extrinsic factors such as antigenic variation and also by intrinsically inappropriate immune responses (Doolan et al., 2009). This is particularly evident in Theileria infections of immunocompromised cattle, which often results in the death of the host animal. It is theorised that the ability of Theileria to interfere with the host's apoptotic pathways is the crucial factor contributing to mortality (Dobbelaere and Heussler, 1999; Dobbelaere and Rottenberg, 2003). Once inside the host cell, Theileria resides free in the cytoplasm and induces uncontrolled proliferation of the infected cell. Some have even compared Theileria infections with cancer development and metastasis. Thus, it appears that during Theileria infection the immune system fails to control this proliferation in time, in turn resulting in potent, nonspecific lysis of both infected and noninfected cells.

Studies using immunocompetent animals have shown that, in addition to innate host resistance, IFN-γ plays a key role in the development of adaptive immunity and clearing of Apicomplexa infections. For example, Cryptosporidium-infected mice, with faulty IFN-γ gene expression, suffered from severe mucosal destruction, and as a result they also secreted more oocysts (Lacroix-Lamande et al., 2002; Laurent et al., 1999). Furthermore, mopping-up the secreted IFN-γ by antibodies in immunocompromised animals seemed to worsen C. parvum infection. In addition, it is now widely accepted that IL-12, known to increase host IFN-γ production, can reduce the severity and even prevent infection by apicomplexan parasites (Aguilar-Delfin et al., 2003). Although believed to be mediated by an IFN-γ-dependent mechanism, the pathways or downstream molecules crucial in this process have not been well defined to date.

1.4 Masters of disguise

Although viruses, which entirely depend on the host machinery for replication and assembly of new viral particles, are the experts in host cell manipulation, the Apicomplexa are considered to be the masters of disguise. This is because they have evolved to evade the host immune system to aid in their own survival. Antigenic variation has been proposed as a key factor in this process. Unlike allelic

polymorphism, which results in different phenotypes or so-called parasite strains (Walliker, 1991), antigenic variation is the tightly regulated expression of different genes of a clonal population of parasites over the natural course of infection. Antigenic variation amongst malarial and Babesia parasites is a prime example of sophistication apicomplexans employed to avoid antibody-mediated inhibition (Al-Khedery and Allred, 2006; Allred, 1998; Dent et al., 2008). P. falciparum achieves this by secreting a single type of a variant molecule (parasite-derived erythrocyte membrane protein 1 - PfEMP1) on the surface of the infected erythrocyte at any one time. The PfEMP1 surface proteins are encoded by a family of genes, called var genes, and each individual parasite expresses only a single var gene, keeping all other members of var gene family in a transcriptionally silent state (Hommel et al., 1983; Smith et al., 1995; Su et al., 1995). This strategy in turn induces adhesion of the parasite-infected erythrocytes to the blood vessels to avoid reaching the spleen, whose main function is to rid the body of damaged and/or infected blood cells. Similarly, sequestration of Babesia-infected erythrocytes in the microvasculature enables the Babesia to persist within the host maximizing its chances of transmission (Allred, 1998). This cytoadherence in Babesia is mediated by constant gene conversion of ves family genes encoding the variant erythrocyte surface antigen 1 (VESA1) (Oconnor et al., 1997).

A puzzling question arises from these observations: if infected erythrocytes pass through the body unchecked since they lack major histocompatibility complex (MHC) expression, overwhelming proliferation of the parasites may cause premature death of the host prior to successful transmission to an arthropod vector? Interestingly, in spite of the fact that malaria parasites sequentially express variant surface molecules exposing the immunodominant antigens to the host immune defences, infection is actually prolonged. Thus, the parasite must undergo antigenic variation and rates of growth that enable the host to control infection while allowing for transmission of the parasite prior to its death. This mechanism to prolong infection was also evident in merozoites of Babesia species. Due to coating of the merozoite surface with glycosyl-phosphatidyl-anchored proteins crucial for initial attachment to the host erythrocyte surface, they are targeted by host-protective antibodies (Guevara-Patino et al., 1997). These surface-anchored proteins (Variable Merozoite Surface Antigens-VMSA) exhibit varying degrees of intra-species antigenic polymorphisms allowing these parasites to evade the host immune system at the population level (Doolan et al., 2009). Nevertheless, studies

involving African children have shown that variant specific immunity, namely, secretion of IgG antibodies directed against P. falciparum variant surface antigens (VSA), has been correlated with protection from clinical malaria in Ghana, Kenya, and Tanzania (Dent et al., 2008; Dent et al., 2009; Dent et al., 2005; Kinyanjui et al., 2004). Thus, VSA antigens have been proposed as excellent candidates for malaria and Babesia vaccine development.

1.5 Humoral immunity protects against challenge infections

Although B cells have been regarded as minor contributors to protective immunity and resistance to primary infections with Apicomplexa, numerous studies have shown that hosts infected with these parasites are capable of producing protective, parasite-specific immunoglobulins (Ig) of all major classes after an episode of infection and recovery (Hogh, 1996; Mahoney, 1967; Meeusen et al., 1984b; Mineo et al., 1993; Precigout et al., 1993). Thus, early work by Rose and colleagues has shown that humoral antibodies, induced by live *Eimeria* infection, can provide excellent passive protection against challenge infections with the same parasite (Rose, 1971; Rose et al., 2000). Likewise, studies on mice infected with T. gondii have shown that intestinal IgA antibodies to major surface protein SAG-1 (P30) were produced after peroral infection and found to inhibit infection of murine enterocytes by directly blocking the parasite entry (Mineo et al., 1993). In addition, Precigout et al. have demonstrated an inhibitory effect of antibodies directed against a 17-kDa merozoites membrane protein on B. divergens parasite growth (Precigout et al., 1993). Furthermore, studies on invasion of red blood cells by P. falciparum merozoites have revealed that since RBCs do not express the MHC complex, parasite killing by T lymphocytes is not important. Instead, antibodies specific to merozoite surface molecules (MSP-1) and proteins externalised from the apical complex play a major role in immunity to asexual blood stages (Hui and Hashimoto, 2007).

The Plasmodium merozoite surface protein 1 (MSP-1) is a 200 kDa multicomponent precursor complex derived by proteolytic processing during erythrocyte invasion. The 42 kDa C-terminal component is cleaved (i.e., secondary processing) to produce soluble 33 kDa and 19 kDa fragments that remain on the merozoites surface (Kauth et al.,

2003). Studies have shown that anti-merozoite antibodies are capable of neutralizing parasites by Fc-dependent mechanisms involving macrophages, thus reducing the parasitemia and clinical disease (Elliott et al., 2007; Kassim et al., 2000). In addition, a number of recent studies have shown that children naturally infected with malaria secrete anti-MSP-1 antibodies (MSP-119 mAb) that block the binding of Plasmodium merozoites to the surface of the red blood cells and also inhibit secondary processing of MSP-1. In addition, studies investigating the protective properties of maternally derived IgG and IgM antibodies to the 19 kDa domain of MSP-1 of P. falciparum have shown that mothers who have tested positive for anti-MSP-1 (19 kDa fragment) IgG antibodies conferred protection against placental infection and infection in their infants (Broen et al., 2007).

It has been shown that, in babesiosis infection, IgG antibodies produced as a result of live infection can prevent infection of erythrocytes by binding and neutralizing sporozoites before they invade their target cells. Similar observations were reported in chickens where antisporozoite antibodies specific to glycosyl-phosphatidylinositol-anchored *E. tenella* surface antigen 1 (EtSAG1) appeared to inhibit parasite binding and invasion of the host cell (Danforth, 1983). However, it seems that the protective role of these antibodies is limited since it can only neutralize sporozoites from the time the parasites egress and the time they gain access to new cells. Thus, it is hoped that genome-wide fingerprinting techniques (Blake et al., 2012; Blake et al., 2011; Blake et al., 2004) will aid in the identification of additional immunoprotective antigens that can be used in combination to induce the maximal inhibitory humoral immune response.

In addition to antigen-specific polyclonal and monoclonal antibodies capable of inhibiting asexual stages, antibodies raised to antigens localized exclusively to gametocyte/zygote stages were also found to be highly immunogenic and capable of providing passive protection in vivo (Krucken et al., 2008; Wallach et al., 1989). Early experiments involving immunisation with purified sexual-stage gametes of P. gallinaceum in chickens showed that effective transmission-blocking immunity can be achieved by reducing the infectivity of gametocytes and oocyst development (Huff and Marchbank, 1955; Huff et al., 1958). Thus, Pfs25 and Pvs25 proteins expressed on the surface of ookinetes in the mosquito stage of P. falciparum and P. vivax have been used extensively as candidates for malaria transmission-blocking vaccines, since lowering the

density of circulating parasites would not produce sterilizing immunity, instead it would allow individuals to develop long-lasting, naturally acquired immunity to malaria (Kaslow et al., 1992; Williamson et al., 1993).

Work by Wallach and coworkers, aimed at applying transmission-blocking immunity to control infections caused by *Eimeria*, hypothesised that antibodies raised against the gametocyte/zygote stages of development can act to inhibit oocyst development and thereby provide a block in parasite transmission (see Figure 1). A method was developed for purifying *E. maxima* gametocytes from the infected chicken gut mucosa and immunodominant gametocyte antigens, namely, Emgam56, Emgam82, and Emgam230 localized to the WFBs and the oocyst wall of the maturing zygote, were extracted (Wallach et al., 1992). Passive immunisation experiments showed that there was a good correlation between the intensity of IgG and IgM antibodies binding to gametocyte antigens by Western and ELISA with the ability of those sera to provide passive protection in vivo (Wallach et al., 1994; Wallach et al., 1995). The mechanisms by which these antibodies inhibit oocyst maturation are still obscure; however, it is hypothesised that antibodies raised to the immunodominant antigens retard zygote development by interfering with the processing of wall proteins or the wall-hardening processes (Wallach, 2010). In addition, a protective monoclonal antibody raised against Emgam56 localised to the WFB2 (1E11-11), as well as the inner layer of the oocyst wall, was also found to react strongly with the Stieda body of the sporulated oocysts (M. Wallach, unpublished data). Similar results were reported by Krücken et al. using a monoclonal antibody E2E5 raised to WFB2s of *E. tenella* (Krucken et al., 2008). The in vitro excystation inhibition assay showed that the antibody E2E5 can significantly interfere with parasite development by impairing sporozoite excystation. It is tempting to speculate that the 1E11-11 monoclonal antibody inhibits or blocks excystation of the sporocyst in a similar manner, thereby reducing the number of infectious sporozoites released in the intestine of infected birds allowing them to develop protective immunity induced by exposure to low doses of parasites.

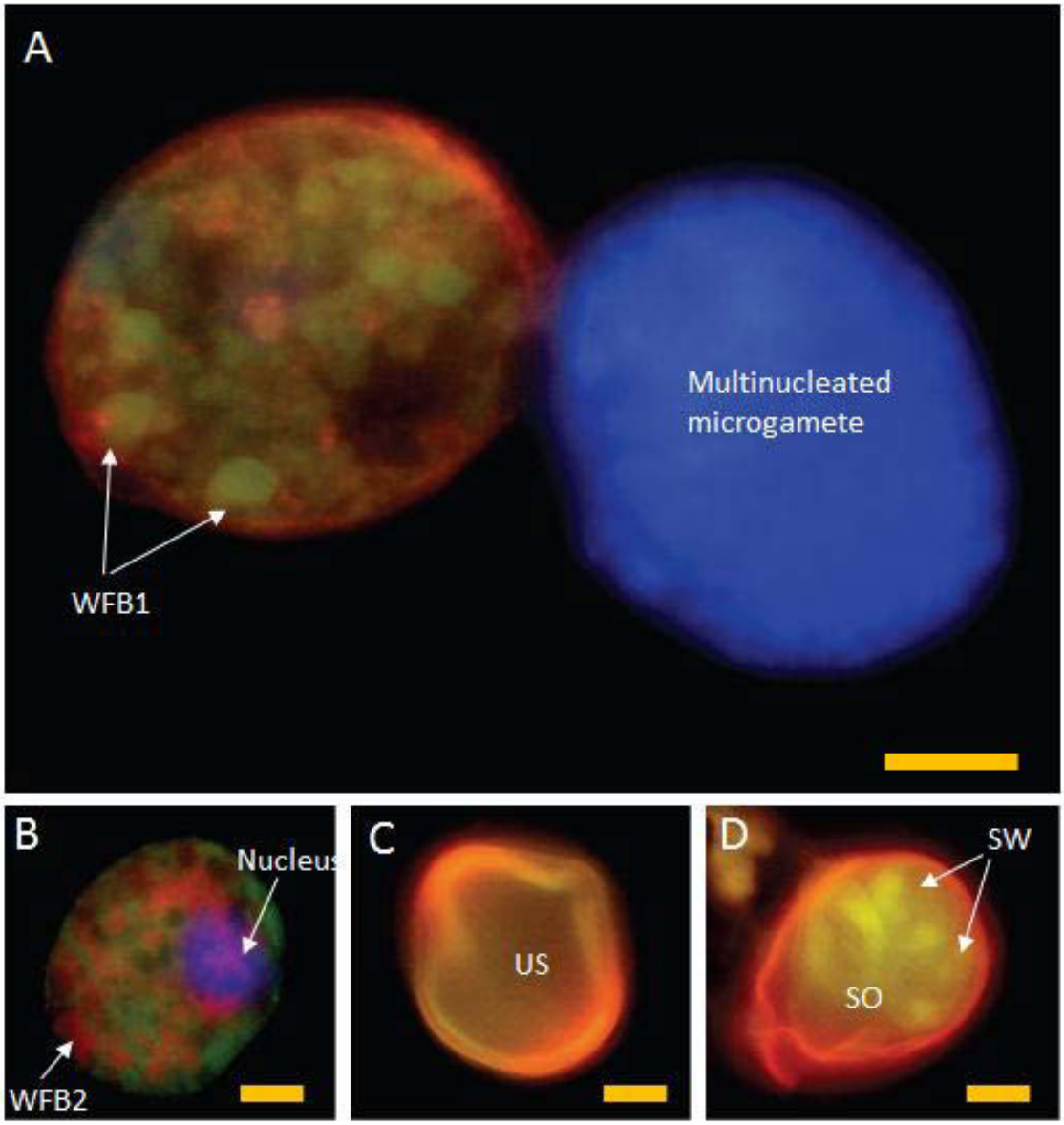

Figure 1: Developing and mature micro- and macrogametes and oocysts harvested from the infected chicken intestine 134 h post infection (p.i.) and double-labelled with a monoclonal antibody raised to antigens confound to WFB1s (E1D8) [107], and a polyclonal affinity purified gametocyte antigens Emgam56, Emgam82, and Emgam230, amongst other molecules (anti-APGA) specific to molecules contained within the wall-forming bodies (1 and 2) [53] and visualised with fluorescein isothiocyanate (green) or revealed with rhodamine-conjugated goat anti-mouse IgG secondary antibody (red). Counterstained with DAPI. Abbreviations: N, nucleus; SO, sporulated oocysts; SW, sporocyst wall; US, unsporulated oocyst; WFB1, wall-forming body type 1; WFB2, wall-forming body type 2. Bars represent 5 µm.

Jenkins and colleagues have shown that ruminants immunized with a DNA vaccine expressing a gene isolated from C. parvum encoding a sporozoite antigen (CP 15/60) were capable of inducing antigen-specific antibodies (Jenkins et al., 1995; Jenkins, 2004). In that study, it was found that using various routes of vaccination resulted in differing antibody responses and titres. The authors, therefore, suggested that the route of antigen delivery of any protozoan vaccine requires careful formulation and optimisation of delivery systems.

Finally, in studies carried out by Wallach and co-workers on *Eimeria* (Wallach et al., 1994), it was found that in order to achieve protective immunity using parasite extracts requires the inclusion of the correct antigens and exclusion of the irrelevant ones. Their results indicated that while some parasite-specific antigens induce protective immunity, others actually induce an exacerbation of the infection. Therefore, in the design of any parasitic vaccine, it is crucial that the combination of various antigens maximizes their inhibitory effect on parasite growth and development.

1.6 The apicomplexa are the manipulators of host defence mechanisms

One of the main defence mechanisms employed by host cells is programmed cell death (apoptosis) ensuring regulated removal of damaged and infected cells (Green, 2000). But because the survival and development of intracellular apicomplexan parasites is dependent upon the continuous supply of host cell nutrients and protection from immune attack, the parasites have adapted to extend the life of the infected cells by inhibiting the host cell apoptotic machinery through interference with the intracellular signalling molecules, notably phosphatidylinositol 3-kinase (PI3-K). PI3-K is involved in a variety of functions including cell growth, proliferation, and intracellular trafficking, amongst others (Chen et al., 2001; Kuenzi et al., 2003; Lang et al., 2006; Leiriao et al., 2005). P. falciparum is a good example of how parasite secreted proteins prevent host cell death to ensure its own development and survival. Sporozoites of Plasmodium species are stealthy invaders that first travel to the liver (hepatocyte) cells, where the growth and development of the daughter cells, hepatic merozoites, takes place. Recent results have shown that prior to the establishment of the PV, sporozoites

of P. falciparum transmigrate through a number of hepatocytes before they anchor to and invade the suitable cell via exocytosis of proteins contained within the apical complex. It has been shown that the thrombospondin-related adhesive-protein- (TRAP-) like protein plays a role in this process. Additionally, the wounding of the hepatocyte induced by invading sporozoites releases growth factors which in turn appear to inhibit PI3-K and block the signalling pathways destined for apoptosis. Leirião and colleagues have shown that once the parasite is established in the hepatocyte, it secretes HGF/MET signalling molecules into the host cell cytoplasm, thereby conferring resistance to apoptosis to ensure survival and maturation of the daughter cells. However, which signalling upstream of PI3-K occurs during Plasmodium infection is yet to be determined. Interestingly, upon maturation of merozoites, Plasmodium seems to be able to induce host cell death to liberate the motile progeny. Strum et al. have shown that this process involves cysteine proteases (Sturm et al., 2006; Sturm and Heussler, 2007). Moreover, similar mechanisms were found to play a role in release of sporozoites from the oocysts (Aly and Matuschewski, 2005). Although work is ongoing to try and elucidate the mechanisms involved in these processes, it appears that the Apicomplexa have learned to inhibit host cell death during parasite development and subsequently activate it, liberating thousands of new progeny.

T. gondii has also evolved a broad spectrum of adaptations to challenges presented by its life style (Sinai et al., 2004; Sinai et al., 1997). Chronic toxoplasmosis is the trademark of the parasite's success and is induced by the slow-replicating bradyzoites safely tucked away in the remodelled PV, the tissue cyst. Like Plasmodium, T. gondii modulates host cell apoptosis by both inhibiting and triggering the programmed cell death (Payne et al., 2003). Chen et al. have shown that Fas/FasL ligand-dependent mechanisms mediate the inflammatory responses induced by the apicomplexan infection (Chen et al., 1999). But the parasites have evolved to neutralize granzyme/perforin-mediated killing of infected T cells and natural killer cells (NK) by modifying transcription and posttranscriptional modification of IFN-γ-regulated genes, the major mediators of resistance to T. gondii infections. Likewise, del Cacho et al. have demonstrated that *E. tenella* and E. necatrix second-generation schizonts first induce NF-κβ activation to protect the transformed cells from apoptosis, allowing the

schizonts to mature and later cause NF-κβ inhibition to trigger host cell apoptosis to facilitate the release of merozoites (del Cacho et al., 2010).

The Apicomplexa have evolved to live in synergy with their infected hosts because they completely depend on it for survival; however, some apicomplexan infections induce a great deal of immunopathology and can lead to host cell death. For example, *Eimeria* and Cyclospora both interfere with the absorption of nutrients across the intestinal mucosa and can cause death due to malaise, diarrhoea, and dehydration. Because apicomplexans increase in numbers while in their hosts, the severity of infection is proportional to the parasite density—the smaller the number, the greater the chance of asymptomatic infection and the greater the chances of the parasite survival. However, the immunological defence of a host can also cause extensive tissue damage and clinical symptoms. Patients with cerebral malaria usually have elevated levels of tumour necrosis factor alpha (TNF-α) and IgE considered to be responsible for fever and tissue lesions to an extent where vital functions of the host fail leading to a coma (Marsh and Snow, 1997).

1.7 Are we losing the battle against apicomplexan parasites?

Despite a great deal of effort and technological advancements in biotechnology, molecular biology, genetics, immunology, and vaccinology, there are no vaccines for humans against malaria and toxoplasmosis at the present time, and it seems that we are losing the battle in the fight against pathogenic protozoans. The current failure to develop a practical vaccine may well be attributed to our inadequate understanding of the mechanisms underlying (1) the naturally acquired immunity against apicomplexans, (2) acquired parasite resistance to most (if not all) antimicrobial compounds used to date, and (3) in the case of arthropod transmitted protozoans, failure to implement adequate vector control programs in tropical and subtropical regions.

The life cycles of the Apicomplexa are complex, thus, it is hoped that a multivalent, multistage vaccine will alleviate the problems caused by these pathogenic protozoans. Although this approach has attracted a great deal of commercial and research interest, the critical issues to be addressed include the identification of stage-specific antigens capable of inducing protective immunity and the delivery methods in a form that will

stimulate an adequate protective immune response. The main impediment in the search and selection for immunostimulatory antigens is the lack of in vitro assays to analyse and predict immune responses. The transmission blocking assays, relying on counting the number of oocysts produced, and the inhibition of sporozoite invasion assays have both been used extensively to evaluate parasite inhibition induced by neutralizing antibodies.

Although in vivo experimentation is extremely difficult for malaria, other model systems can be used to dissect the fine details and the effect of neutralizing antibodies. It is very possible that, in the development of an antiprotozoan vaccine capable of inducing only partial immunity, resistant mutants would be selected that are even more pathogenic than existing strains. In the malaria scenario, this could be catastrophic since the parasite would undergo recycling and be transmitted throughout the community leading to an increase in morbidity and mortality. It is, therefore, of great hope that in the battle against these pathogenic protozoan parasites, including Plasmodium, Cryptosporidium, and *Toxoplasma*, the completion of their genomes and proteomes may provide information needed to design vaccines, assess the effects of immunization on parasite pathogenicity and the selection of unwanted mutants, and in the final analysis control the diseases caused by this class of parasites.

Chapter Two

Background on the subjects presented in this thesis

Eimeria is a cyst-forming intracellular parasite that causes the economically important disease, coccidiosis, in intensely reared broiler chickens worldwide. *Eimeria* typically infect defined regions of the gastrointestinal tract leading to impaired nutrient absorption, weight loss, diarrhoea and in severe cases mortality (Belli et al., 2004). The poultry industry incurs major economic losses since chemoprophylaxis, the preferred method of preventing and controlling the disease, is ineffective because the resilient parasites do not respond to therapy.

The molecular machinery responsible for the synthesis of the resistant oocyst is housed in the wall forming bodies (WFBs) of the parasite's sexual stages. The collaborative effort of the parasitology team at the iThree Institute (UTS) with scientists worldwide has led to the development of a maternally based subunit vaccine against coccidiosis. The currently available subunit vaccine, CoxAbic®, is based on transmission blocking immunity, which provides protection to chicks upon hatching. It contains antibodies that interfere directly with the parasite development into an infective form (oocyst). However, it is not certain when and by what mechanisms these antibodies retard the wall formation. It has been postulated that protective antibodies inhibit development by preventing either the processing, cross-linking or wall hardening process (Wallach, 2010). Although macrogametogenesis has been well documented at the ultrastructural level (Ferguson et al., 2003; Ferguson et al., 1977b, c; Lee and Millard, 1971; Mehlhorn, 1971; Mehlhorn, 1972; Pittilo and Ball, 1979a, 1980; Pittilo et al., 1981), reports describing the molecular mechanisms involved in the assembly of the oocyst wall have been limited.

2.1 The life cycle of cyst-forming Coccidia

The life cycle of the *Eimeria* parasite (Figure 2) is complex and includes asexual sporozoites and merozoites (Hammond, 1973; Mehlhorn, 1974; Pittilo and Ball, 1985; Ryley et al., 1972), and the sexual gametocyte stages (Mehlhorn, 1971; Mehlhorn, 1972; Pittilo et al., 1981). Coccidiosis is transmitted via the faecal-oral route by the ingestion of the resistant oocyst, which is excreted in the faeces contaminating food and

water. The excreted oocyst is unsporulated and non-infectious, and is essentially the zygote of the parasite surrounded by a protective wall (figure 2, step 11) (Ferguson et al., 2003; Ferguson et al., 1977a, b, 1978a; Pittilo and Ball, 1979b, 1980). Optimum humidity and temperature stimulate oocysts to sporulate by meiotic division to form the infectious sporozoites (Figure 2, steps 12-13) (Ferguson et al., 1978a; Lee and Millard, 1971; Pittilo and Ball, 1980; Ryley et al., 1972). The sporulated oocysts are picked up from the litter and ingested. Following ingestion, the oocysts are cracked open in the gizzard of the host releasing sporocysts (Figure 2, step 1). The excystation allows motile sporozoites to break out and invade epithelial cells of the intestinal mucosa (Figure 2, step 2). The sporozoites differentiate into merozoites, the asexual stage parasites (Mehlhorn, 1974). After 120 h post infection (h p.i.), three or four rounds of merogony take place (Figure 2, steps 3-5). The final generation merozoites erupt out of the host cell and invade new epithelial cells to enter the phase of sexual development (Figure 2, steps 7-9). To date, no explanation exists as to why a specific number of genetically predetermined asexual stages occur before gametogony. Within the epithelial cells the merozoites develop into male and female gametes (microgametocytes and/or macrogametocytes). The microgametocytes fertilize macrogametocytes to stimulate wall formation and the production of oocysts (Figure 2, steps 7i-8i) prior to excretion in the faeces (Figure 2, steps 9-10). Although there is evidence for zygotic meiosis in Coccidia, little is known of the process of "fertilization". Whether this process is necessary to stimulate wall formation is still controversial (Ferguson, 2002; Hammond, 1973; West et al., 2003; West et al., 2000). The two oocyst layers originate from the material stored in highly specialised organelles, the wall forming bodies (WFBs), found exclusively in the macrogametocyte stage of the life cycle (Ferguson et al., 2003; Ferguson et al., 1977a; Ferguson et al., 1975; Mehlhorn, 1971; Mehlhorn, 1972). There are two types of WFBs; type 1 (WFB1) form the outer oocyst layer, whereas type 2 (WFB2) form the inner oocyst layer (Mehlhorn, 1988). The two oocyst layers protect the fragile zygote from immune confrontations, mechanical damage and the harsh external environment (Stotish et al., 1978). Therefore, unravelling the molecular mechanisms involved in oocyst wall biogenesis in *Eimeria* spp. will provide valuable insights into the fundamental biology of other related cyst-forming Apicomplexans.

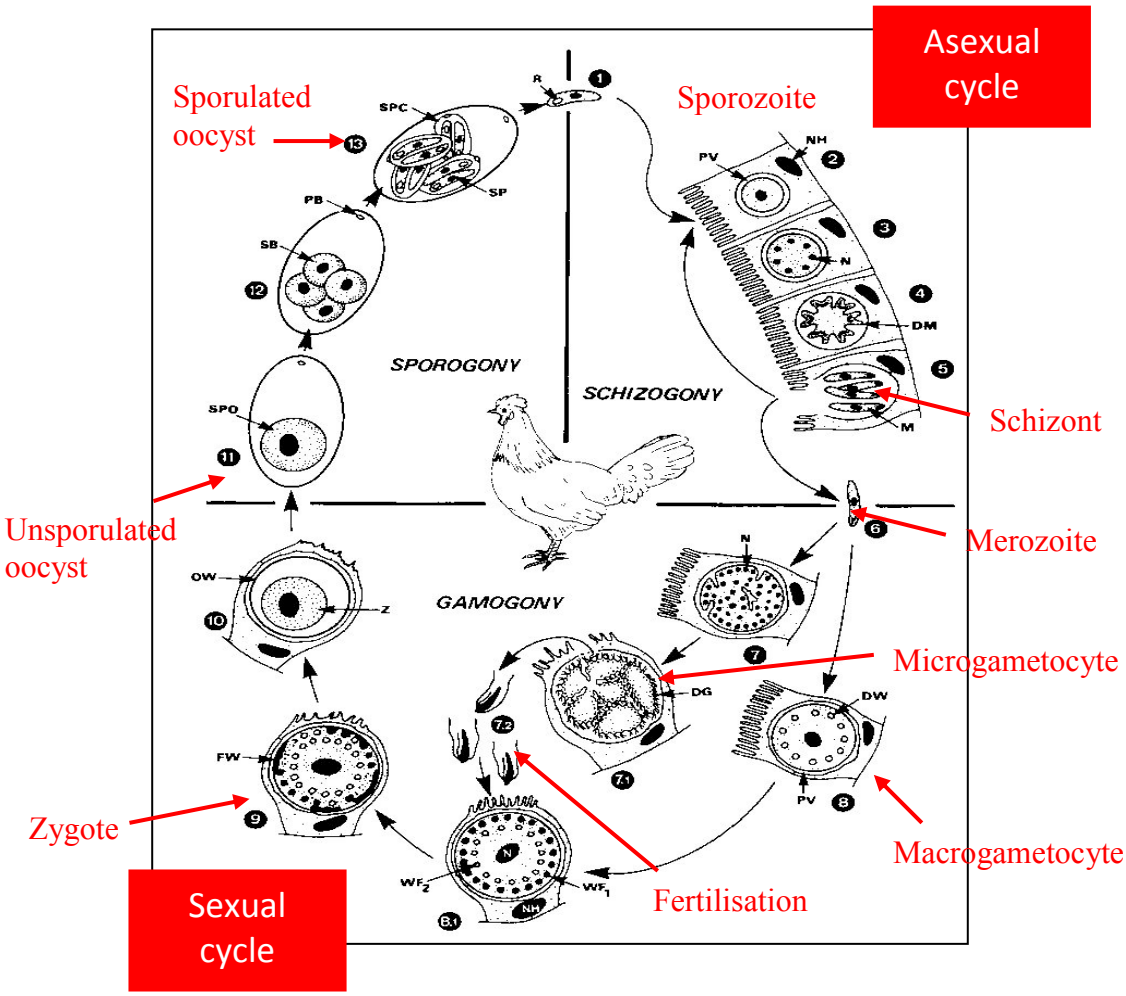

Figure 2: Life cycle of *Eimeria.* (1) Excystation of the sporulated oocyst releases eight motile sporozoites; (2-5) sporozoites invade epithelium of the gut, and go through asexual replication (schizogony) to produce merozoites; (6) merozoites rupture from schizonts and re-infect the host epithelium, or differentiate into micro- (7) or macrogametocytes (8); microgametocytes fertilize the macrogametocytes to form a zygote (9); the zygote develops into an unsporulated oocyst (10), which ruptures from the host cells into the gut and is released in the faeces (11), where they sporulate (12-13). [Adapted and modified from (Mehlhorn, 1971; Mehlhorn, 1988). Abbreviations DG = developing microgamete, DM = developing merozoite, DW = developing wall forming body, FW = fusion of wall forming bodies, M = merozoite, N = nucleus, OW = oocyst wall, PB = polar body, PV= parasitophorous vacuole, R= refractile body, SB = sporoblast, SP = sporozoite, SPO = sporont, SPC = sporocyst, WF1= wall forming body type 1, WF2 = wall forming body type 2, Z = cytoplasm of the zygote

2.2 Gametocyte biogenesis

The basic morphology of macrogametogenesis and oocyst wall formation of *Eimeria spp*. has been described in the 1970s. The young gametocyte stages are easily identified as male or female, when the organelles characteristic of both emerge. These early studies have shown that two types of wall forming bodies (WFB1 and WFB2) were synthesised exclusively during maturation of macrogametes and appeared to give rise to the two distinct layers that formed the oocyst wall (Ferguson et al., 2003; Ferguson et al., 1977a, b, 1978a, b; Hammond, 1973; Mehlhorn, 1971; Pittilo and Ball, 1979b, 1980). An additional structure, termed the oocyst veil, enclosing the developing oocyst has also been reported (Ferguson et al., 1977b; Ferguson et al., 1975; Pittilo and Ball, 1980). The loose veil appeared to be lost during excretion with the faeces. In contrast, a number of studies concerning the basic morphology of male gametes reported that the microgametocytes lack these specialised organelles and instead contain numerous nuclei (Ferguson et al., 1977c; Mehlhorn, 1972).

The early *E. maxima* macrogametocyte (Figure 3), situated within the parasitophorous vacuole that fulfils parasite's anabolic needs, can reach 17 μm in diameter. The cytoplasm contains a large central nucleus and a prominent nucleolus with areas of dilated endoplasmic reticulum (ER) designated as early WFBs (Figure 3, panel a). The mid-stage macrogametocyte contains a number of WFB2s intermixed with veil forming bodies (VFBs) arranged concentrically around the nucleus (Figure 3, panel b). The diameter of the WFB2s can reach up to 1.4 μm. It is well documented that the WFB2s consist of filamentous material with a compact centre, giving it the typical "donut-shaped" appearance (Ferguson et al., 2003; Mehlhorn, 1971; Pittilo and Ball, 1979a). The marginal regions of the WFB2s are closely associated with the Golgi complex. The close association of the WFB2s with the rER and Golgi complex appears to be characteristic of many coccidian parasites, including the related cyst-forming Apicomplexans, *Toxoplasma* and *Isospora* (Ferguson et al., 1977b, 1978b; Ferguson et al., 1975; Mehlhorn, 1971; Pittilo and Ball, 1979b). The late-stage macrogametocyte is identified by the increase in size to accommodate newly synthesized lipid and polysaccharide inclusions, which serve as stores of energy (Mehlhorn, 1971). At this stage, numerous WFB1s emerge as membrane-bound vesicles (Figure 3, panel b). The

appearance of the WFB1s as a large membrane-bound structure with homogenous contents is typical of storage granules (Ferguson et al., 2003). The subcellular origin of the WFB1s is not exactly clear. Mehlhorn *et al.* (1971) proposed that the WFB1s appear as membrane-bound vesicles originating from mitochondria, since similar inclusions were observed there. However, other authors have suggested that the WFB1s arise directly from the Golgi complex and sometimes, but not always, contain a limiting membrane (Lee and Millard, 1971). In contrast, morphological studies of *E. maxima* microgametocytes revealed the absence of the WFBs and presence of numerous peripheral nuclei, typically 0.7 μm in diameter closely associated with flagella and mitochondria (Figure 3, panel e). Dark blobs, which concentrated at the periphery of the nuclei, were identified as chromatin (Ferguson et al., 1977c; Mehlhorn, 1972).

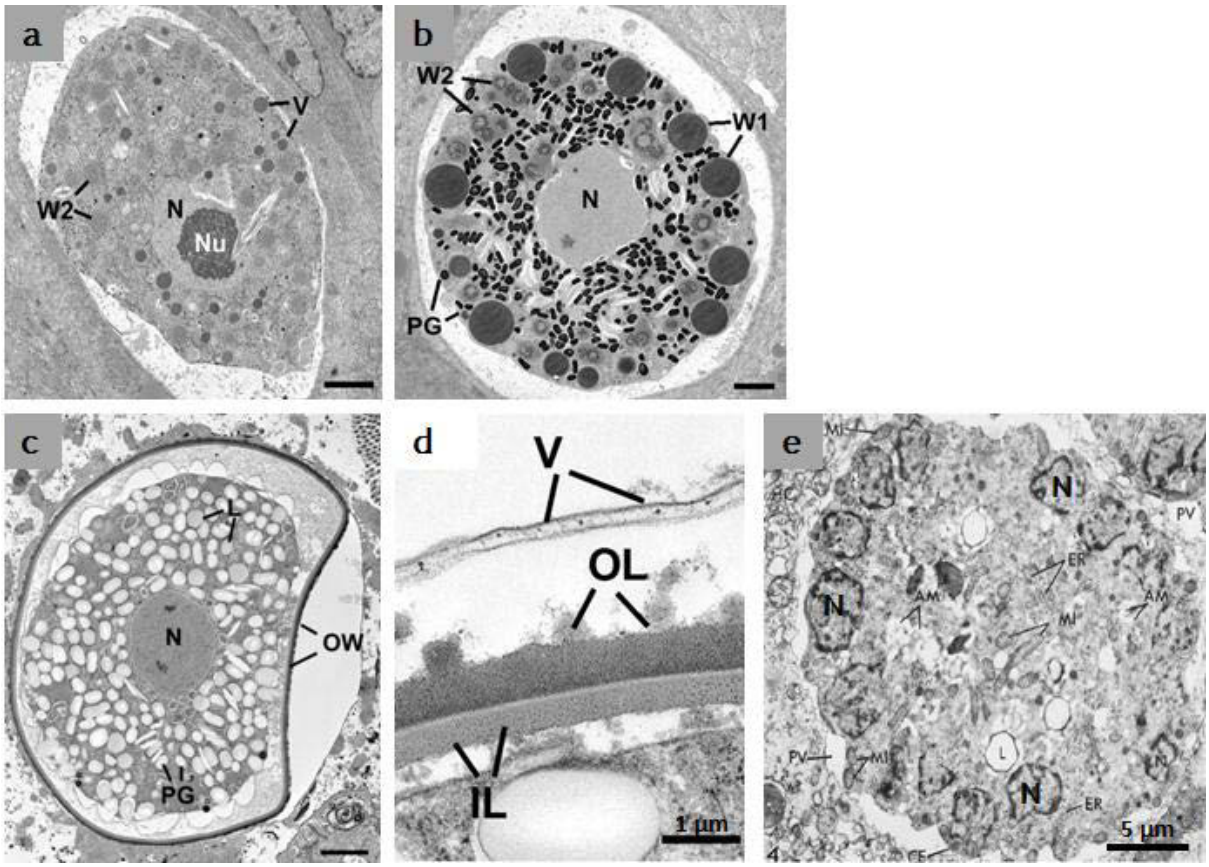

Figure 3: Transmission electron microscopy of developing macro- (female) and micro- (male) gametocytes. (a) Early macrogametocyte with a large centrally located nucleus (N) and nucleolus (Nu). The cytoplasm contains veil forming bodies (VFBs) and areas of dilated rough endoplasmic reticulum designated as early wall forming bodies type 1 (WFB2s). (b) A mature macrogametocyte showing the central nucleus and a number of large peripherally located wall forming bodies type 1 (WFB1) inter-mixed with donut-shaped WFB2. The cytoplasm contains a large number of electron dense polysaccharide granules (PG). (c) Fully formed oocyst showing the outer oocyst wall. The cytoplasm contains polysaccharide granules (PG) and lipid droplets (L) of less than 200 nm in diameter. (d) A cross-section of the oocyst wall showing the loose outermost veil (V), the thick electron dense outer layer (OL) and thin electron lucent inner layer (IL). (e) A mature microgametocyte with numerous peripherally located nuclei (N). Bar is 5 µm. (Ferguson et al., 2003; Mehlhorn, 1971).

2.3 Biogenesis of the oocyst wall

Early electron microscopic studies of macrogametogenesis in *E. maxima* and related parasites have provided evidence for the role of WFB1s and WFB2s in oocyst wall biosynthesis (Ferguson et al., 2003; Ferguson et al., 1977b, 1978b; Mehlhorn, 1971; Pittilo and Ball, 1980; Ryley et al., 1972). The common belief is that following the fertilization of macrogametes by microgametes, the macrogametocyte differentiates into a zygote (young oocyst). The veil forming bodies (VFBs) migrate to the parasite's periphery giving rise to the outermost layer, the veil (Figure 3, panel d, V). The WFBs, situated in the peripheral cytoplasm of the zygote, align beneath the limiting membrane to release the material stored in the WFBs to form the bi-layered oocyst (Figure 3, panels b) (Mehlhorn, 1971; Pittilo and Ball, 1980). During this process, the WFB1s undergo disaggregation to release their contents. The released material becomes fused together to form the membrane bound layer at the periphery of the parasite (Figure 3, panel c-d, OL). This process initially coordinates the formation of an irregular thick outer layer (0.7 μm), which later becomes thinner and smoother through unknown molecular changes (Figure 3, panel d). At this stage, the WFB1s can no longer be seen since they were utilized in the process. Following outer layer formation, the WFB2s assume peripheral position and aggregate into islands of amorphous material with loss of their typical donut-shaped structure, to form the inner layer of the oocyst wall 0.2 μm in thickness (Figure 3, panel d, IL). Following the formation of the oocyst wall, the WFBs can no longer be seen in the young zygote. The oocyst remains enclosed within the parasitophorous vacuole until the complete formation of the multi-layered oocyst. After 164 h p.i., fully formed bi-layered oocysts are then excreted with the faeces contaminating the food and water.

Recently, Ferguson *et al*. (2003) studied oocyst wall formation by *in situ* immuno-histology and immuno-electron microscopy with antibodies specific to WFBs, and provided further evidence to support the mechanisms proposed by Mehlhorn *et al.* (1971) and Pittilo and Ball (1980). The antibodies raised to the WFB-specific proteins Gam56 and Gam82, and to an affinity purified gametocyte antigen preparation (APGA), which contains both of these antigens along with Gam230, are the best characterised gametocyte proteins to date (Ferguson et al., 2003). Antibodies to these proteins localize

either to WFB2s and the inner wall only, as is the case for Gam56, Gam82 and Gam230, or to both WFBs and both layers of
the oocyst wall, as seen for APGA (Wallach et al., 1989) (Figure 4a-c, green fluorescence). Ferguson *et al.* (2003) used these antibodies as markers to follow the secretion of the contents stored in the VFBs and WFBs during macrogamete maturation. These studies have demonstrated that the organization of the oocyst wall requires a co-ordinated synthesis and release of the VFBs and WFBs controlled at the level of the rER and Golgi complex (Figure 4, panels a-c, green fluorescence). Based on these findings it has been proposed (Belli et al., 2006; Ferguson et al., 2003) that following fertilization of the macrogametocytes, the parasite receives an (undefined) signal that initiates wall formation and stimulates the WFB1 migration to the periphery of the macrogametocyte and synchronous disaggregation of their contents (Figure 4, b-c). The released material undergoes further molecular modifications to form a membrane bound outer layer at the periphery of the cell (Figure 4, d). After the release of the WFB1-contents, the WFB2 material retained in the rER is transferred via the Golgi body to the periphery of the parasite where it is released to form the inner oocyst layer (Figure 4, a-d, fluorescing "donut-shaped" structures), thus completing oocyst wall formation prior to excretion from the host.

Studies involving antigenicity of the major *E. maxima* gametocyte proteins in mice, rabbits and chickens have shown that the Gam56, Gam82 and Gam230 are highly antigenic (Fried et al., 1992; Pugatsch et al., 1989; Wallach, 1997; Wallach et al., 1992; Wallach et al., 1990; Wallach et al., 1995a; Wallach et al., 2008; Wallach et al., 1989). The affinity purified Gam56 and Gam82 (APGA) antigens were used to immunise breeder hens and found to stimulate the production of large amount of protective IgG antibodies. The maternally derived antibodies are transferred to the offspring via the egg yolk, and provide protection for newborn chicks (Smith et al., 1994a; Smith et al., 1994b; Wallach et al., 1994; Wallach et al., 1995b). This concept is the basis for transmission blocking immunity of the subunit vaccine, CoxAbic®, which induces maternal antibodies that retard the processing of gametocyte wall forming glycoproteins, cross-linking of the peptides or wall hardening of the oocyst. However, further experimentation is needed to elucidate the mechanism(s) by which these antibodies interfere with oocyst wall formation. A number of studies in this area have

led to ground breaking discoveries regarding the biochemical nature of the oocyst wall and the molecular machinery involved in oocyst wall assembly.

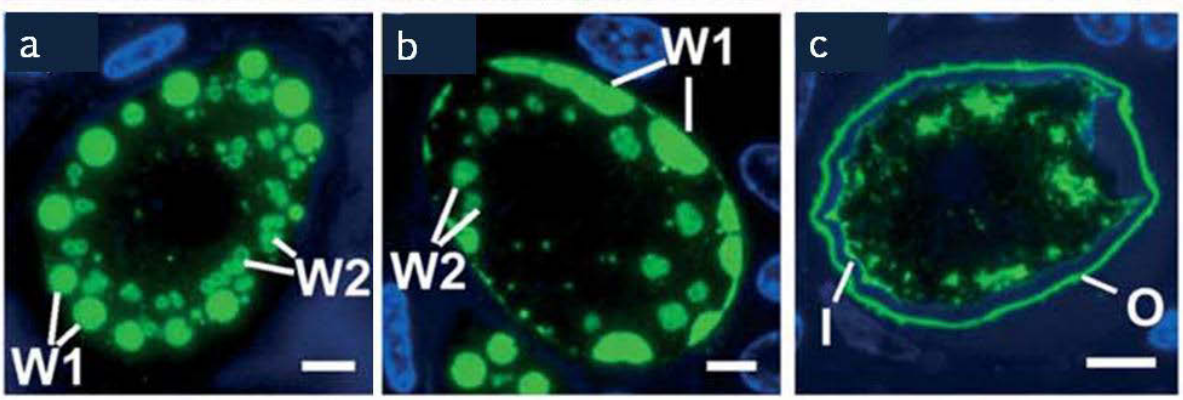

Figure 4: Structural development of the oocyst wall in *E. maxima.* The developing zygote was immuno-labelled with anti-APGA and visualised with fluorescein isothiocyanate (FITC). (a) Mature macrogametocyte with large type 1 WFBs (W1) and donut-shaped type 2 WFBs (W2) dispersed in the cytoplasm. (b-c) Type 1 WFBs disaggregate and fuse to form the outer oocyst layer (O), donut-shaped type 2 WFBs contents fuses to form the inner oocyst layer (I). Bar is 5 µm (Ferguson et al., 2003).

2.4 Biochemical composition of the oocyst wall and molecular basis of inner oocyst wall formation

Due to the lack of a good culture system for the gametocyte stages of *Eimeria*, studies on the molecular mechanisms involved in macrogametocyte development and oocyst wall formation have been limited. Despite the technical challenges, studies involving SDS-PAGE, immunoblotting, immunofluorescence and biochemical analysis of the oocyst wall proteins, provided valuable insights into the molecular mechanisms involved in inner oocyst wall formation (Belli et al., 2003a; Ferguson et al., 2003; Mai et al., 2009; Mouafo et al., 2002). The genes encoding gam56 and gam82 have been fully cloned and sequenced, and a partial sequence is available for gam230 (Belli et al., 2003b; Belli et al., 2002b; Fried et al., 1992). *Mai et al.,* (2009) investigated the biochemical composition of the sporulated and unsporulated oocyst walls of *E. tenella* and *E. maxima* that may contribute to its formation and resilience. The oocyst wall was shown to be predominantly composed of proteins (>90%), a small amount of

carbohydrate (0.3-2.0%) and lipid (1.4-7.6%). SDS-PAGE analysis and western blots of the *E. maxima* oocyst wall identified a number of tyrosine-rich, highly hydrophobic small molecular weight glycoproteins (Belli et al., 2002a). N-terminal amino acid sequences revealed that these small molecular weight oocyst wall proteins are derived from larger precursor proteins, namely Gam56 and Gam82, found in the WFB2 of *E. maxima* macrogametocytes (Figure 5, A). A closer analysis of the gametocyte proteins (gam56 and gam82) showed that the proteins underwent N- and C- terminal processing, preserving the tyrosine-rich domains of the molecule. The polypeptides are then tyrosine cross-linked, dehydrated and hardened to give rise to the inner wall proteins (Figure 5, b) (Belli et al., 2006; Belli et al., 2003a; Belli et al., 2003b; Belli et al., 2002b; Wallach, 2010). The tyrosine rich proteins have been identified in oocyst walls of other *Eimeria spp*. (Eschenbacher et al., 1996; Fried et al., 1992; Krucken et al., 2008; Mai et al., 2009; Mouafo et al., 2002; Stotish et al., 1978), as well as the closely related parasite *Toxoplasma spp.* (Fritz et al., 2012a; Fritz et al., 2012b), further providing the evidence supporting the role of tyrosine in oocyst wall formation most likely through the formation of dityrosine-protein bonds.

Based on the detection of dityrosine in *E. maxima*, as well as 3,4-dihydroxyphenylalanine (DOPA), a derivative of tyrosine, by high performance liquid chromatography and UV detectors (Belli et al., 2003a), stemmed the hypothesis of quinone tanning as the molecular mechanism driving oocyst wall biogenesis. According to Belli et al., (2006) "quinone tanning is a mechanism of sclerotization involving the modification of tyrosine residues of structural proteins. It involves the conversion of soft proteinaceous material to a hard resistant structure" (Belli et al., 2006). The model hypothesises that large tyrosine-rich protein precursors (Gam56 and Gam82) are synthesised by the macrogametocytes and stockpiled in the WFB2s (Figure 5, A). An unknown stimulus initiates their processing into smaller, tyrosine–rich proteins (Figure 5, B). Recently, studies focusing on enzymes that may be involved in processing of the precursor proteins have shown that six protease genes were specifically expressed or upregulated in gametocytes of *E. tenella* (Katrib et al., 2012). Based on the finding that serine protease inhibitors prevented processing of EtGam56, it was concluded that these subtilisin-like proteases play a key role in the formation of the oocyst wall (Figure 5, C). These findings have clearly shown that the molecular machinery required for oocyst

wall formation is enzymatically processed when material stored in the WFB2s is delivered to the periphery of the zygote. In a similar model to that of oocyst wall formation, the model for cuticle formation in nematodes hypothesises that collagens are synthesised as proproteins and cleaved at the N-terminus by a subtilisin-like protease prior to cuticle formation (Stepek et al., 2010; Thacker and Rose, 2000; Thacker et al., 2000). The collagens are held together by di- and tri-tyrosine cross-links by the action of dual oxidase (Page and Johnstone, 2007).

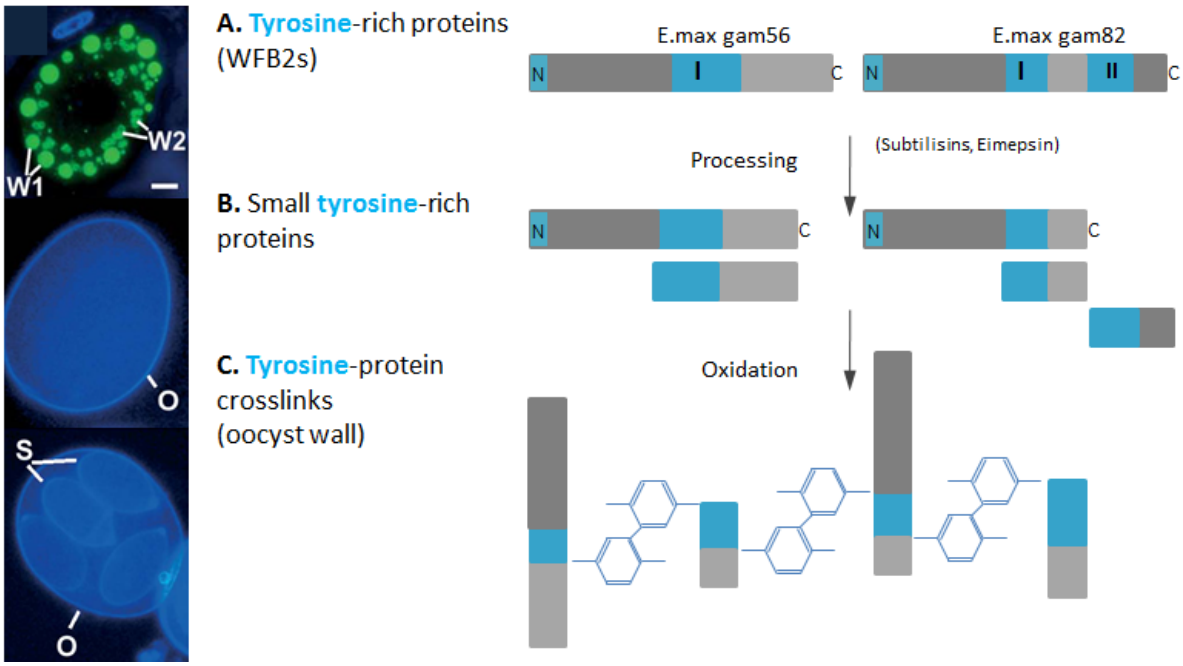

Figure 5: A proposed model for molecular basis of inner oocyst wall formation in *E. maxima*. (A) The precursor proteins, EmGam56 and EmGam82 gametocyte glycoproteins, are synthesised by the macrogametocyte and stored in the donut-shaped WFB2s (W2). (B) During the development, tyrosine rich precursor proteins are processed by proteases into smaller tyrosine-rich subunits, which are subjected to oxidation, dehydration and crosslinking to form the hard oocyst wall (C) (Belli et al., 2006; Katrib et al., 2012).

The quinone-tanned structures are observed throughout the animal kingdom, including egg shells of liver fluke and insect cuticles (Page A.P., 2007; Waite, 1995) and are

implicated in the synthesis of hard, water impermeable structures. Similar to these organisms, the oocyst wall is water impermeable and resistant to proteolytic damage (Ferguson et al., 2003; Ryley et al., 1972), protecting the soft-bodied parasite from the external environment. Such properties explain the difficulty in removing oocysts from poultry houses even when using harsh decontamination procedures.

Dityrosine cross-linked proteins in coccidian parasites are easily visualised by UV light. The inner oocyst walls of *Eimeria* autofluoresce blue when subjected to a wavelength in the range of 330-385 nm (Belli et al., 2006). However, not all oocysts autofluoresce blue indicating that tyrosine cross-linking is not the sole molecular mechanism involved in wall biosynthesis, but additional unidentified molecular mechanisms are at play. Indeed, recent studies examining the process of oocyst wall formation have reported that in addition to tyrosine-rich proteins, oocyst walls of *Eimeria* also contain β-1, 3-glucan (Bushkin et al., 2012), as well as neutral and polar lipids (Bushkin et al., 2013; Frölich et al., 2013; Mai et al., 2009) that also contribute to impermeability and rigidity of the oocyst wall. Interestingly, the EmGam56 and EmGam82 homologues have been identified in the genomes of other coccidia such as *Toxoplasma gondii* (Fritz et al., 2012a; Fritz et al., 2012b). Furthermore, the oocyst walls of *Toxoplasma, Neospora, Sarcocystis, Isospora* and *Cyclospora* autofluoresce blue under UV light (Berlin et al., 1998; Daugschies et al., 2001; Lindquist et al., 2003) further suggesting that they share a common mechanism of oocyst wall formation involving tyrosine crosslinking (Belli et al., 2006; Belli et al., 2003a).

Despite a substantial amount of evidence supporting the proposed model of inner oocyst wall formation, a great deal remains to be elucidated about the sexual stages of *Eimeria.* Very little is known about the morphological appearance of the isolated *Eimeria* gametocytes, the biochemical composition of macrogametocyte WFB1s and the molecular mechanisms driving outer oocyst wall formation. An understanding of these processes may provide additional information on parasite developmental biology and new potential drug and vaccine targets for the control of coccidiosis caused by cyst-forming Apicomplexans.

2.5 Aims and approaches of this project

This project aimed to:

1. Characterize the subcellular localisation and spatial organization of the WFBs at various stages of parasite development in isolated gametocytes using wide-field and fluorescent microscopy;

2. Characterize the molecular mechanisms of outer oocyst wall formation;

3. Develop a method for the isolation of gametocyte WFBs in order to analyse their molecular make up;

4. Gain insights into the nature and mechanisms of nutrient acquisition in developing *E. maxima* macrogametocytes *in vitro;*

5. Determine if anti-gametocyte antibodies have the ability to gain access to an intracellular parasite *in vivo*.

In order to address the listed objectives *E. maxima* was used as a model cyst-forming organism since it is relatively easily visualised microscopically and extraction of relatively large quantities of gametocyte stages is feasible. The parasitology group at the iThree Institute (UTS) have worked to develop a method for extracting and purifying WFBs from *E. maxima* gametocytes, which was adapted and modified from subcellular fractionation and organelle purification of micronemes from *E. tenella* sporozoites (Tomley, 1997). However, further experimentation is required to first isolate the WFBs in large quantities and then to purify WFBs to a level required for accurate biochemical and proteomic analysis.

To gain an understanding of gametocyte development and differentiation at the morphological and molecular level, Australorp cockerels will be infected with *E. maxima*, and samples will be extracted from infected intestine at 134 hrs post infection (p.i.) to isolate sexual stage parasites (macro- an microgametocytes). The harvesting of

E. maxima gametocytes will be carried out according to a protocol developed by Wallach et al., (1989). It involves the addition of hyaluronidase III enzyme and subsequent filtration through a defined pore-sized polymon filters, which is a very fast and efficient way to release the gametocytes from surrounding host material (Wallach et al., 1990). The type and quality of isolated gametocytes will be assessed by comparison to *in situ* stained infected tissue sections (Figure 5).

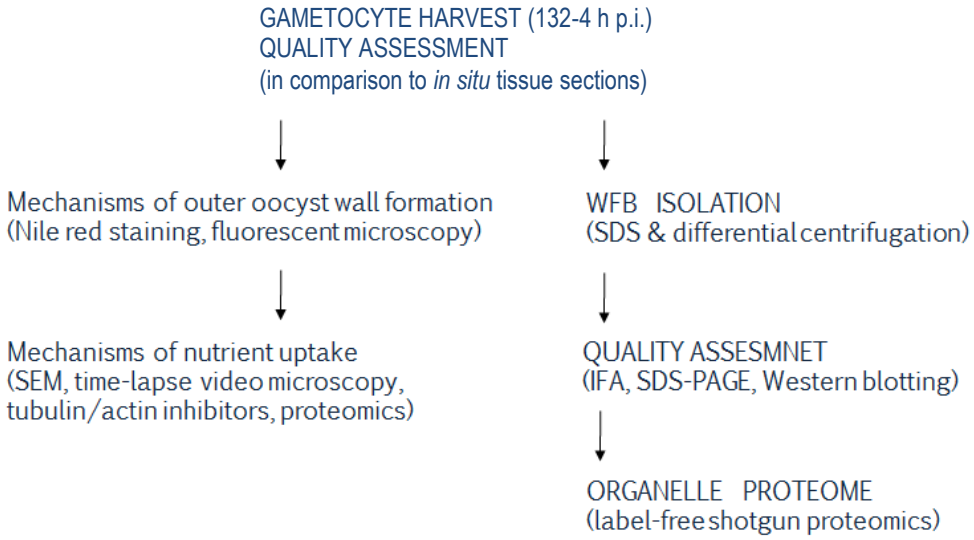

Figure 6: Experimental plan outlining the steps involved in isolation of the wall forming bodies and protein analysis.

The detection of WFBs currently relies on immunofluorescence analysis using gametocyte specific antibodies. Although effective, this method is time consuming. A simple, rapid method to assess the presence of wall forming bodies in the isolated gametocytes is therefore needed. Various histological methods, such as Haematoxylin and Eosin (H&E) and Nile red staining, were optimised for rapid routine identification of WFBs, and to evaluate whether or not they are intact within the isolated gametocytes prior to the start of the isolation procedures.

The isolation of the WFBs involved a number of steps. First, gametocytes were disrupted to release all cellular contents. Sonication was employed to disrupt the

gametocytes and release WFBs. Differential centrifugation was then used to enrich for WFBs. Taking into the account that the density of *E. maxima* WFBs is not known, a few rotational centrifugal forces were tested and outcomes analysed. Strong ionic detergent (i.e. sodium dodecyl sulphate) was added to aliquots of high-speed pellets and re-centrifuged to solubilize cell debris leaving WFBs intact. Aliquots of high-speed supernatants and pellets were assessed for the presence of the WFBs by staining, western blotting and immuno-labeling.

SDS-PAGE was used to analyse the proteins found within the isolated WFBs according to their molecular weight. The proteins were visualised using Silver staining and Coomassie Brilliant blue R250 to increase detection sensitivity of proteins present in trace amounts. Western blotting was employed to determine the type and purity of WFBs by using monoclonal (E11-11, E1d8) and polyclonal (anti-APGA) antibodies to discern which type of WFB is isolated using the enrichment methods described above. Once an appropriate sample was available proteomic methods were employed to identify and analyse proteins stored within the isolated WFBs.

The fourth aim is to gain a better understanding of the nature and mechanisms underlying nutrient acquisition in developing *E. maxima* macrogametocytes and oocysts. A study was designed to elucidate the mechanisms of particle uptake and intracellular transport of wall forming bodies mediated by the sexual stage (gametocyte) cytoskeleton and host/parasite endocytotic pathways. This work was carried out *in vitro* by combining SEM and fluorescent confocal microscopy to provide detailed images of the surface of the *Eimeria maxima* infected chicken enterocyte as well as to analyse the uptake of 40 nm and 100 nm beads into the parasite cytoplasm. In addition, biochemical and proteomic strategies were used to analyse the vesicular trafficking proteins and other regulators, and localize them to their subcellular compartments. Data from these studies indicate that gametocytes and early stage oocysts contain surface pores and are capable of actively taking up and internalizing nano beads via endocytosis. Upon incubation with colchicine and cytochalasin D, the ability of developing gametocytes to internalize particles was inhibited. Moreover, there was a dispersion of WFB type 1 material in the parasite cytosol, suggesting a disruption in the cytoskeleton-vesicle signalling pathways. Finally, biochemical and proteomic methods were employed to

identify and analyse vesicular trafficking proteins and other putative regulators of endocytosis and transport. These results indicate that endocytosis is crucial for normal development of the sexual stage parasites and that the molecules involved in this process may be a potential target for the development of novel transmission-blocking drugs.

Chapter Three

Paper II: The spatial organization and extraction of the wall forming bodies of Eimeria maxima

Declaration

I declare that the following publication included in this thesis in lieu of a chapter meets the following criteria:

- More than 50% of the content in the following publication included in this chapter has been planned, executed and prepared for publication by me
- The work presented here has been peer-reviewed and accepted for publication
- I have obtained approval to include the publication in this thesis from the Publisher
- The initial draft of the work has been written by me and any subsequent changes in response to co-authors and editors reviews was performed by me
- The publication is not subject to any obligations or contractual agreements with a third party that would constrain its inclusion in the thesis

Publication title: The spatial organization and extraction of the wall-forming bodies of *Eimeria maxima*

Authors: Sonja Frölich, Michael Johnson, Michelle Robinson, Rolf Entzeroth and Michael Wallach

Candidate's contribution (%): above 50 %

Journal name: Parasitology

Volume/ page numbers: Volume 140, Issue 07, pages 876-887

Status: Published 14 March 2013

I declare that the publication above meets the requirements to be included in the thesis.

Candidate's name: Candidate's signature: Date (dd/mm/yy):

3.1 Brief introduction

Apicomplexan parasites cause some of the world's most debilitating diseases including malaria and toxoplasmosis in humans, babesiosis and theileriosis in cattle and coccidiosis in chickens. In the case of the *Plasmodium* parasite, malaria is still one of the world's biggest killers leading to the death in 2010 of more than half a million people, most of these deaths occurring in young African children (WHO, 2012). *Eimeria*, the causative agent of coccidiosis in chickens and other animals, has had a major economic impact on the meat industry and, in spite of 70 years of drug development, is still difficult to control. Most of these parasites undergo complex life cycles going through both asexual and sexual stages of development, leading to the production of oocysts that act to transmit the parasite in either an insect vector, as is the case for malaria, or the environment as in the case of Coccidia. Coccidian oocysts remain viable under hostile conditions due to the presence of an oocyst wall; a structure that enables parasite survival while preventing the influx of toxic substances.

A great deal of research has focused on elucidating the structure, biochemical composition and developmental biology of the oocyst wall of *Eimeria* spp. *Eimeria maxima* is an apicomplexan parasite that is 1 of the 3 major species of *Eimeria* that cause coccidiosis in chickens. *In situ* studies using fluorescent microscopy to observe sexual stage development in tissue sections of chicken intestines infected with *E. maxima*, revealed that the 2 types of wall-forming bodies (WFBs), Type 1 and 2 (WFB1s and WFB2s), migrate to the periphery of the parasite, undergo fusion and form the outer and inner layer of the wall respectively (Ferguson et al., 2003; Mehlhorn, 1971; Mehlhorn, 1972; Pittilo and Ball, 1979).

In previous studies it was found that a collection of gametocyte antigens, termed Affinity Purified Gametocyte Antigen (APGA), prepared using a monoclonal antibody to the gametocyte 56 kDa antigen, elicit a protective immune response against parasite transmission. APGA has been used as the basis of a commercial transmission-blocking vaccine against coccidiosis, CoxAbic® (Smith et al., 1994a; Smith et al., 1994b; Smith et al., 1994c; Wallach et al., 1992; Wallach et al., 2008). The 56 and 82 kDa gametocyte antigens contained in APGA and their peptide fragments have been localized to the WFB2, and have been shown to compose the inner layer of the oocyst wall (Belli et al.,

2002a; Ferguson et al., 2003). Furthermore, the genes encoding these antigens have been cloned and sequenced where it was found that they are very rich in the amino acid tyrosine (Belli et al., 2002a; Belli et al., 2003a; Belli et al., 2003b; Belli et al., 2002b; Mai et al., 2009; Mai et al., 2011). Based on the finding that when zygotes and oocysts of *E. maxima* are exposed to UV light they autofluoresce blue, work was carried out in which it was shown that during oocyst wall formation these proteins are processed into smaller peptides, enzymatically cross-linked via the formation of di-tyrosine (the molecule that fluoresces blue) and inserted into the inner oocyst wall.

In spite of all of the above research, little is known about the molecular composition and biosynthesis of the WFB1s and the molecular mechanisms underlying outer oocyst wall formation. In addition, the proteomic analysis of the 2 types of WFBs is still incomplete. Therefore, in the present study confocal and wide-field fluorescent microscopy combined with a variety of staining techniques, were used for the first time to observe in 3 dimensions the subcellular location and spatial organization of the WFBs at various stages of parasite development in isolated and purified gametocytes. In addition, it was shown that extracted WFBs had the same size, shape and staining properties as *in situ* WFBs of macrogametocytes extracted from the *E. maxima*-infected intestine, and contained the expected glycoproteins previously shown to be present in these organelles. This work therefore is the first step in the purification of the WFBs that can then be used for future biochemical and proteomic analysis.

3.2 Materials and Methods

3.2.1 Oocyst, gametocyte and enterocyte production

The Houghton strain of *E. maxima* was originally provided by Dr Martin Shirley (Institute for Animal Health, Compton, Newbury, Berkshire, UK). Oocysts were routinely passaged through 4-week-old chickens (Australorps; S. F. Barter and Sons) and purified as described previously (Belli et al., 2002a). Fresh oocysts were used to infect chickens and macro- and microgametocytes, which after concentration on a 10 μm polymon filter, were then purified from infected intestines 134 h post-infection (h p.i.) as described previously (Pugatsch et al., 1989). The harvested macrogametocytes

were then assessed for the presence of WFBs by cytochemical stains, Western blotting and immunofluorescence microscopy using WFB-specific antibodies, as described below.

For chicken enterocyte preparation, a total of 5 uninfected Australorp cockerels were euthanized at 4 weeks of age and their intestines removed and immediately washed with ice-cold phosphate-buffered saline (PBS, pH 7), slit open and cut into small pieces measuring approximately 1 cm^2. Tissue was then incubated with 0·5 mg mL^{-1} hyaluronidase in PBS (pH 7) and placed in a 41 °C water bath for 30 min. At the end of the incubation period the intestines were filtered through cheesecloth and the material retained on the cheesecloth was discarded and the flowthrough, containing the enterocytes, was filtered through a 10 μm polymon filter (Sefar Filter Specialist Pty Ltd). The enterocytes, which pass through the filter, were collected and washed 3 times by centrifugation at 1000 ***g*** for 10 min. The enterocytes were then examined microscopically and diluted to 2×10^6 mL^{-1} and stored at −20 °C until needed. Staining with haematoxylin and eosin (H&E) was performed to check the quality of the harvested cells.

3.2.2 Live cell imaging of harvested *E. maxima* gametocytes

Freshly harvested gametocytes re-suspended in 200 μL of TNEP buffer (10 mM Tris-HCl, pH 7·4, 50 mM NaCl, 2 mM EDTA) were placed on 0·1% (v/v) poly-L-lysine-coated glass microscope slides before imaging in a microscope heated chamber warmed to 37 °C. Images were captured with a high-speed charge-coupled device (CCD) camera using the NIS-Elements acquisition software mounted on a Nikon Ti inverted microscope equipped with 60× oil objective lens (Plan Apo NA 1.4 aperture) and the Perfect Focus System™ for continuous maintenance of focus. Blue autofluorescence was monitored with a bandpass excitation/emission filter (330–385/435–485 nm). Time-lapse images were collected every 30 min over a 17 h period. Exposure time and brightness/contrast settings were kept constant for each using the NIS Elements acquisition software.

3.2.3 Tissue processing and H&E staining of *in situ* and isolated gametocytes

Portions of the small intestine containing *E. maxima* gametocytes were fixed in 10% neutral buffered formalin (pH 7). Fixed tissues were embedded in paraffin, 5 μm thick sections were cut and stained with H&E at the Histopathology Laboratory (Faculty of Veterinary Science, University of Sydney, New South Wales, Australia). Colour images were acquired with the Olympus BX51 upright epifluorescence microscope equipped with a DP70 Charged Couple Device (CCD) Microscope Camera.

Freshly harvested gametocytes were placed on glass slides pre-coated with 0·1% poly-L-lysine (Sigma) for 30 min, at room temperature. The unbound material was washed off and the slides air-dried and fixed in 95% ice-cold methanol for 5 s or left unfixed, and the organelle composition of preparations was determined by staining with H&E, nile red and oil red O, or alternatively, probed with antibodies as described below.

H&E staining was carried out on unfixed parasites using a modified staining protocol. Briefly, the samples were soaked in Harris haematoxylin for 1 min; rinsed in tap water; treated with 1% acid alcohol, and then rinsed again with tap water for 10 s. The samples were then soaked in Scott's water for 1 min; rinsed; treated with 1% alcoholic eosin for 1 min, and de-stained twice in 95% ethanol for 30 s. Samples were dehydrated in 100% ethanol for 1 min, and submerged in xylene; 2 changes at 2 min intervals. Once dehydrated, the samples were mounted under cover slips in D.P.X. mounting medium and visualized under bright field using an Olympus BX51 upright microscope with 100× objective.

3.2.4 Indirect immunofluorescence analysis

Gametocytes and extracted WFBs were fixed for 5 min at room temperature in 95% ice-cold methanol, permeabilized in 0·1% TWEEN20/PBS and non-specific staining was blocked with 2% BSA in PBS for 1 h, at room temperature. The harvested gametocytes were then incubated with either a mouse monoclonal anti-WFB1 antibody E1D8, raised against an antigen in the WFB1 of *E. tenella* gametocytes (Mouafo et al., 2002), or incubated with a mouse monoclonal anti-WFB2 antibody (1 : 200 dilution) raised

against *E. maxima* gametocyte glycoprotein EmGAM56 (Fried et al., 1992) and counterstained with diamidino-2-phenylindole (DAPI). Primary antibodies were detected with Alexa Fluor 488 – conjugated goat anti-mouse IgM (1 : 500 dilution, Invitrogen, Australia). Normal chicken and mouse sera, or isotype-matched purified mouse myeloma IgM, kappa antibody (Sigma), were used as a negative control. Localization of bound antibodies was visualized with an Olympus BX51 upright epifluorescence microscope with a bandpass excitation/emission filter (470–490/510–550 nm). Multinucleated microgametes stained with DAPI were examined with a Nikon A1 Confocal Scanning Laser Microscope equipped with a 100× oil immersion objective lens (N.A. 1.4) and a violet laser (405/425–475 nm). The three-dimensional volumes of blue fluorescing microgametes were then deconvolved using AutoQuant deconvolution software (7.5.1 Bitplane, Zürich, Switzerland) and displayed as maximum z-projections.

3.2.5 Labelling of *E. maxima* gametocytes with nile red and oil red O

The lipid content of the WFBs was examined by nile red staining according to the method of Greenspan *et al*. (Greenspan et al., 1984, 1985). For the detection of both brilliant yellow gold fluorescence typical of neutral lipids (cholesterol and triglycerides), and red fluorescence characteristic of glycoproteins, phospholipids, amphipathic lipids and strongly hydrophobic membrane proteins, cells were examined with an Olympus BX51 upright microscope (Olympus, Australia) using 100× oil immersion objective (N.A. 1.3) and a DP70 colour CCD camera (Olympus Australia Pty Ltd). Nile red-stained red and yellow emission was observed with 460–490 nm excitation and 510 nm long-pass emission filters. In order to achieve a three-dimensional visualization the subcellular location and distribution of lipids/glycoproteins in the membranes/walls surrounding the developing zygotes/oocysts, a Nikon A1 Confocal Scanning Laser Microscope equipped with a 100× oil immersion objective lens (N.A. 1.4) was employed. Cells stained with nile red were excited with the 488 nm laser and yellow and red emissions were observed with 525/50 nm and 595/50 nm emission filters, respectively. To acquire three-dimensional volumes, 106-z serial optical sections were collected with a step size of 0·2 μm, using NIS Elements software (Nikon). Images were deconvolved using AutoQuant blind

deconvolution software (7.5.1 Bitplane, Zürich, Switzerland) and displayed as maximum z-projections.

Oil red O staining was performed as described previously (Pittenger et al., 1999). Briefly, harvested gametocytes were covered with 60% isopropanol in PBS (pH 7) for 2–5 min at room temperature. Isopropanol was poured off and 20 μL of oil red O dye was added to each sample for 5 min. After incubation, slides were washed in distilled water for 5 min, and counter-stained in Mayer's Haematoxylin and mounted in D.P.X. (Fronine, Australia) prior to visualization under bright field, as described above.

3.2.6 Extraction of gametocyte WFBs

Purified *E. maxima* gametocytes (2×10^6 cells mL^{-1}) were re-suspended in TNEP (10 mM Tris-HCl, pH 7·4, 50 mM NaCl, 2 mM EDTA) buffer and mechanically disrupted by sonication (Vibra Cell Sonicator) using a 2-mm microtip and a wave amplitude of 2·5 W for consecutive 10-s intervals over 0.5 min. To remove released RNA, DNAse-free RNAse A (Sigma) was added to the lysate at a final concentration of 10 μg mL^{-1}, according to the manufacturer's instructions. The sonicate was then centrifuged at 15 000 ***g*** for 10 min and the pellet was re-suspended in 1% sodium-dodecyl-sulphate (w/v) to separate the insoluble material from solubilized debris. The detergent supernatant was then passed through a 1000 kDa cut-off filter (MWCO, VivaSpin) and washed three times in TNEP (pH 7·4) by centrifugation (15 000 ***g*** for 5 min). Fractions were collected and the protein content of each fraction was estimated using the bicinchoninic protein assay (Pierce), according to the manufacturer's instructions and using bovine serum albumin as a standard. All enriched fractions were assessed for the presence of WFBs by cytochemical stains, immunofluorescence microscopy and Western blotting using WFB-specific antibodies.

3.2.7 SDS–PAGE and immunoblotting

The proteins from gametocyte lysates, enriched fractions and host cells were separated by size as described previously (Belli et al., 2002a). Laemmli sample buffer was added

to all fractions prior to boiling for 10 min at 95 °C. Samples were then centrifuged at 12 000 ***g*** for 5 min, at room temperature to remove insoluble and aggregated matter prior to SDS–PAGE on NuPAGE® Novex 4–12% Bis-Tris gradient gels (Invitrogen). Total protein (4 μg) loaded per lane was determined by bicinchoninic protein assay (Pierce). The proteins were then visualized by staining with silver or, alternatively, transferred to polyvinylidene difluoride (PVDF, Pall Corporation) membranes and incubated with mouse anti-1E11–11 monoclonal antibody or anti-APGA at a 1 : 1000 dilution (Wallach et al., 1990), or normal serum (1 : 1000). PVDF membranes were then incubated with alkaline-phosphatase conjugated rabbit anti-mouse IgM or anti-chicken IgG (1 : 1000; Sigma) and developed with 5-bromo-4-chloro-3-indolyl-phosphate/nitro blue tetrazolium (SIGMA *FAST* ™ BCI/NBT, Sigma) according to the manufacturer's instructions.

3.3 Results

3.3.1 *E. maxima* macrogametocytes continue to develop *in vitro* and contain intact WFB*s*

To visualize autofluorescence in isolated macrogametocytes, time-lapse video microscopy of developing parasites was used to observe UV-excited fluorescence. Sporulated oocysts, which were used as an internal control for autofluorescence, were added to the gametocyte sample. During the 17-h time-period, the isolated macrogametocytes increased in autofluorescence while, simultaneously, the WFBs became detectable at the periphery of the parasite (Figure 7) whilst the sporulated oocyst wall showed no increase in fluorescent intensity. These results indicated that macrogametocyte maturation continues even after *E. maxima* macrogametocytes are removed from the infected intestine.

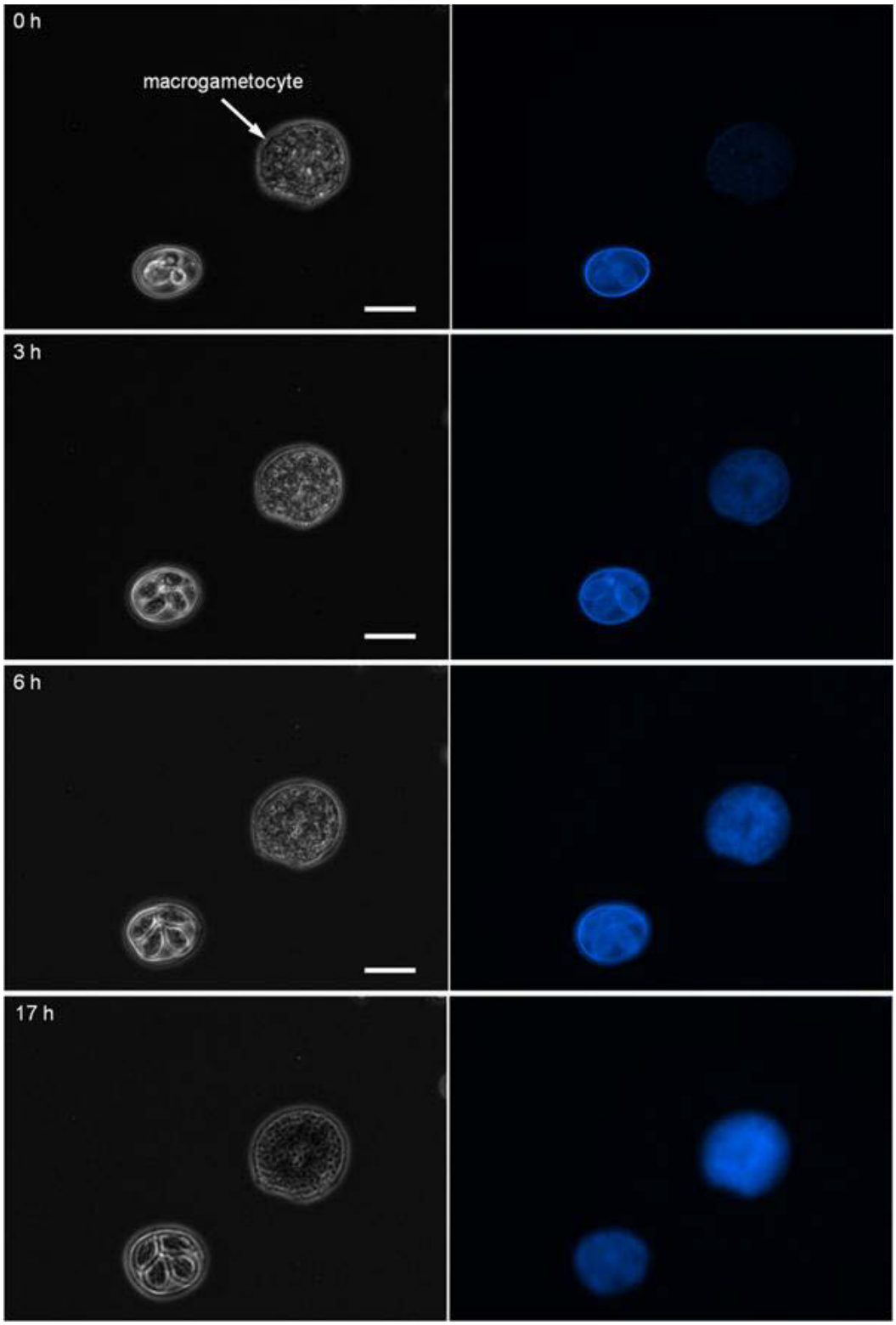

Figure 7: Time-lapse live cell imaging of freshly harvested *Eimeria maxima* macrogametocytes. The maturation of freshly isolated macrogametocytes is revealed by an increase in autofluorescence over a 17 h period. Sporulated oocysts were used as a reference for autofluorescence. In each series, the images on the left-hand side represent the phase-contrast micrographs and the images on the right-hand side show autofluorescence at 330–385 nm excitation wavelength. Bar = 20 μm.

To visualize the WFBs and gain further insights into oocyst wall formation, macrogametocytes at various stages of maturation were examined by H&E staining. Microscopic analysis of gametocytes purified 134 h post-infection from the infected intestine revealed that all stages of sexual development are present (Figure 8,_A–K), consistent with previous reports that 134 h is the peak time-point for gametocyte production (Ferguson et al., 2003). The early macrogametocytes, which were identified by their single centrally located nucleus, appeared to contain a number of eosinophilic bodies of approximately 0·5 to 1 μm in diameter (Figure 8, A and B, arrows). These eosinophilic bodies appeared to extend outward from the nucleus and were therefore identified as early macrogametocyte WFBs. In addition, numerous basophilic granules appeared dispersed in the cytoplasm of an early macrogametocyte (Figure 8, A and B, arrowheads). These granules reached a diameter of $0{\cdot}4 \pm 0{\cdot}1$ μm and, based on their appearance and distribution, were identified as veil-forming bodies (VFBs) (Figure 8, A and B, arrowheads). At this stage, using the H&E dye it was not possible to detect the 'doughnut-shaped' granules, characteristic of the WFB2s in the cytoplasm of the isolated macrogametocytes. However, mature macrogametocytes, which were larger in size, possessed large WFB1s, which appeared in the peripheral cytoplasm with narrow bridges linking them together into chains (Figure 8, C and D). These WFB1s reached a maximum 2·5 μm in diameter and appeared to be coated by a membranous basophilic structure and were cross-linked via eosinophilic 'bridges' extending laterally from each organelle (Figure 7, D). In some specimens, we observed the coalescence of the WFB1s to form the thick eosinophilic outer oocyst wall (Figure 8, E and F). In newly formed oocysts, the thin basophilic layer, presumably the inner layer of the oocyst wall was detected directly underneath the thick outer oocyst wall (Figure 8, G and H).

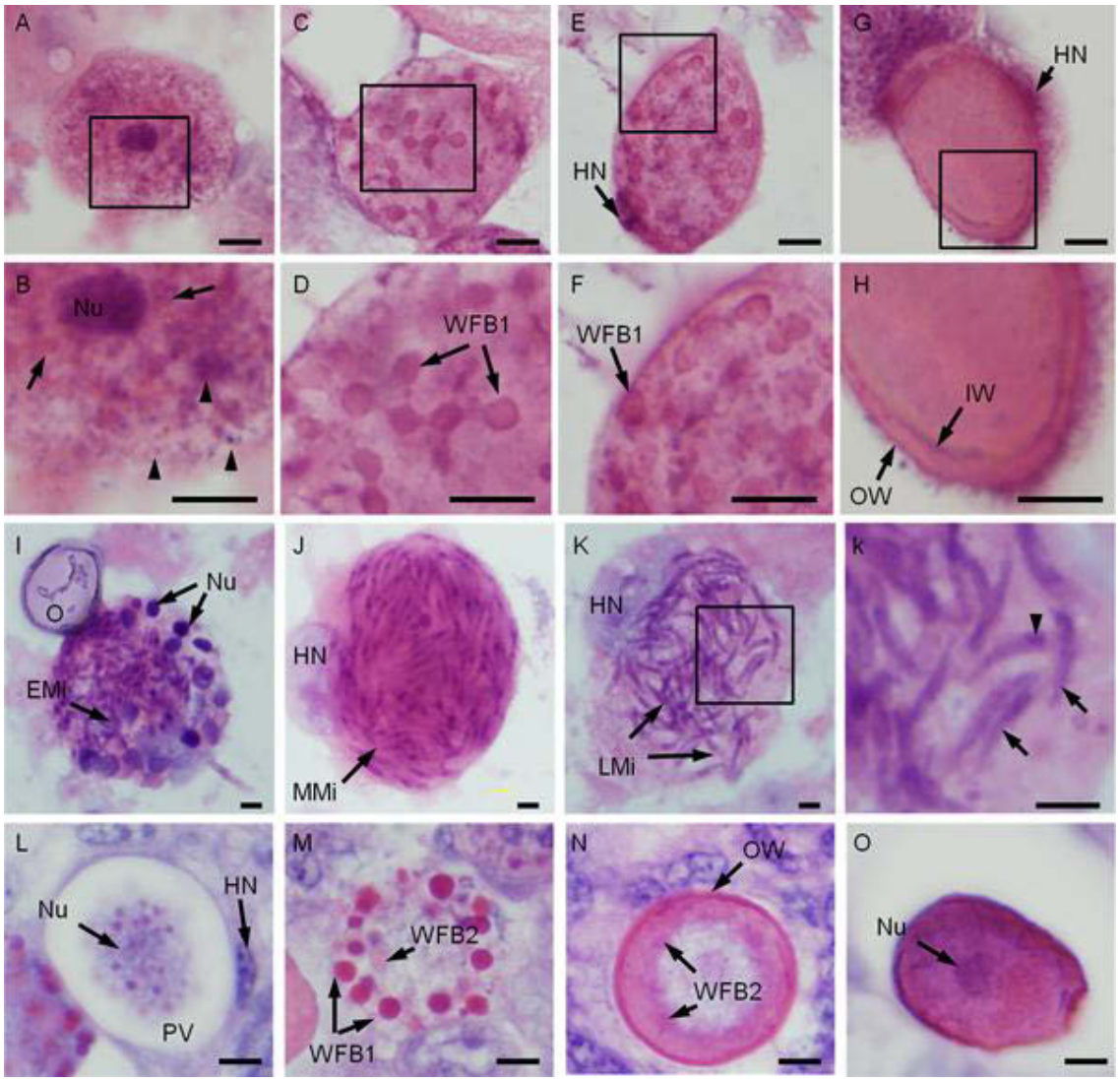

Figure 8: Light microscopy of freshly harvested (A–K) and *in situ* (L–O) macro- and micro-gametocytes stained with H&E. (A) An early harvested macrogametocyte showing a single basophilic centrally located nucleus with eosinophilic and basophilic bodies dispersed in the cytoplasm. (B) Detail of a part of the isolated macrogametocyte showing eosinophilic granules (arrows), presumably early WFBs concentrically arranged around the nucleus (Nu). Note the presence of numerous basophilic bodies, resembling the VFBs (arrowheads). (C) A mature isolated macrogametocyte showing large Type 1 WFBs (WFB1) arranged into necklace-like structures in the peripheral cytoplasm. (D) Enlargement of the section shown in (C), illustrating the membrane surrounding the WFB Type 1 organelles (arrows) and their arrangement into 'bunch of grapes' with narrow bridges linking them together. (E, F) A forming oocyst showing large WFB1s (arrows) fusing with the parasite's limiting membrane. (G, H) A newly formed oocyst showing 3 distinct layers, including a basophilic loose outermost layer, presumably the veil, a thick eosinophilic outer oocyst wall (OW) and a thin basophilic inner layer (IW). (I–K) Microgametocytes isolated 134 h p.i. at various stages of maturation revealed with H&E stain. (I) An early microgametocyte showing peripheral basophilic nuclei (Nu) approximately 7 μm in diameter and a number of undifferentiated early microgametes (EMi). An oocyst (O) attached to the surface of a microgametocyte. (J) A mature microgametocyte with fully formed microgametes

(MMi), each reaching 5–7 μm in length and containing a small basophilic nucleus. Note the swollen host nucleus protruding from the host cell. (K-k) A late-stage microgametocyte (LMi), showing protrusion of fully formed microgametes into the exterior (arrows). Mature microgametes appear comma-shaped, each containing a posterior basophilic nucleus (k). (L–O) Macrogametocytogenesis of *Eimeria maxima* in tissue sections of infected chicken intestine. (L) An early *in situ* macrogametocyte situated in the parasitophorous vacuole (PV) showing a basophilic nucleus (Nu) and a number of small eosinophilic early WFBs. (M) A mature macrogametocyte showing large, membrane-bound eosinophilic WFB1s in the peripheral cytoplasm and eosinophilic masses, the aggregated WFB2s. (N) An early oocyst showing a number of coalescing WFB2s (arrows) underneath the outer OW. (O) Formed oocyst. Bar corresponds to 5 μm. Abbreviations: HN, host nucleus; Emi, early microgametocyte; Mi, microgametocyte; MMi, mature microgametocyte; LMi, late microgametocyte; Nu, nucleus; O, oocyst; OW, outer oocyst wall; PV, parasitophorous vacuole; WFB1, Type 1 wall-forming bodies; WFB2, Type 2 wall-forming bodies.

In addition to macrogametocytes, a few microgametocytes at various stages of maturation were also observed. The early to mid-stage microgametocytes were identified as they lack WFBs, and instead were found to contain a number of large, basophilic peripherally located nuclei, typically 7 μm in diameter (Figure 8, I). Dark-stained granules, which concentrated at the periphery of these nuclei, were identified as chromatin. At this stage, the individual microgametes were barely detectable while in later stages of microgametocytogenesis large numbers of microgametes occupied a single host cell with the host nucleus swollen and pushed to the periphery (Figure 8, J). Microgametes, 5 to 7 μm in length, appeared comma-shaped and contained a small, posterior basophilic nucleus (Figure 8, K-k). Finally, in isolated microgametocytes we observed fully formed microgametes that protruded into the parasitophorous vacuole and were detached from the host cell (Figure 8, K-k).

To further demonstrate that the WFBs observed in isolated gametocytes were intact, a comparison was made with WFBs seen in stained tissue sections (Figure 8, L–O). Serial thin sections of H&E-stained *in situ* macrogametocytes revealed a similar size, shape and distribution of WFBs to those seen in isolated gametocytes (Figure 8, A–H). The early gametocytes in tissue sections contained a single centrally located nucleus with distinguishable eosinophilic early WFBs arranged around it. Once again, it was difficult to discern Type 2 from Type 1 WFBs at this stage of macrogametocyte maturation (Figure 8, L). In contrast, the mature macrogametocytes contained 2 distinct populations

of WFBs situated in the peripheral cytoplasm (Figure 8, M). The large, membrane-bound eosinophilic WFB1s were seen in the peripheral cytoplasm of the mature macrogametocyte, whereas the smaller eosinophilic WFB2s appeared aggregated, forming amorphous eosinophilic masses. Similar to WFB1s of isolated gametocytes, the membrane-bound WFB1s in tissue sections were situated near the parasite's surface, occasionally fused with the parasite's limiting membrane to form the thick, outer oocyst layer (Figure 8, N). The amorphous WFB2s aggregated into eosinophilic masses that formed the inner oocyst layer (Figure 8, N and O), consistent with a previous publication (Mehlhorn, 1971).

To more specifically assess the presence of antigenic glycoproteins in the gametocyte WFBs, harvested gametocytes and/or zygotes were analysed by immunofluorescent microscopy. Monoclonal antibody 1E11-11, raised against the EmGAM56 glycoprotein localized to the 'doughnut-shaped' WFB2s dispersed in the cytoplasm of an early macrogametocyte (Figure 9, A and B), and the inner wall of the forming oocyst (Figure 8, C), consistent with a previous report (Ferguson *et al*. 2003). No reaction was detected when control serum was used (Figure 9, D). The WFB1s were detected with the monoclonal antibody, E1D8, that is specific to an antigen found in the WFB1s of *E. tenella* (Mouafo et al., 2002). This antibody reacted to the WFB1s of macrogametocytes (Figure 9, E), and material deposited on the parasite's surface (Figure 9, F), in agreement with a previous report (Frölich et al., 2012). Interestingly, E1D8 also bound to material within the zygote's cytoplasm even after the outer wall was clearly visible (Figure 9, F, double arrows). No reaction was detected when isotype-matched purified mouse myeloma IgM, kappa antibody (Sigma) was used as a control (Figure 9, G). In addition, DAPI staining revealed a number of multi-nucleated, large microgametocytes (Figure 9, H). Taken together, these results indicate that the isolated macrogametocytes were not harmed during isolation from the infected chicken intestine, both in terms of morphology, as well as in terms of the molecular and antigenic composition of the WFBs.

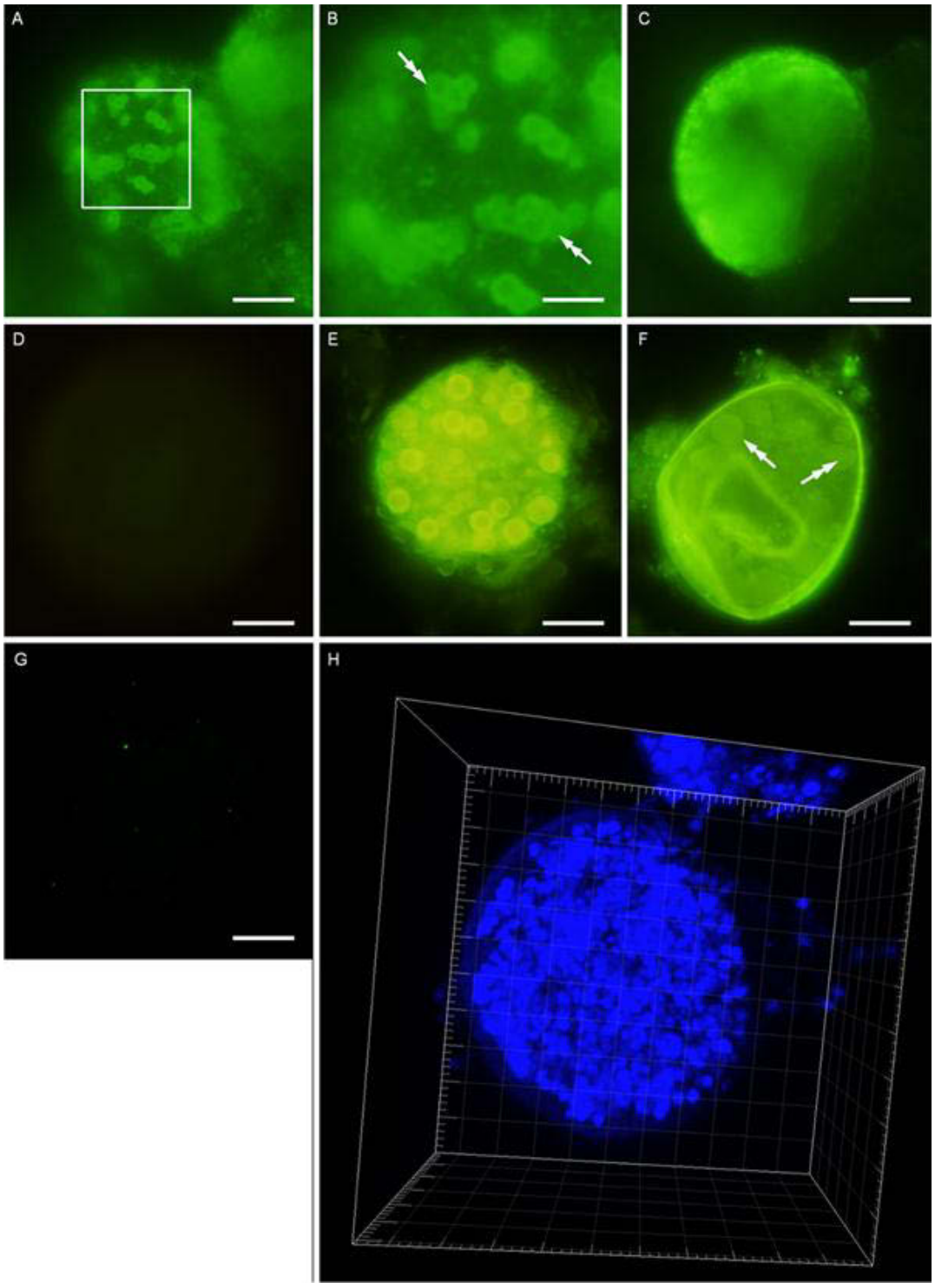

Figure 9: Distribution of Type 1 and Type 2 wall forming bodies during sexual-stage development in macrogametocytes isolated 134 h p.i. from the infected chicken intestine. (A–C) Fluorescent micrographs of isolated macrogametocytes probed with a monoclonal antibody raised to *Eimeria maxima* glycoprotein EmGAM56. (A) An early macrogametocyte showing numerous positively stained 'doughnut-shaped' WFB2s dispersed in the cytoplasm. (B) Shows the enlarged 'doughnut-shaped' WFB2s detected in A. (C) Shows an early oocyst in which numerous 1E11-11-positive granules (green) are accumulated at the surface of the parasite, representing the initiation of inner

wall formation. (D) Normal mouse serum control. (E, F) Isolated macrogametocytes immune-labelled with anti-WFB1 antibody, E1D8, generated to a set of antigens localized in the WFB1 of *E. tenella* gametocytes (Mouafo et al., 2002). (E) A mature macrogametocyte showing numerous large E1D8-positive WFB1s (green). (F) An oocyst showing E1D8-positive outer oocyst wall and a few 'left-over' WFB1s underneath (double arrows). (G) Isotype-matched purified mouse myeloma IgM, kappa antibody (Sigma) control. (H) A three-dimensional confocal reconstruction of harvested microgametocytes stained with a nuclear stain, DAPI (blue). Note the presence of numerous nuclei in the cytoplasm of the microgametocyte. The bar represents 5 μm.

3.3.2 Use of nile red and oil red O to stain the WFBs of developing macrogametocytes

Nile red and oil red O lipophilic stains were used to stain WFBs during gametocyte development and oocyst wall formation (Fowler and Greenspan, 1985; Greenspan and Fowler, 1985; Greenspan et al., 1985). Nile red staining patterns were examined by fluorescence microscopy as described above. As can be seen, nile red revealed numerous 'doughnut-shaped' Type 2 WFBs intermixed with a number of small, brightly staining yellow-gold granules in the cytoplasm of an early macrogametocyte (Figure 10, A and B). At the mid-stage of development, the yellow-gold fluorescence characteristic of neutral lipids localized to the large WFB1s, which reached a maximum diameter of 2·5 μm. In comparison, the 'doughnut-shaped' WFB2s appeared to be 1·8 μm in diameter and orange/red in colour indicating the presence of glycoproteins, amphipathic and/or polar lipids (Figure 10, C and D).

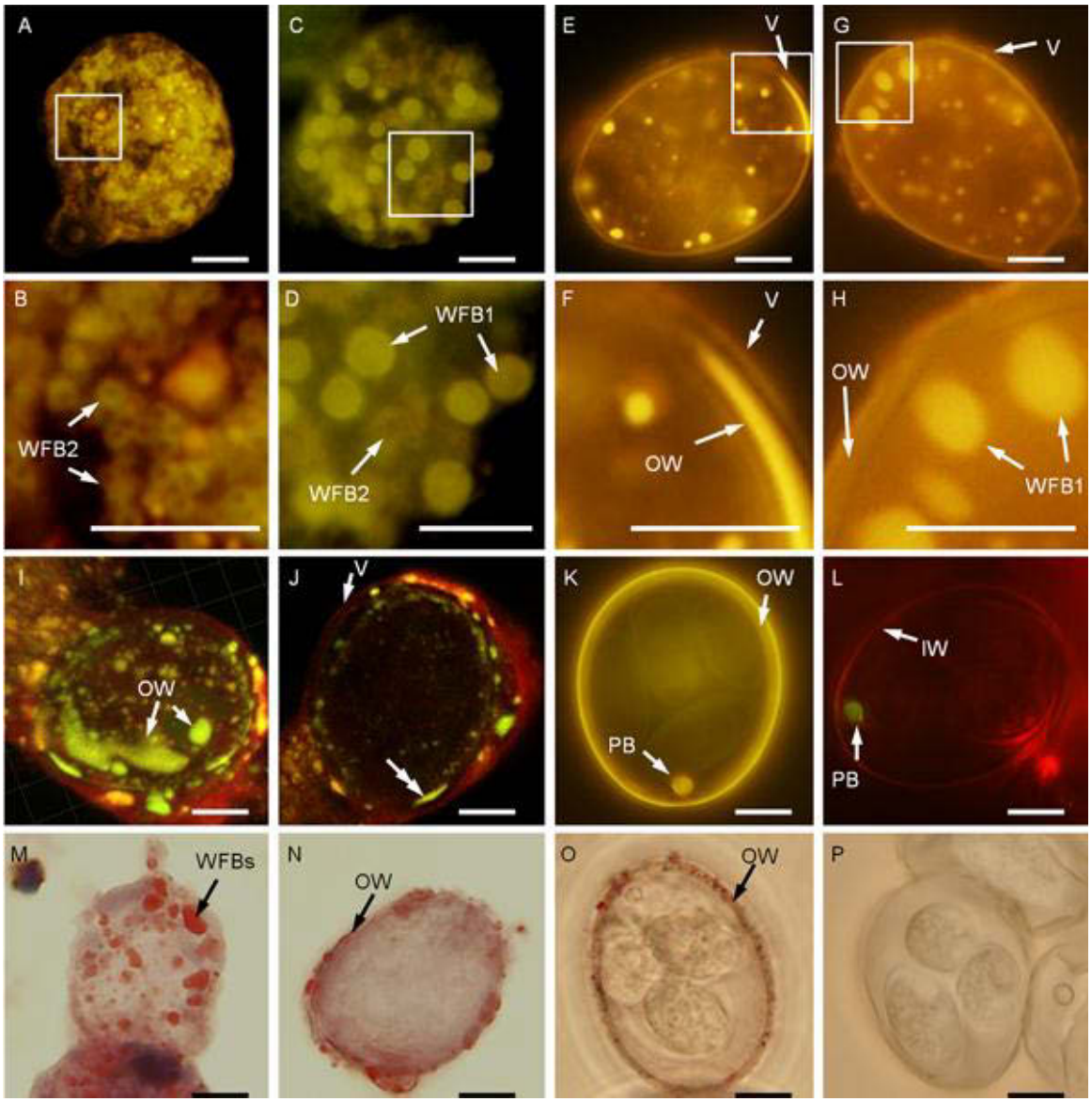

Figure 10: Stage-specific localization of neutral lipids, polar lipids and glycoproteins in freshly harvested macrogametocytes with lipid stains nile red and oil red O. (A) A fluorescent micrograph showing numerous 'doughnut-shaped' WFB2s dispersed in the cytoplasm of an early macrogametocyte. (B) Enlargement of the enclosed area in (A), highlighting the 'doughnut-shaped' WFB2s intermixed with small brightly stained lipid granules (yellow) of various sizes. (C) A mature macrogametocyte showing localization of neutral lipids (yellow) to the large WFB1s and localization of polar lipids and/or glycoproteins (orange/red) to the 'doughnut-shaped' WFB2s aggregated in the cytoplasm. (D) Detail of a part of a mature macrogametocyte, shown in C. (E) An early oocyst showing coalescence of the lipid-rich WFB1s (yellow) at the parasite's surface. (F) Enlargement of the enclosed area displayed in (F) showing deposition of the yellow-gold Type 1 WFBs into the empty space between the 2 parasite-derived membranes representing initiation of outer wall formation (OW). Note the presence of orange/red fluorescing loose outermost veil (V) surrounding the early oocyst. (G) A later stage to that in panel E, showing a loose orange/red fluorescing veil (arrow) and a yellow-gold outer oocyst wall underneath (OW). (H) A few 'left-over' large yellow-gold WFB1s, located at the periphery, are seen directly underneath the

thick yellow-gold outer oocyst wall (OW). (I) A 3-dimensional confocal microscopy image showing an isolated forming oocyst stained with nile red, highlighting lipid-rich patches coded green (double arrow) and the parasite veil (V) and plasma membranes coded red; overlapping lipid-rich, phospholipid- and/or glycoprotein-rich regions appear yellow. (J) Three-dimensional confocal reconstructions of through-focal optical sections showing coalescence and deposition of lipid-rich patches (coded green) between the 2 parasite-derived membranes (red) giving rise to the lipid-rich outer layer of the oocyst wall. (K, L) A fluorescent microscopy image showing localization of the lipids (yellow) to the thick outer oocyst wall (OW) and a polar body (PB) in the unbleached sporulated oocysts (K) and the localization of the lipids (yellow) to the polar body of the bleached sporulated oocyst (L). Note the absence of a yellow-fluorescing outer oocyst wall and a remaining red-fluorescing thin inner oocyst wall (IW) in panel L. (M–P) Light microscopy of the isolated gametocytes (M), early oocyst (N), sporulated unbleached (O) and bleached oocysts (P) stained with oil red O. Note the accumulation of the oil red O dye in the large WFB1s and the outer oocyst wall of immature and mature unbleached oocysts (arrows) and the absence of the dye from bleached oocysts. Scale bar = 5 μm. Abbreviations: IW, inner oocyst wall; Nu, parasite nucleus; PB, polar body; OW, outer oocyst wall; WFB1, Type 1 wall-forming bodies WFB2, Type 2 wall-forming bodies.

In mature macrogametocytes, a red fluorescing membraneous structure was present surrounding the parasite (Figure 10, E). At this stage, large yellow-gold WFB1s were situated just below the parasite's plasmalemma and formed the thick yellow-gold layer filling the empty space between the two parasite-derived membranes lying internal to the red fluorescing outermost membrane, presumably the veil (Figure 10, F). Using nile red stain, it appeared that not all yellow-gold WFB1s were completely consumed in this process, and in some instances they remained as large organelles in the cytoplasm of formed oocysts (Figure 10, G and H, arrows). Also in the cytoplasm of forming oocysts, an additional group of brightly staining bodies became apparent. This population of granules appears to consist mainly of very small, brightly staining bodies, which reached a maximum diameter of only a 100 nanometers and therefore were significantly smaller than the large WFB1s. These granules were predicted to be lipid droplets, as described in previous studies (Ferguson et al., 2003). According to the nile red staining, these small brightly stained lipid granules appeared to be the most abundant at the very late stages of oocyst biogenesis (Figure 10, G).

Finally, three-dimensional confocal microscopy was used to observe macrogametocytes at various stages of maturation. Three-dimensional confocal images of merged yellow and red emissions were acquired of an early oocyst. The image shows coalesced lipid-

rich WFB1s coded yellow at the parasite's surface forming yellow lipid-rich patches initiating the beginning of the outer oocyst wall formation (Figure 10, I). The two-dimensional focal micrograph of the same specimen showed the accumulation and condensation of the yellow-fluorescing material at the parasite's membrane lying internal to the red fluorescing layer, presumably the veil (Figure 10, J). It was found that these yellow patches had formed in a scattered fashion on the surface of the macrogametocyte.

Upon completion of oocyst wall formation and sporulation it was found that the entire surface was coated in a yellow-gold fluorescing outer layer (Figure 10, K). Treatment of the sporulated oocysts with bleach, completely stripped off the thick yellow-fluorescing outer oocyst wall, leaving the thin red-fluorescing inner wall intact (Figure 10, L). This result further supports the contention that the outer oocyst wall, like the WFB1s, is mainly composed of neutral lipids (e.g. triglycerides and cholesterol). Similar subcellular localization and distribution of lipid-rich material was evident based on staining with oil red O, which specifically binds to lipids and lipoproteins (Figure 10, M–P).

3.3.3 Extraction, staining and protein analysis of the WFBs of *E. maxima*

An extraction process was developed in order to isolate and enrich for gametocyte WFBs. The results of staining and immunofluorescence analysis of these enriched WFBs are shown in Figure 10. As can be seen, organelles that appeared purple-pink after H&E staining or gold when labelled with nile red were detected in the WFB-enriched fraction (Figure 10, A and B). Based on a comparison of morphology, staining characteristics and size with the WFBs observed in isolated macrogametocytes (Figure 11, A, insert), it was concluded that the organelles detected in these fractions are indeed intact parasite Type 1 and 2 WFBs (Figure 11, B, insert). This view was further supported by immunofluorescence analysis which showed that the ‘doughnut-shaped’ WFB2s reacted strongly with the 1E11-11 monoclonal antibody to EmGAM 56 (Figure 11, C), whereas the large WFB1s reacted strongly with the polyclonal anti-APGA and the monoclonal E1D8 antibodies (Figure 11, D and E). The E1D8 antibody reacted exclusively with the membrane surrounding the extracted WFB1s of *E. maxima*, as

shown in the two-dimensional focal slice of the same sample (Figure 11, E, insert). Interestingly, after a period of incubation the WFB1s seen in the detergent suspension spontaneously aggregated into ‘necklace-like’ structures similar to that seen under the surface of purified macrogametocytes (Figure 10, A–E).

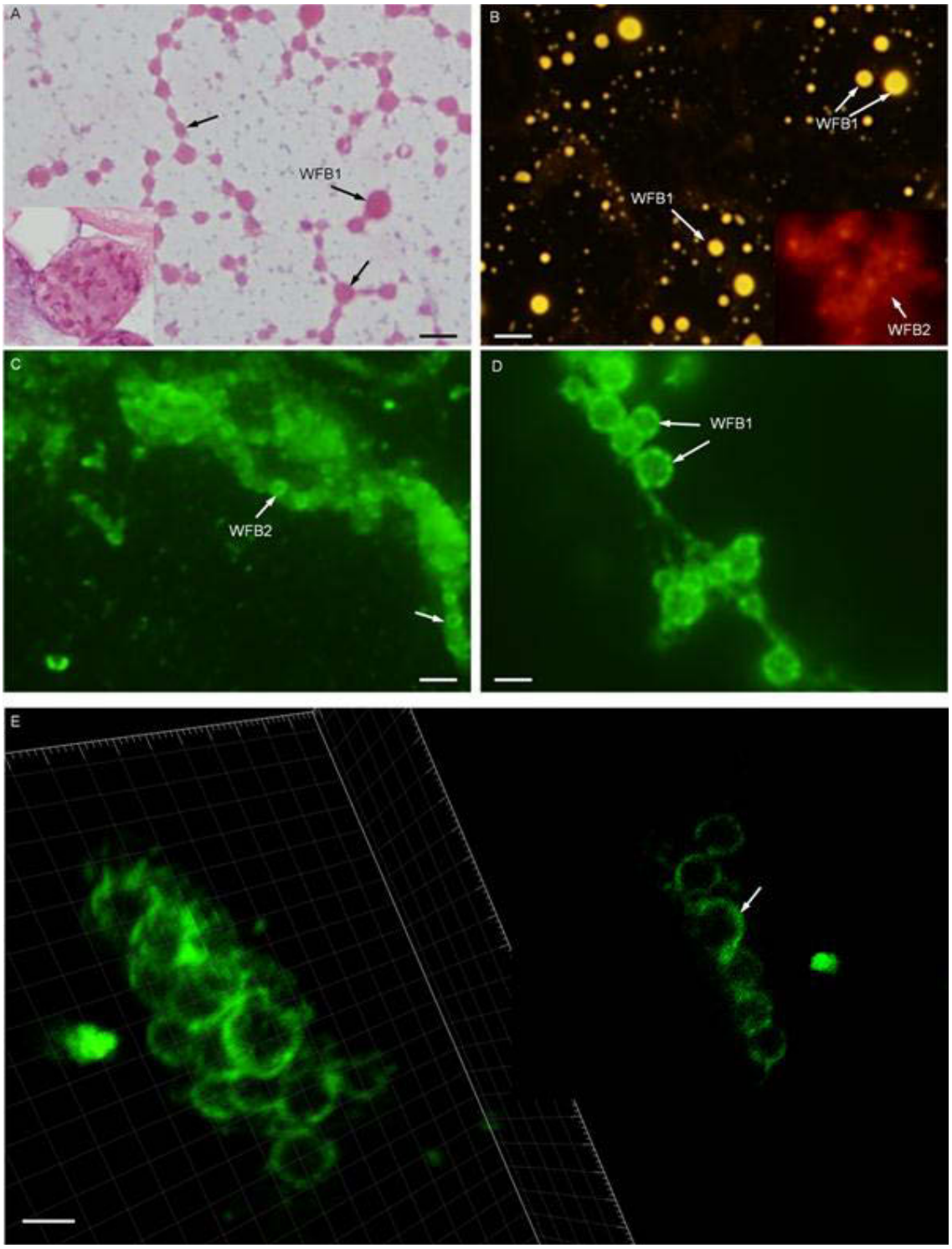

Figure 11: Light microscopy and fluorescent micrographs of the WFB-rich extract. (A) Light microscopy of the WFB-rich extract stained with H&E, highlighting extraction of the large WFB1s and their arrangement into necklace-like structures similar to that seen in the macrogametocytes harvested from the chicken intestine 134 h p.i. (insert). (B) The WFB-rich extract (same to that shown in (A)) incubated with nile red showing the localization of the lipids (yellow) to the extracted large WFB1s and glycoproteins and/or polar lipids (orange/red) to the 'doughnut-shaped' aggregated WFB2s (insert). (C) Immunofluorescent micrographs of the WFB-rich extract incubated

with a monoclonal antibody 1E11-11 specific to EmGAM56, showing the clustered 1E11-11-positive 'doughnut-shaped' WFB2s (green). (D) An immunostained image of the WFB-rich extract showing the large APGA-positive WFB1s (green) clustered into 'necklace-like' structures. (E) The WFB-rich extract was incubated with a monoclonal anti-WFB1 antibody E1D8 and analysed by confocal laser scanning microscopy. Shown is the three-dimensional confocal reconstruction of immunofluorescence signals. Note the aggregation of the E1D8-positive WFB1s and the E1D8 accumulation (green) to the membrane located at the surface of the WFB1 organelle (insert; the three-dimensional confocal reconstructions of through-focal optical section). Bar = 2 μm.

The lysates of isolated gametocytes and uninfected enterocytes, as well as an extract of isolated WFBs, were analysed by SDS–PAGE. Silver staining of proteins collected from the enterocyte host control lysate showed a number of protein bands migrating between 170 and 15 kDa, with the 170, 135, 35 and 17 kDa bands being the most prominently stained (Figure 12, A, Host). In comparison, the gametocyte lysate showed a very different banding pattern, and several of the major protein bands observed in the enterocyte lysate were undetectable in the silver-stained gametocyte extract, indicating that there was minimal host protein contamination. Of all the parasite-specific proteins detected in the gametocyte lysate, the 62, 58 and 56 kDa bands were the most prominent, representing a significant proportion of the total protein extracted (Figure 12, A, Gametocyte). Four prominent bands were also detected between 80 and 120 kDa and several other prominent bands were observed between 12 and 45 kDa in this lysate. One of these bands of 17 kDa was RNase which was used in the extraction process.

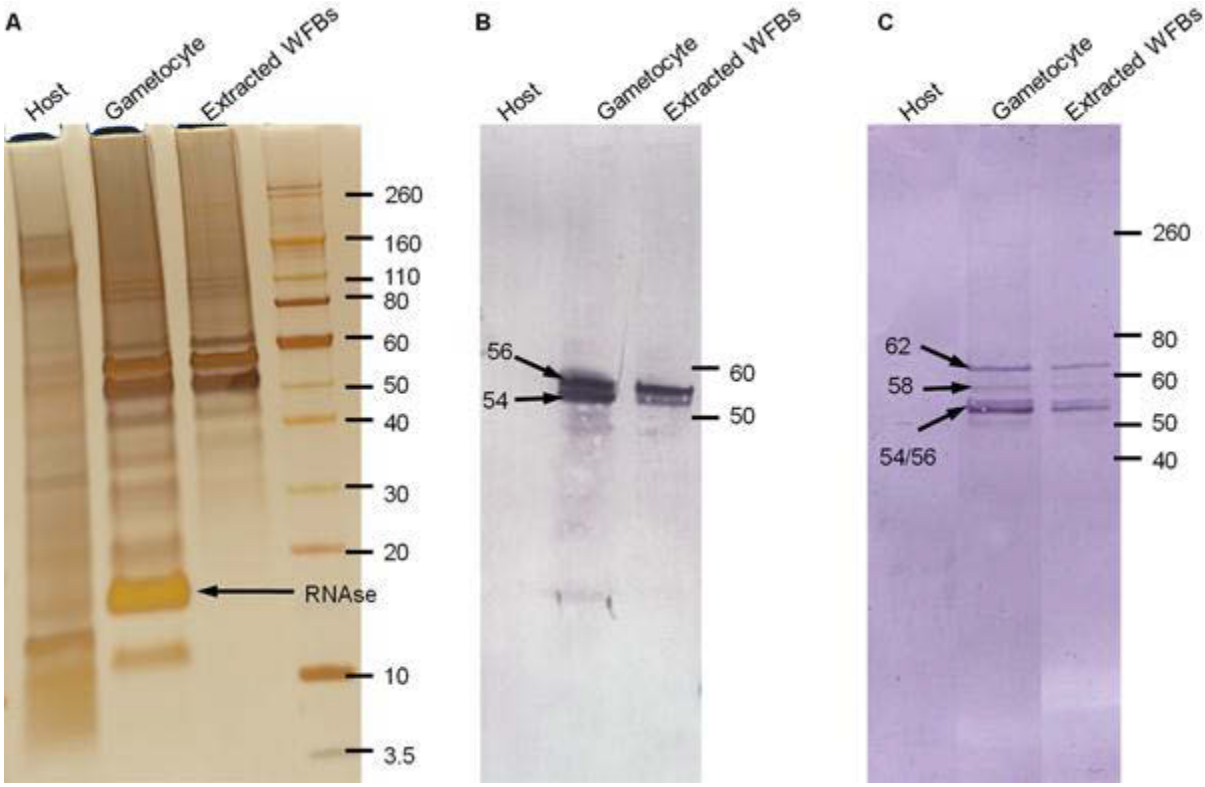

Figure 12: SDS-PAGE and Western blot, in which lane 1 shows the uninfected control enterocytes, lane 2 shows the gametocyte lysate, lane 3 shows the WFB-rich extract (colloid suspension formed by the detergent treatment of the pelleted lysate) retained on top of the 1000 kDa filter. (A) A silver-stained gel of extracts from uninfected enterocytes, gametocytes and WFBs. (B) An immunoblot probed with anti-WFB2 monoclonal antibody, 1E11-11. Note the major gametocyte antigen, EmGAM 54/56 doublet (lanes 2 and 3). (C) An immunoblot probed with anti-APGA. The 3 gels were loaded with 4 μg of protein per lane. The position and molecular mass (in kDa) of protein standards are indicated on the right.

Prominent protein bands having molecular weights of 62, 58 and 56 kDa were also visualized in the extract prepared from isolated WFBs (Figure 12, A). In addition, 4 bands ranging in size between 80 and 120 kDa were also observed in the extracted WFBs. Finally, there were only 2 smaller molecular weight proteins of 45 and 38 kDa observed in the extracted WFBs with the complete absence of the RNase band, which further supports the contention that fractionation has resulted in the isolation of an extract that is substantially enriched with the WFBs.

By Western blotting, using the mouse anti-WFB2 monoclonal antibody 1E11-11, the gametocyte protein EmGAM 56 was detected as a doublet 56/54 kDa band in the

gametocyte lysate and the extracted WFBs (Figure 12, B). The only difference was that it appears that the relative amount of the 56 kDa band within the doublet is higher in the extracted WFBs as compared with the starting gametocyte lysate. As a control, the uninfected enterocyte extract probed with 1E11-11 antibody showed no reactivity (Figure 12, B, Host).

Using anti-APGA on a Western blot we found that the 3 major gametocyte protein bands of 56/54, 58 and 62 kDa all reacted with the antiserum (Figure 12, C). Only when we loaded 10-fold more protein were we able to detect the 82 and 230 kDa proteins (not shown). Interestingly, using anti-APGA the 56/54 doublet band showed that the 54 kDa protein lower band was greater in intensity than the upper band in contrast to the opposite result seen using the monoclonal antibody to the 56 kDa antigen.

3.4 Discussion

The results of the present study show that isolated gametocytes are both intact and metabolically active. This is based on the finding that the wall forming bodiess in isolated macrogametocytes have the same size, shape and staining properties as those seen in tissue sections. In addition, it was found by time-lapse imaging of purified macrogametocytes that during *in vitro* incubation the WFBs become visible in the periphery of the parasite with a corresponding increase in autofluorescence. Furthermore, we observed the presence of well-formed microgametes budding off from the microgametocyte. These results, together with a previous study showing the incorporation of L-[S^{35}] methionine into antigenic proteins from isolated gametocytes (Mencher et al., 1989; Pugatsch et al., 1989), indicate that macrogametocyte maturation does continue even after *E. maxima* gametocytes are removed from the infected intestine. Our results also indicate that the enzymes and other molecules required for parasite growth and development are intact and active in purified gametocytes although further work is required to demonstrate their presence.

During the course of gametocyte development, there is a large burst in the biosynthesis of WFBs in which nearly all of its cytoplasm is filled by WFBs. Nile red and oil red O staining showed that the WFB1s migrate to the periphery of the parasite and release

their contents in patches in the empty space between the 2 macrogametocyte-specific membranes. Nile red staining of purified sporulated oocysts indicates that these patches eventually fuse together to form the outer wall of the oocyst. It was also observed that the WFB1s form links and chains on the surface of the parasite indicating the start of WFB1 joining and exocytosis. Shortly afterwards, the WFB2s start to fuse, forming the inner layer of the oocyst wall through proteolytic processing and di-tyrosine cross-linking of EmGAM56 and EmGAM82 as described previously (Belli et al., 2003a; Mai et al., 2009).

In our studies using nile red we found that the WFB1s and outer oocyst wall stained bright yellow gold. This result indicates that the major components of these organelles are neutral lipids such as cholesterol and triglycerides. Previous studies from our laboratory have shown that the oocyst wall contains relatively large quantities of cholesterol and triglycerides even after bleaching of both unsporulated or sporulated oocysts (Mai et al., 2009). Therefore, it was not surprising to find that both nile red and oil red O, which are sensitive lipophilic probes, strongly reacted with the WFB1s, lighting up the entire organelle.

It was found that a monoclonal antibody previously shown to specifically bind to the WFB1s of *E. tenella* (Mouafo et al., 2002) reacted with antigens localized to the membrane surrounding the WFB1s of *E. maxima*. This was particularly evident in a z-series of confocal images collected through the isolated WFB1s, which showed the concentration of green fluorescence in the rim of the organelle (Figure 11, E). Together with nile red results, it was therefore postulated that these organelles contain a lipid core with a protein-rich surface coat. The role of this WFB1 protein in outer oocyst wall formation is currently being investigated.

A simple method to extract WFBs from purified gametocytes was developed and it was shown by light and fluorescent microscopy, immunofluorescence and Western blotting that they were intact and contained the major WFB1 and WFB2 antigens. In addition, it was shown by SDS-PAGE that in both gametocyte lysate and WFB-enriched fractions, the 56, 58 and 62 kDa antigens were the most prominent bands, representing a large proportion of the total gametocyte protein. Based on silver staining of the SDS-PAGE gel, it appeared that the extraction procedure resulted in a significant enrichment of the

major WFB proteins as most of the smaller molecular weight proteins detected in the gametocyte lysate were absent in the WFB-rich extract.

We had shown previously that the 56 and 82 kDa gametocyte antigens are partially insoluble even in strong detergent (Belli *et al*. 2002*a*), and based on this study it would appear that these organelles form a stable colloidal suspension in 1% SDS. This conclusion is supported by the finding that even after concentrating and washing the organelles with PBS buffer using a 1000 kDa MWCO filter, the major WFB1 and WFB2 proteins remained associated with the intact WFBs. This biophysical property of the WFBs is most likely due to the relative insolubility of the major protein and lipid components of these organelles, which maintain their integrity until a signal is given to release their contents possibly after fertilization.

3.5 Conclusions

The results of the present study help to elucidate the biosynthesis and spatial organization of WFBs during the development of the oocyst wall of *E. maxima* using isolated and purified gametocytes. The picture that emerges from all of these studies is as follows: as the macrogametocytes mature the veil-forming and WFBs are synthesized as small vesicles that enlarge and spread out in the cytoplasm during development. Once the parasite has reached its final size the veil, which contains mainly proteins/glycoproteins, is laid down surrounding the parasite membrane. In mid- and late-stage macrogametocytes the neutral lipid containing WFB1s align themselves at the periphery of the parasite, form links and chains, and then their contents are exocytosed as lipid patches (‘rafts’) into the space between 2 parasite membranes in a patchwork fashion. During outer wall formation the WFB2s, which are rich in the glycoproteins EmGAM 56, EmGAM 82 and EmGAM 230, begin to coalesce in the gametocyte cytoplasm. Then, these tyrosine-rich glycoproteins are enzymatically cleaved into smaller peptides that are cross-linked and inserted into the inner wall. Finally, there are some ‘leftover’ WFBs that remain in the cytoplasm of the newly formed oocyst/zygote.

Chapter Four

Paper III: Endocytosis and intracellular trafficking of wall forming bodies in sexual stages of E. maxima

Declaration

I declare that the following publication included in this thesis in lieu of a chapter meets the following:

- More than 50% of the content in the following publication included in this chapter has been planned, executed and prepared for publication by me
- The work presented here has been peer-reviewed and accepted for publication
- I have obtained approval to include the publication in this thesis from the Publisher
- The initial draft of the work has been written by me and any subsequent changes in reponse to co-authors and editors reviews was performed by me
- The publication is not subject to any obligations or contractual agreements with a third party that would constrain its inclusion in the thesis.

Publication title: Particle uptake and intracellular trafficking of wall forming bodies in the sexual stages of *Eimeria maxima*
Authors: Sonja Frölich, Valerie C. Wasinger, Matthew P. Padula and Michael Wallach
Candidate's contribution (%): above 50 %
Journal name: Plos One
Volume/ page numbers: N/A
Status: under review (manuscript number: PONE-D-13-49560)

I declare that the publication above meets the requirements to be included in the thesis

Candidate's name: Candidate's signature: Date (dd/mm/yy):

4.1 Brief introduction

Eimeria is an obligate intracellular parasite that inhabits the small intestine of the domestic chicken causing the disease coccidiosis in commercial poultry. The disease is characterised by nutrient malabsorption, lethargy, diarrhoea and severe growth retardation. Many anti-coccidial drugs have been used over the past 50 years to treat the disease, however, due to the development of drug resistance by the parasite, new drugs and vaccines are urgently needed to be able to continue to control this major veterinary health problem.

The establishment of an *Eimeria* infection is dependent upon the parasite's ability to invade and develop within a parasitophorous vacuole (PV) of the enterocyte of its chicken host. The PV serves as a physical barrier protecting the intracellular parasite from the harmful environment of the host cell cytosol. It also serves as a molecular sieve for acquisition of solutes keeping the parasite's osmotic balance in check (Entzeroth et al., 1998). As it develops, the *Eimeria* parasite eventually differentiates into the sexual stages, male (micro-) and female (macro-) gametocytes that upon fertilisation form an oocyst.

The oocyst is the transmissible form of the parasite, which is released into the external environment with the faeces. To survive and successfully transmit between hosts, the *Eimeria* parasite needs a rigid protective barrier, an oocyst wall. When challenged with toxic compounds and mechanical damage in the external environment, the oocyst wall protects the parasite and allows it to survive for extended periods of time.

The mechanisms of oocyst wall formation have been particularly well studied in *Eimeria maxima* and are known to involve incorporation of tyrosine-rich precursor glycoproteins, EmGam230, EmGam82 and EmGam56 glycoproteins, synthesised by the female gametocytes (Belli et al., 2002a; Belli et al., 2003a; Belli et al., 2003b; Belli et al., 2002b; Ferguson et al., 2003; Mai et al., 2011; Wallach et al., 1995). The cross-linking of tyrosine residues forms a rigid matrix contributing to the robustness and impermeability of the oocyst wall. Furthermore, recent studies examining the process of oocyst wall formation have reported that in addition to tyrosine-rich proteins, oocyst

walls of *Eimeria* also contain β-1, 3-glucan (Bushkin et al., 2012), as well as neutral and polar lipids (Bushkin et al., 2013; Frölich et al., 2013; Mai et al., 2009) that also contribute to impermeability and rigidity of the oocyst wall. However, exactly how the parasite assembles these molecules into an impervious oocyst wall while maintaining the ability to acquire nutrients needed for development into an infectious cyst form remains an open question.

Early studies of the encapsulation process in *E. maxima*-infected enterocytes indicated that surface membranes of developing macrogametocytes contain micropores and intravacuolar tubules (Mehlhorn, 1971). These membranous structures were proposed to play a role in nutrient intake. However, since the first description of these structures, little work has been done to validate their role and explain the mechanisms by which nutrients transverse the plasma membrane and reach intracellular compartments.

In the present study, we were able to harvest and maintain viable *E. maxima* gametocytes *in vitro* for several hours. We used this model system to study the nature and mechanism of particle intake in *Eimeria* by visualising the structure and dynamics of the parasite surface membrane. We combined scanning electron microscopy with live-cell imaging and a series of endocytosis assays to study uptake and the intracellular location of internalised particles. Furthermore, we used three-dimensional confocal microscopy to determine the subcellular location of the cytoskeletal elements in purified macrogametocytes and oocysts *in vitro*. Finally, we used label-free comparative LC-MS/MS-based shotgun differential proteomics for the analysis of the wall forming body proteome in *E. maxima*. The results reported here reveal valuable insights into the mechanisms by which the parasite is able to acquire nutrients essential for development, transport organelles and at the same time synthesise the impervious oocyst wall.

4.2 Materials and Methods

4.2.1 *E. maxima* viability assay

Ethidium bromide and acridine orange staining is routinely used as a permeability assay to differentiate between viable and non-viable (i.e. apoptotic and necrotic) cells. Acridine orange (AO) is taken up by both viable and non-viable cells and emits green fluorescence indicating intercalation of the dye into double stranded nucleic acids. In contrast, ethidium bromide (EB) is taken up by cells whose membrane integrity has been compromised (e.g. apoptotic and necrotic cells) and emits red fluorescence due to intercalation into the DNA. To evaluate the viability of freshly prepared parasites, *E. maxima* freshly harvested and freeze-thawed gametocytes, unsporulated and sporulated oocysts were incubated in a solution of EB and AO, as descried previously (Borel et al., 1998; Rieux et al., 2012). Parasites were washed three times by centrifugation (1,000 x g, 10 min) and stained cells examined by a fluorescence Olympus BX51 microscope equipped with a 100 X oil objective (N.A. 1.3), a narrow green (ex 450-480 nm/515 nm) and a long pass excitation/emission red (510-550 nm/590 nm) fluorescence filters, and a DP70 colour CCD camera (Olympus Australia Pty. Ltd.). In addition, gametocytes were also examined using a Nikon A1 laser scanning confocal microscope and appropriate fluorescence filters to obtain three-dimensional stacks and single focal slices of stained cells. According to fluorescence emitted by the stained parasites and the nucleus appearance, the cells were differentiated and categorized according to previously published methods (Ribble et al., 2005), as follows: living viable cells (green nucleus), apoptotic cells (orange nucleus with chromatin fragmentation) and necrotic cells (uniformly red stained cell nuclei).

4.2.2 Live cell time-lapse imaging of freshly harvested *E. maxima* gametocytes

Live-cell imaging of freshly harvested and freeze-thawed gametocytes, used as a control for these experiments, was performed using time-lapse video microscopy, as follows.

Freshly harvested gametocytes (2 x 10^6) were resuspended in 1 ml of TNEP buffer (pH 7.4) and a drop of gametocyte suspension was placed on a round 35-mm glass-bottom dish pre-coated with 0.1% poly-L-lysine. The cells were left to settle for 15 min in a microscope heated chamber pre-warmed to 37˚C and humidified (5% CO_2) before imaging on a Nikon Eclipse Ti-U inverted microscope (Nikon, Tokyo, Japan) equipped with a 60 X oil objective lens (Plan Apo NA 1.4 aperture) and the Perfect Focus System™ for continuous maintenance of focus. Blue autofluorescence was monitored with a bandpass excitation/emission filter (330-385/435-485). Fluorescing and differential interference (DIC) images were were collected every 30 minutes over a 17 hour period with a 5 mega-pixel high-speed charge-coupled device (CCD) camera. Exposute time and brightness/contrast settings were kept constant foe each and subsequently analysed using the NIS-Elements acquisition software.

4.2.3 Scanning electron microscopy (SEM) of freshly harvested *E. maxima* gametocytes

Purified gametocytes were allowed to adhere to poly-L-lysine coated cover slips, coated with 10 nm carbon or left uncoated for subsequent SEM imaging. All SEM imaging was conducted on the LEO Supra 55VP (ZEiss) SEM using secondary and backscatter mode to allow visualisation of cellular surface. The SEM was set to variable pressure in high current at 10 and 20 kV using a 120 nm aperature.

4.2.4 In vitro experiments with fluorescent nano beads

Freshly harvested sexual stage parasites were incubated in TNEP buffer supplemented with 40 and 100 nm fluorescent polystyrene beads (Life Technologies, USA). The carboxylate-modified yellow-green or red FluoSpheres® nano bead solutions were sonicated for 15 min in a water bath to disperse particles and avoid aggregation, and introduced to a parasite suspension at a 1:1000 v/v dilution. Samples were incubated for 45 min at different temperatures (4˚C, room temperature and 37˚C) and washed twice with TNEP (1,000 x g, 5 min) prior to fixation with 95% ice-cold acetone. As a control

for these experiments, freeze-thawed parasites, which do not have intact membranes based on viability staining, were also incubated with the nano beads and processed as above. Cells were then mounted in Vectashield® (Vector Laboratories, Burlingame, CA, USA) prior to analysis by a Nikon A1 laser scanning confocal microscope, as described below.

4.2.5 Drug effects on endocytosis and distribution of macrogametocyte WFBs

To evaluate the effects of specific endocytosis inhibitors, the freshly harvested macrogametocytes were first pre-incubated with the tubulin inhibitor, colchicine, or the actin blocker, cytochalasin D, for 1 h before exposure to 40 or 100 nm green fluorescent nano beads (Life Technologies, USA). Each inhibitor was tested at different concentrations in order to establish working concentrations for maximum inhibition with minimum toxic effects on cells. Cytochalasin D (Sigma) was tested at concentrations of 0.01, 0.1, 10 and 100 μM and colchicine (Sigma) was tested at concentrations of 0.05, 0.5, 5 and 50 mM. The effect of DMSO, the drug vehicle, was tested separately as a control. All experiments were performed in triplicates. In labelling experiments designed to study morphologically whether microfilaments and microtubules play a role in trafficking of WFBs, cells were first exposed to drugs for 1 h. They were then gently rinsed three times with PBS prior to double-labelling (see below).

.

4.2.6 Analysis of actin distribution in gametocytes and during oocyst biogenesis

Actin in fixed and permeabilized gametocytes was visualized using Oregon Green 514 conjugated phalloidin (LifeTechnologies, USA) prepared in methanol and 1% bovine serum albumin (BSA), as described by the manufacturer. The gametocyte suspension (100 μL) was mixed with 10 μL of the phalloidin staining solution and allowed to stain for 30 - 45 min at room temperature. The cells were washed once by centrifugation (1,000xg, 5 min) and placed on 35-mm round glass-bottom dishes coated with poly-L-lysine (Sigma). Macrogametocyte type 1 WFBs (WFB1s) and the outer oocyst wall material were visualized by incubating parasites in the presence of Evans blue, as

described previously (Ferguson et al., 2003). All staining procedures were performed in a dark room at room temperature.

4.2.7 Confocal microscopy

Labelled specimens were examined by confocal laser scanning microscopy using a Nikon A1 microscope equipped with 60 and 100 X oil immersion objective lenses (N.A. 1.4) and appropriate lasers to obtain 2D and 3D images. Green and red fluorescence were excited with the 488 and 637 nm laser and collected with 500-550 nm and 662-737 nm emission filters respectively. To acquire three-dimensional volumes, approximately 30-z serial optical sections were collected with a Z-step size of 0.1-0.4 µm, using the NIS Elements software (Nikon, Melville, NY, USA). Raw images were reconstructed and rendered in 3D using IMARIS v.7 software (Bitplane Scientific, Zurich, Swizerland). Images for all figures were processed in Photoshop (Adobe).

4.2.8 Proteomic analysis of the isolated Wall Forming Bodies

Whole gametocyte lysate and WFBs-rich extract were resuspended in a minimal volume of PBS and a small aliquot was taken for protein quantification using the BCA Protein Assay (Pierce) with bovine serum albumin (BSA) as the standard. One hundred micrograms of protein was used for in-solution trypsin digestion.

4.2.9 Acetone precipitation and in-solution trypsin digestion

The in-solution trypsin digestion of the proteins and acetone precipitation was performed as follows. Four volumes of ice-cold acetone were added to the solution and stored at -20°C overnight. The proteins were pelleted by centrifugation at 15,000xg for 10 min and the resulting pellets air-dried at room temperature and then reconstituted in 8M urea/100 mM ammonium bicarbonate (Sigma). The samples were then reduced (14 mM dithiothreitol 45 min, 56°C), alkylated (55 mM iodoacetamide, 45 min, 56˚C) and

diluted fivefold using 100 mM ammonium bicarbonate solution (pH 8) prior to overnight digestion at 37˚C using sequencing grade trypsin (1 mg/ml) prepared in 1 mM HCl (Sigma). The digested peptides were then cleaned up using C_{18} Zip-Tip® pipette tips (Millipore, USA) for enrichment of the peptides and salt removal prior to MS analysis as follows. POROS 20 R2 media (Applied Biosystems, California) was used for peptide extraction. Poros beads, 100 ng, were used for each sample in 5% formic acid and 0.2% TFA in water to a total of 25 µl. Samples were shaken at 4°C for 4 hours. Beads were put into a Zip Tip (Millipore, Massachusetts) using gel loading tips and centrifuged at 1000 x g for 1 minute. Samples were washed twice with 50 µl of 0.1% aqueous TFA which was placed onto tips and centrifuged. Zip tips were washed three times with 50 µl, 0.1% aqueous TFA. Peptides were then eluted into a fresh tube with 20 µl 40% acetonitrile and 0.25 µm ML peptide in 0.1% TFA, then 80% acetonitrile and 0.25 µm ML peptide in 0.1% TFA, centrifuging at 3000 rpm for 2 mins. Samples were then dried in a speed-vac and stored at -20°C.

4.2.10 In-solution digestion and liquid chromatography tandem mass spectrometry (LC-MS/MS)

Analyses of soluble peptides were performed at the Bioanalytical Mass Spectrometry Facility, The University of New South Wales (Sydney) using an ESI-LC-MS/MS on an LTQ-Orbitrap Velos (Thermo Fisher Scientific, Massachusetts, USA). Each sample was reconstituted in 10 µL of 0.1% formic acid and separated by nano-LC using an Ultimate 3000 HPLC and autosampler (Dionex, Amsterdam, Netherlands). Samples were divided into three technical replicates. 0.2 µl was injected into a micro C_{18} precolumn (500 µm × 2 mm, Michrom Bioresources, Auburn, CA, USA) with Buffer A (98% H_2O, 2% CH_3CN, 0.1% TFA) at 10 µl min^{-1}. After a 4 min wash the pre-column was switched (Valco 10 port valve, Dionex) into line with a fritless nano column (75 µm i.d × 11 cm) containing reverse phase C18 media (5 µm, 200 Å Magic, Michrom Bioresources). Peptides were eluted using a linear gradient of Buffer A (98% H_2O, 2% CH_3CN, 0.1% TFA) to Buffer B (98% CH_3CN, 2% H_2O, 0.1% formic acid) at 250 nl min^{-1} over 70min. High voltage (2000 V) was applied to low volume (Upchurch Scientific, Oak Harbor, WA, USA) and the column tip positioned approx. 0.5 cm from the heated

capillary (T=280°C) of an Orbitrap Velos (Thermo Electron, Bremen, Germany) mass spectrometer. Positive ions were generated by electrospray and the Orbitrap operated in data-dependent acquisition mode. A survey scan m/z 350–1750 was acquired in the Orbitrap (Resolution=30,000 at m/z 400, with an accumulation target value of 1 e^6 ions). Up to the 10 most abundant ions (>5,000 counts) with charge states 2+ to 4+ were sequentially isolated and fragmented within the linear ion trap using collisionally induced dissociation with an activation q=0.25 and activation time of 30 ms at a target value of 30,000 ions. The m/z ratios selected for MS/MS were dynamically excluded for 30 s.

4.2.11 Database searches and protein identification

Mass spectra peak list files generated by the Protein Pilot v1.0 software (Applied Biosystems) were searched using Mascot Daemon search engine (Matrix Science, London, UK) against a non-redundant protein database (24_8_12, containing 19,941,864 entries for all species). The search parameters were set to oxidation of methionine as a variable modification, with 4.0 ppm peptide tolerance and 0.60 Da MS/MS peptide tolerance and an allowance for up to three missed cleavages for tryptic searches were used. To maximise the number of quantifiable proteins but at the same time keep the false discovery rate at acceptable levels, only peptides with ion scores above 20 and the presence of at least one unique peptide were considered for further analysis. For each protein matching the above criteria, the quality of the MS/MS spectra of peptides with scores lower than 50 were manually verified. The mass spectra remaining after filtering were quantified using spectral counting by Scaffold (see below).

In order to maximise the identification of peptides obtained from the LC-MS/MS analysis of *E. maxima*, which lacks an annotated genome sequence, raw spectra were analysed using PEAKS Studio v6.0 software (Bioinformatics Solutions Inc.). Peptides were matched against a custom-made database containing the predicted protein sequences of a related cyst-forming apicomplexan parasites, *Eimeria* tenella (housed within www.ToxoDB.org, version 8.2). The first draft genome of Houghton strain *E. tenella* was annotated by the Parasite Genomics Group at the Welcome Trust Sanger Institute using Workflow-based Automatic Genome Annotation (WAGA) and has been

provided prepublication. To identify host proteins and common contaminants, the parasite database was supplemented with complete Gallus gallus database and a contaminant database from NCBI. The enzyme specificity was set to trypsin, propionamide (acrylamide) modification of cysteine, oxidation of methionine and deamidation of asparagine and glutamate were set as variable modifications, with a tolerance of ± 4.0 ppm for precursor ions and ± 0.60 Da for fragment ions. Three missed cleavages were allowed. In order to be included in the list, a protein needed to exhibit a minimum score of 20 (false discovery rate of 2%) and be identified by at least two unique peptide, further enhancing the probability of true identification. Proteins identified as unknowns or hypothetical were identified by searching the peptide sequences using BLASTP algorithm (www.blast.ncbi.nlm.nih.gov) for short, nearly exact matches. If there were multiple possibilities for peptide ID, the top scoring hit was selected.

4.2.12 Label-free quantification of proteins identified in the WFB extract

Label free quantification of peptide spectral matches was performed using Scaffold (v4.0.5, Proteome Software Inc., Portland, OR). Peptide identifications were accepted if they could be established at greater than 95.0% probability ($p<0.05$). Peptide probabilities from Mascot were assigned by the Peptide Prophet algorithm (Keller et al., 2002) with Scaffold delta-mass correction. Protein identifications were accepted if they could be established at greater than 95.0% confidence and contained at least 2 identified peptides. Protein probabilities were assigned by the Protein Prophet algorithm (Nesvizhskii et al., 2003). The relative abundance of the identified proteins in the WFB extract in comparison to the gametocyte lysate was determined by spectral counting (Paoletti and Washburn, 2006). Proteins that contained similar peptides and could not be differentiated based on MS/MS analysis alone were grouped to satisfy the principles of parsimony. Proteins sharing significant peptide evidence were grouped into clusters. Proteins were annotated with Gene Ontology (GO) terms from gene_association.goa_uniprot (downloaded Jun 28, 2013) (Ashburner et al., 2000).

4.3 Results

4.3.1 Freshly harvested macrogametocytes and oocysts are viable and exclude the Ethidium bromide stain

Gametocytes freshly purified from the infected chicken intestine were subjected to ethidium bromide/ acridine orange (EB/AO) double staining to differentiate between the viable and non-viable (apoptotic/nectrotic) parasites. Staining and appearance of nuclei were used to classify the parasites as live (green fluorescing) or dead and apoptotic (red fluorescing). No dead macrogametocytes were detected in fresh parasite preparation (Figure 13, A-A2). Red nuclei of surrounding host enterocytes were clearly visible with host cells often aggregated into clusters in close proximity to the gametocytes (Figure 13, A1). The red nuclei of parasitised host cells could also be readily discernible, suggesting that the host cells are undergoing apoptosis induced by the infection (Figure 13, A2 white arrows). In contrast, freeze-thawed micro- and macrogametocytes and oocysts, which were used as a control for this experiment, when incubated with EB/AO all displayed compromised membrane integrity as they stained red with the ethidium bromide dye (Figure 13. B-B2). Interestingly, the multinucleated microgametocytes, the Type 1 wall forming bodies and the oocyst wall of freeze-thawed parasites were easily discernible as red structures, implying the presence of nucleic acids (Figure 13, B1 and B2).

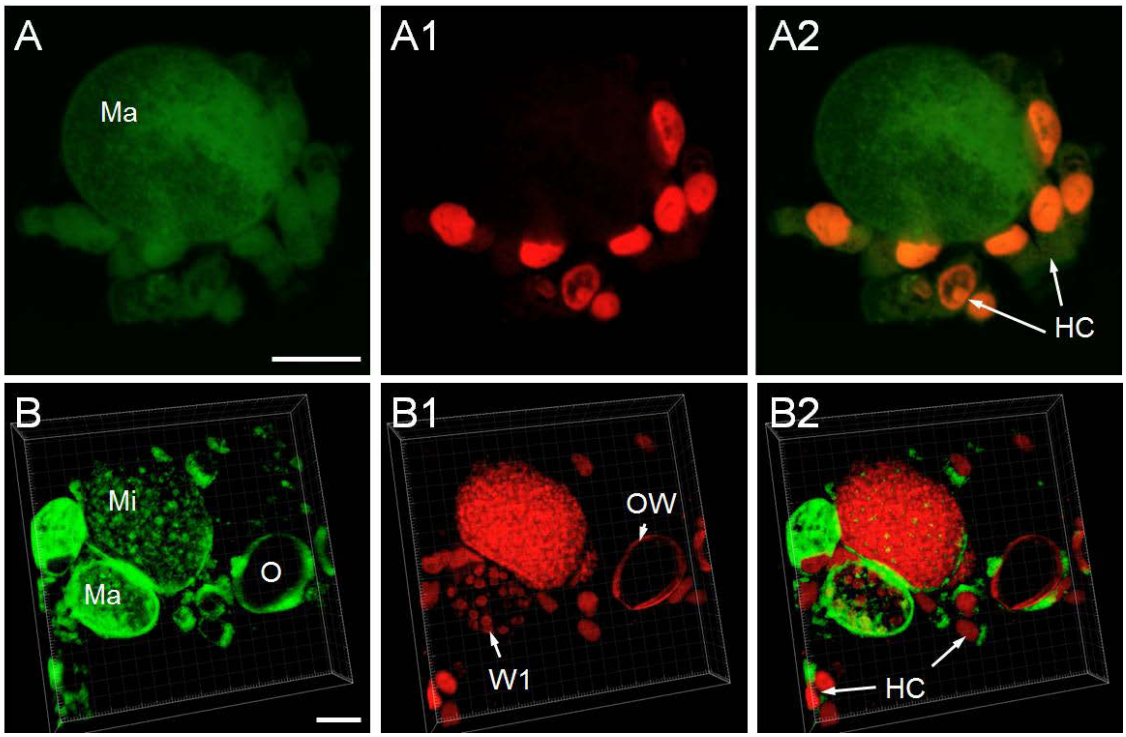

Fig 13: Ethidium bromide (EB) and acridine orange (AO) double staining of freshly harvested and freeze-thawed gametocytes. Unfixed, freshly harvested gametocytes were incubated with EB/AO stain immediately (top), or after freeze-thawing (bottom) used as controls for the experiment. **A** and **B** show AO stained fresh and viable (**A1**), and freeze-thawed, non-viable (**B1**) gametocytes and host enterocytes all emitting green fluorescence. **A2** and **B2** show the EB stained fresh (**A2**) and freeze-thawed (**B2**) gametocytes. Note the penetration of the EB stain (red) and its specific localisation within the host nuclei in fresh gametocyte preparation (A2, white arrows). The EB stain is excluded from the macrogametocyte (A2). In contrast, the EB stain penetrates membranes of all freeze-thawed parasites (microgametocytes; Mi, macrogametocytes; Ma and oocysts; O), including the host cell nuclei (B1-2). **A2** and **B2** show overlays of the data collected using green and red fluorescence filters. The fresh macrogametocytes exclude the EB stain and remain green. Black bars represent 10 µm. Ma; macrogametocyte, Mi; microgametocyte, HN; host nucleus.

4.3.2 Surface membranes of developing oocysts display micropores

To obtain high resolution structural information of surface membranes, fresh sexual stage parasites extracted 132-134 hours post-infection were allowed to adhere to poly-l-lysine coated glass slides and examined by SEM (Figure 14). Low acceleration voltages were used to prevent damage of the observed specimens. Secondary electron images showing surface structural detail of macrogametocytes and early stage oocysts revealed a number of micropores, of varying diameter and depth (Figure 14, A-B1, arrows). Ovoid macrogametocytes, presumably at early stages of oocyst wall biogenesis, could also be identified (Figure 14, C). Secondary electron images of the surfaces of these gametocytes enabled the visualisation of the numerous pores of varying diameter and depth (Figure 14, C1, C2). These structures were observed in all macrogametocytes and early stage oocysts examined.

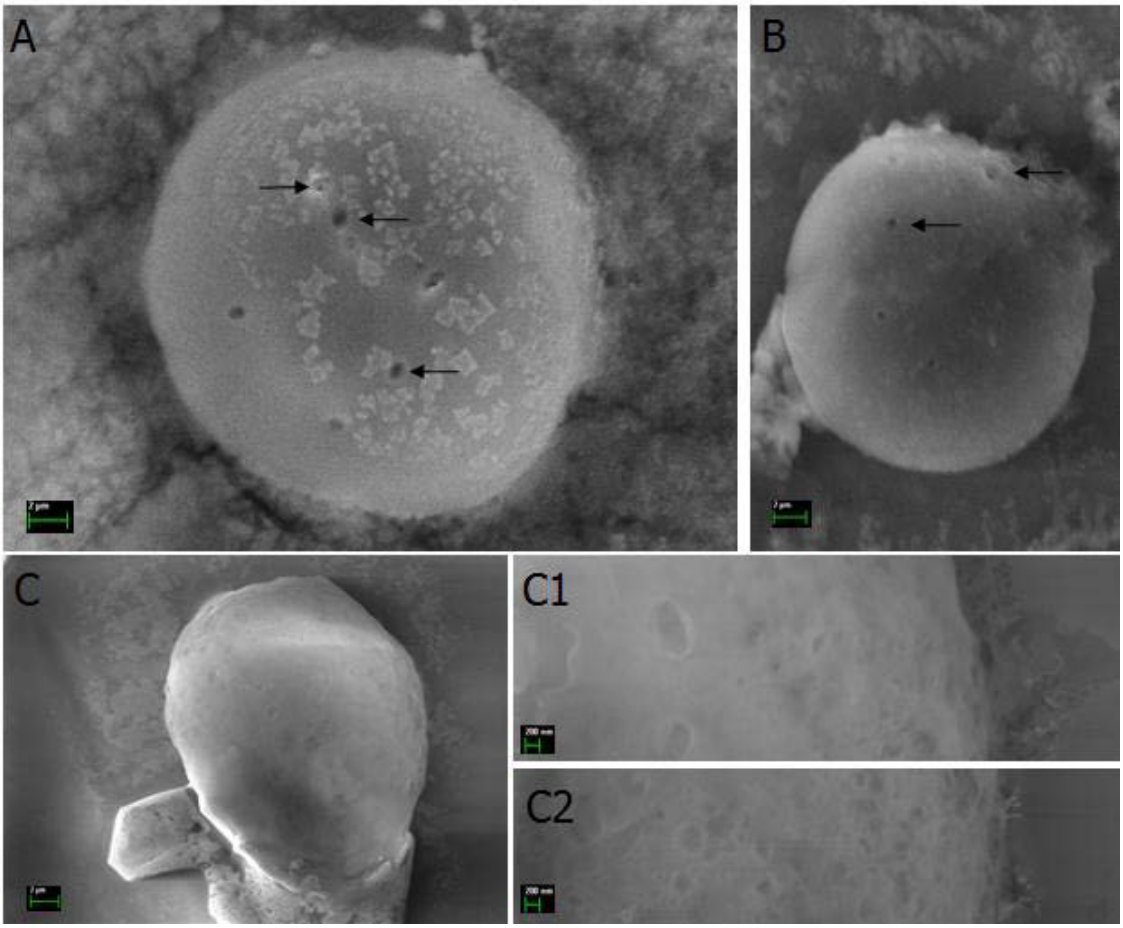

Figure 14: SEM analysis of the cell surface in the freshly extracted sexual stage *E. maxima* parasites. Secondary electron images of gametocytes (A, B) and early oocysts (C) show pores of varying diameter and depth on the parasite's surface (arrows) and in the wall of a young oocyst (C1, C2). Scale bars are indicated.

4.3.3 Developing macrogametocytes and oocysts take up nano beads *in vitro*

We made use of carboxylate-modified green and red FluoSpheres® beads of 40 and 100 nm in diameter to test the endocytic capability of freshly harvested sexual stage parasites. First, gametocytes and early stage oocysts were incubated with green fluorescing nano beads of 40 nm in diameter at room temperature. The 40 nm beads were observed as small green aggregates or droplets (each of which containing a large number of nano beads) approximately 0.5 - 1 μm in diameter, situated both on the surface and in the cytoplasm of the developing macrogametocyte (Figure 15, A). In addition, diffusely fluorescing filamentous structures appeared to be associated with the strongly fluorescing aggregates. In early stage oocysts with a clearly visible oocyst wall, we observed that the fluorescent signal was seen on the parasite's surface; however, even in those samples internalised beads were observed (Figure 15, A1-2). The 40 nm beads were excluded from the large type 1 WFBs (Figure 15, A2, arrows), which appeared hollow due to the lack of fluorescence. No internalisation was seen in gametocytes incubated at 4°C, as expected (not shown).

Figure 15 illustrates that the 100 nm beads were also taken up and internalized by the parasites. The green fluorescent signal was mainly visible within the vesicles resembling large type 1 WFBs (arrows) with a diffuse pattern seen in portions of the macrogametocyte or early stage oocyst cytoplasm (Figure 15, B1 and B2). In addition, there was no apparent fluorescence seen on the surface of the parasites. Evans blue staining was used as a positive control for the detection of large type 1 WFBs and as expected localised to the WFB1s of macrogametocytes and early oocysts (Figure 15, C-C2). Based on the similarity in the size and shape of the WFB1s stained by Evans blue and those in which the 100 nm beads were found to localise, we concluded that these beads specifically are targeted to and accumulate in the WFB1s. Finally, freeze-thawed gametocytes, which do not have intact membranes and were used as a negative control, were incubated with the nano beads as described above; however, no internalisation of the beads was observed (Figure 15).

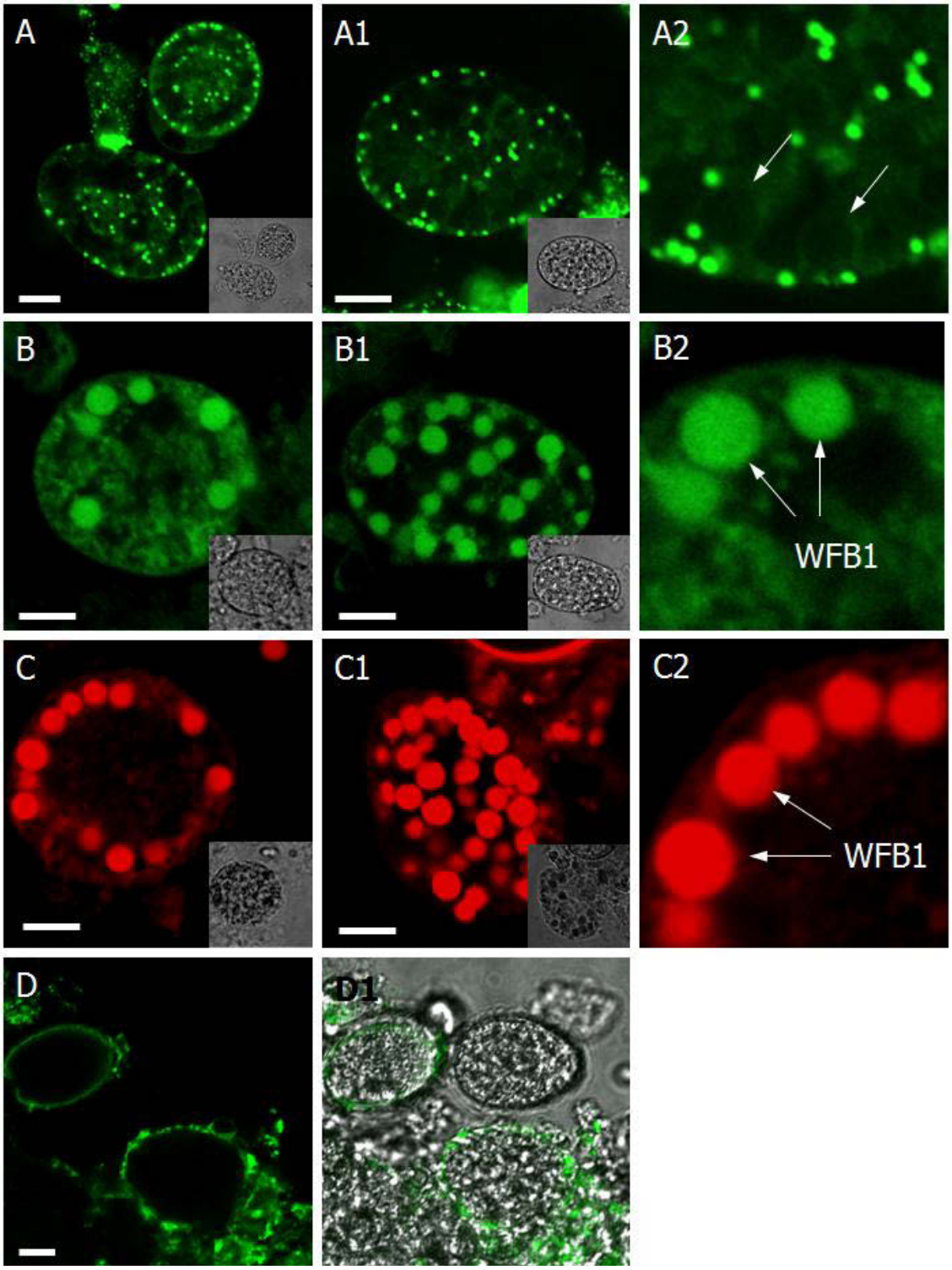

Figure 15: Uptake and internalisation of 40 and 100 nm beads by freshly harvested *E. maxima* gametocytes. Freshly harvested sexual stages were incubated with a solution containing either 40 nm (A-A2) or 100 nm beads (B-B2) for 45 minutes at room temperature. Cells were washed and distribution of the beads analysed by confocal microscopy. Note the different subcellular localisation of the two types of nano beads in the cytosol of mature macrogametocytes. A-A2 show 40 nm beads

concentrating within the small granules less than 2 μm in diameter revealing cytosolic green-fluorescing "trails", whereas the 100 nm beads accumulate within the large type 1 WFBs (arrows) in B-B2. Note the absence of fluorescing beads in WFB1s (arrows) in A2. Note the accumulation of the 100 nm beads in WFB1s in B2 (arrows). C-C2 Evans blue stained *E. maxima* macrogametocytes showing large type 1 WFBs. C2 shows a close-up of the WFB1s. Note the similar size, shape and staining of the WFB1s in C2 and B2.Confocal micrographs of freeze-thawed gametocytes with compromised cell membranes (D-D1), which were used as a negative control for these experiments, shows the lack of intracellular green fluorescence and accumulation of the beads at the surface of these cells. Inserts represent transmission detection. Bars: 5 μm. WFB1; wall forming bodies type 1.

4.3.4 Membrane dynamics of *E. maxima* sexual stages revealed by time-lapse video microscopy

To further analyse the membrane dynamics of macrogametocytes developing inside the infected enterocytes, we used time-lapse video microscopy and collected images at 5 minute intervals for a total of 40 minutes after placing the cells in culture medium. By analysing the time-lapse DIC micrographs, we were able to visualise the process of endocytosis based on the membrane dynamics of the infected enterocyte (Figure 16, A-F). Firstly, the changes in the membrane(s) in response to particle binding were observed in all macrogametocytes analysed (Figure 16, A-A2), indicating that the harvested cells are viable and have not been harmed by the isolation procedures. Secondly, a number of parasite-derived granules, approximately 1.5 μm in diameter, appeared to migrate from the parasite's peripheral cytoplasm toward the site of contact (Figure 16, a-a1). The apparent migration of these granules seemed to correspond with the remodelling of both the parasite's and host cell membrane at the regions of contact (Figure 16, a1-2). Thirdly, the apparent internalisation of the particle by the host cell membrane and subsequent absorption by the parasite membrane, suggests that this phenomenon is both parasite and host-cell dependent.

Analysis of early forming oocysts found in the culture medium by time-lapse microscopy also revealed the ability of the membrane underlying the forming oocyst wall to undergo changes typical of endocytosis as seen in Figure 16, B-B2. Moreover, the oocyst wall, which was identified as a physical barrier separating the parasite from the enterocyte cytosol, appeared continuous and uninterrupted (Figure 16, B, B1, B2). The cytoplasm bordering the oocyst wall appeared to give way to ridges at the parasite's

periphery, which coincided with the shrinkage and collapse of the host enterocytes (Figure 16, B1-B2 and b1-b2, arrowheads). The observed collapse of the host cell coincided with the progressive growth of the parasite. The appearance of a number of small vesicles in the periphery, approximately 2 μm in size, immediately followed this cytoplasmic remodelling (Figure 16, b1, b2, double arrows). This suggests that oocysts developing inside the infected enterocytes are capable of taking up and internalising host cell content. Negative control samples consisted of freeze-thawed gametocytes, which do not have intact membranes, spiked with fully formed and sporulated oocysts. No evidence of endocytosis or other changes in the membrane was observed in the sporulated oocysts (Figure 16, C-C2). Furthermore, the freeze-thawed gametocytes collapsed and disintegrated within the first 10 minutes of the experiment (Figure 16, C2). Based on these observations we concluded that the fresh parasites are capable of endocytosis *in vitro*.

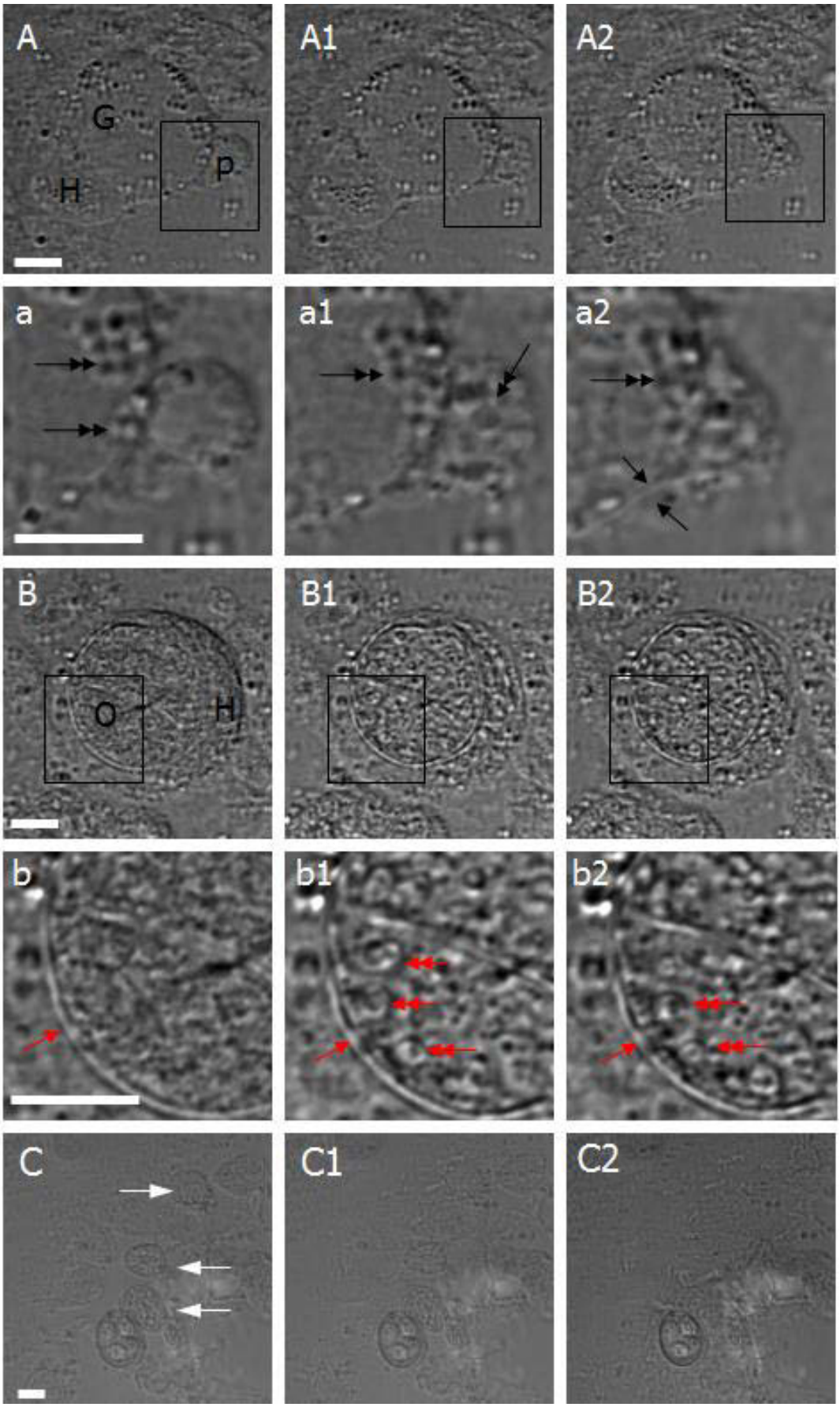
A
G
H
p
A1
A2
a
a1
a2
B
O
H
B1
B2
b
b1
b2
C
C1
C2

Figure 16: Live-cell imaging of freshly harvested *E. maxima* gametocytes using time-lapse video microscopy. Gametocytes were harvested from the infected chicken intestine (A-b2) and monitored *in vitro* by time-lapse video microscopy. (C-C2) Freeze-thawed macrogametocytes with compromised cell membranes were used as controls for these experiments. (A, a) DIC images were acquired at 5 minute intervals. Images of fresh gametocytes in panels A-A2 show intracellular gametocyte (g) occupying a single host cell (h) coming in contact with a large particle floating in the media (p). Note the presence of a few small parasite-derived granules accumulated at the contact site (a, double arrows). A1 Shows binding of the said particle with the parasite and/or host cell membranes, initiating internalisation (a1). Note the remodelling of the parasite and/or host membranes during internalisation (a1, a2), and recruitment of a large number of parasite-derived small vesicles to the contact site (a1, a2, double arrows). The host cell and parasite membranes are labelled with arrows in a2. B-b2 Show time-lapse images of an oocyst (O) developing inside the host cell (h). Note the shrinkage of the host cell with correlates with the growth of the intracellular oocyst. Note in B and b a fully formed oocyst wall (white arrow) separating the parasite from the host cell cytoplasm and a lack of any vesicles in the cytoplasm of a newly formed oocyst. B1-b1 show notable shrinkage of the host cell accompanied by emergence of a number of granules approximately 2 μm in diameter (double arrows) in the peripheral cytoplasm of an oocysts. Note the presence of membrane ridges in panels b1 (arrows). Panels C-C2 show freeze-thawed gametocytes (arrows) disintegrating in the first 10 minutes of the experiment. White bars indicate 10 μm. g; gametocyte, h; host, o; oocyst, p; particle.

4.3.5 Colchicine and cytochalasin D inhibit endocytotic capacity of sexual stage parasites

To gain insight into which of the possible cellular uptake mechanisms were responsible for nano bead internalization, the effect of two different endocytosis inhibitors, colchicine and cytochalasin D, was tested. The inhibitors were added separately at varying concentrations (between 0.01 μM – 100 μM Cytochalasin D and 0.05 mM – 50 mM Colchincine) prior to adding the beads (Figure 17 and 18). Colchicine was used to inhibit formation of microfilaments and microtubules, while cytochalasin D was to block actin elongation. In macrogametocytes, 40 and 100 nm bead endocytosis was reduced by colchicine in a concentration dependent manner (Figure 17). Cytochalasin D was found to reduce the entry into macrogametocytes of 40 and 100 nm beads also in a concentration dependent manner (Figure 18). In both cases, beads were detected only at the parasite's surface after treatment with concentrations of these drugs above 0.1 μM and 0.5 mM for Cytochalasin D and Colchicine respectively.

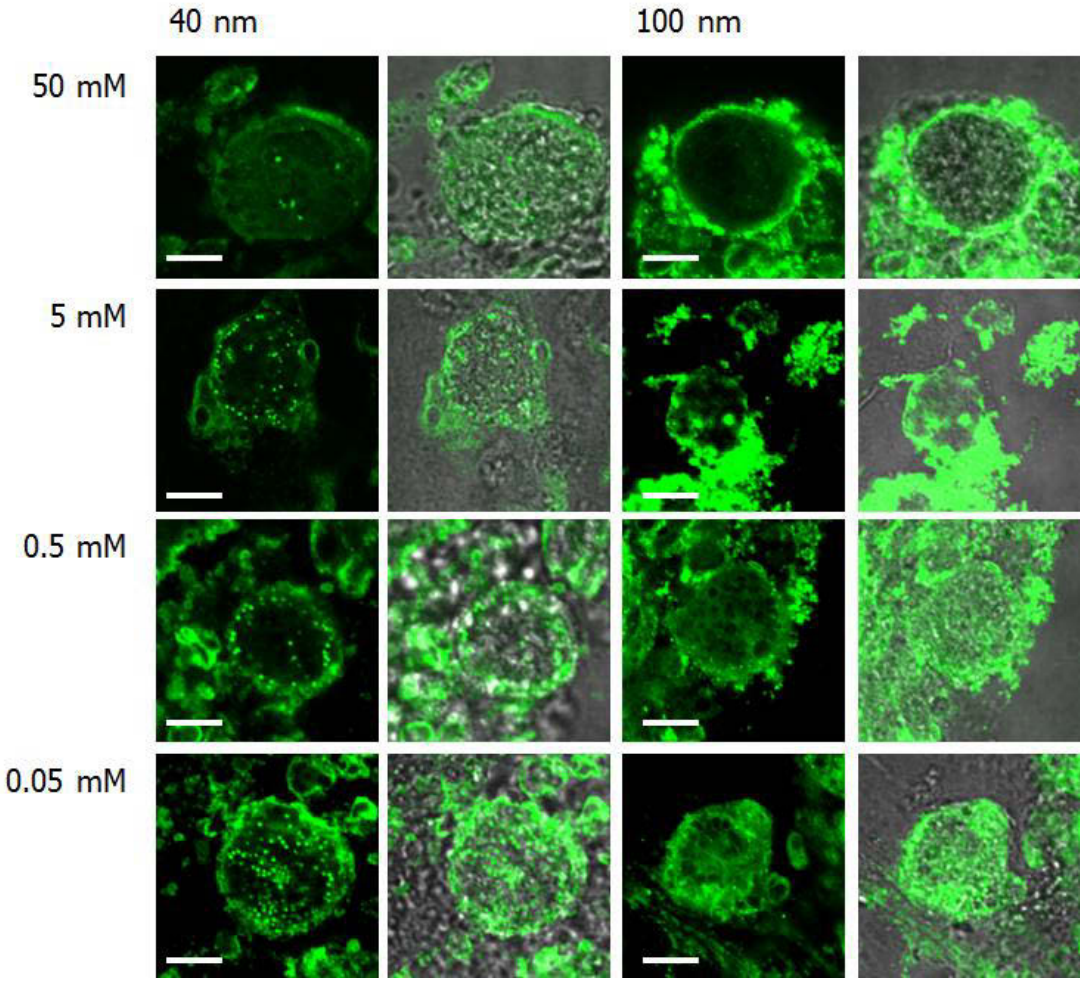

Figure 17: Effects of colchicine on internalization of nano beads. Fresh parasites were incubated in the presence of colcichine (0.05, 0.5, 5, 50 mM) for 45 min and co-incubated with 40 or 100 nm beads (columns indicated). Overlays of green fluorescence and transmission detection are displayed on the right of each column. Note the reduction in green fluorescence in the cytosol of cells incubated with 0.5 - 50 mM colchicne. Also note the gametocyte cell shape degeneration. Bar: 10 µm

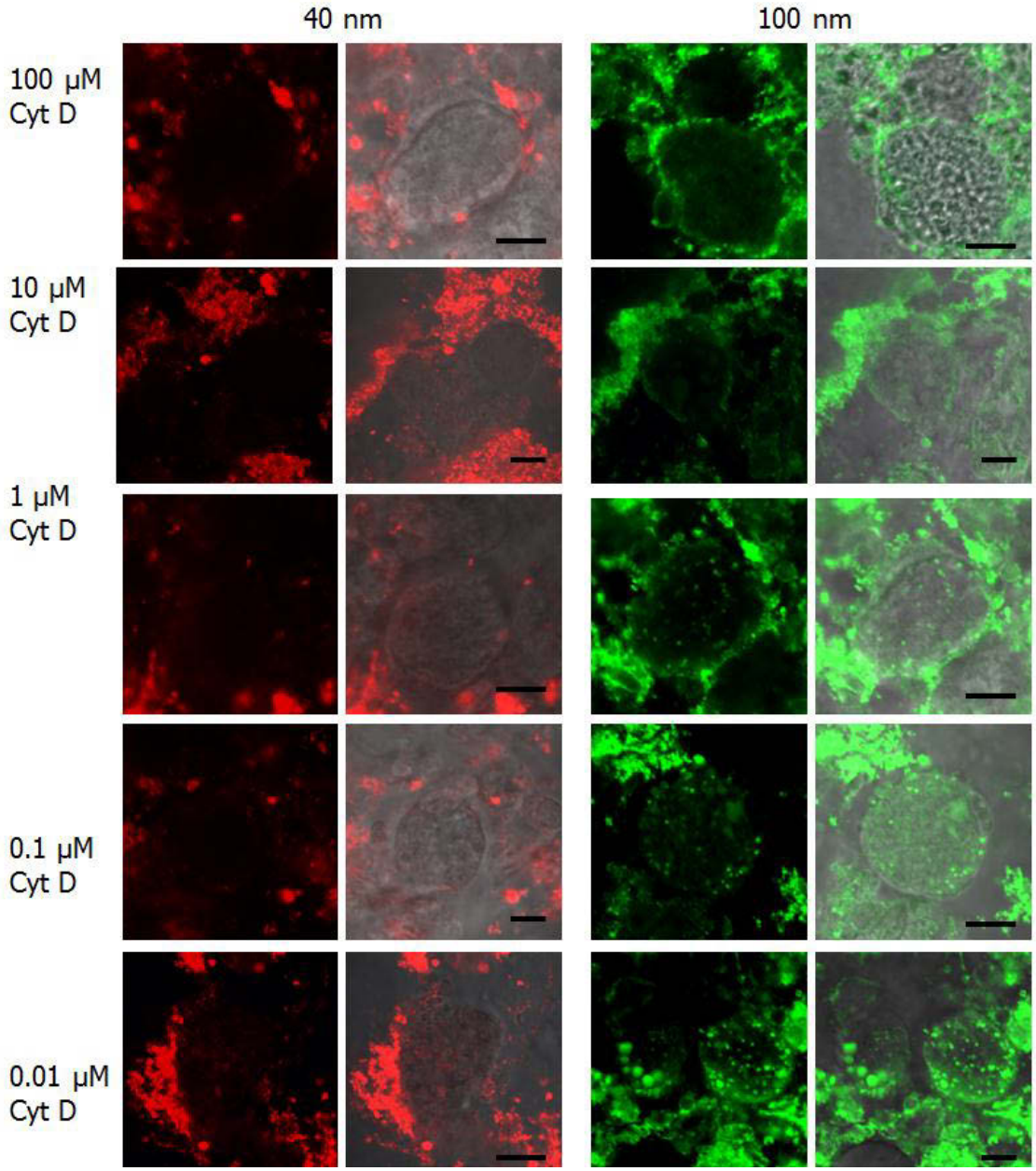

Figure 18: Effects of cytochalasin D on internalization of nano beads. Fresh parasites were incubated in the presence of cytochalasin D (0.01, 0.1, 1, 10, 100 µM) for 45 min and co-incubated with 40 or 100 nm beads (columns indicated). Overlays of green fluorescence and transmission detection are displayed on the right of each column. Note the reduction in the red (40 nm beads) and the green fluorescence (100 nm beads) in the cytosol of cells incubated with 0.1 - 100 µM cytochalasin D. Also note the degeneration of cell shape in drug treated gametocytes. Bar: 10 µm

4.3.6 Spatial distribution of actin and type 1 WFBs at different points of *E. maxima* sexual stage development

Given the central role actin plays in endoctyosis, we first analysed the subcellular distribution of actin at different stages of macrogametocyte maturation. Triton X-100 permeabilized cells were stained with a high-affinity probe for F-actin, Oregon Green 514 conjugated phalloidin (Life Technologies, USA), and co-incubated with Evans blue dye to highlight gametocyte type 1 WFBs and the outer oocyst wall (Figure 19). Using confocal microscopy, actin filaments were visible as longitudinal bundles of filaments occupying the entire cytoplasm of the mature macrogametocyte, and connecting the large type 1 WFBs, making them appear as "a bunch of grapes" (Figure 19, A-A2). Furthermore, type 1 WFBs stained with Evans blue appeared as large F-actin coated vesicles (Figure 19, A2).

In later stages of macrogametocyte maturation, the intensity of the staining and actin localisation changed. In pre-cyst macrogametocytes, actin was mainly localised at the periphery of forming oocysts (Figure 19, B-B2) revealing its ovoid shape, while in fully formed oocysts, actin was mainly localised to the oocyst wall (Figure 19, C-C2). Using Evans blue as a control to follow oocyst biogenesis, the dye highlighted large type 1 WFBs in late macrogametocytes and localised at the periphery of formed oocysts. The overlay of actin and Evans blue showed sites of co-localisation of these subcellular compartments (Figure 19, 3D volumes in C-C2), indicating involvement in the cell shape modification prior to oocyst wall formation.

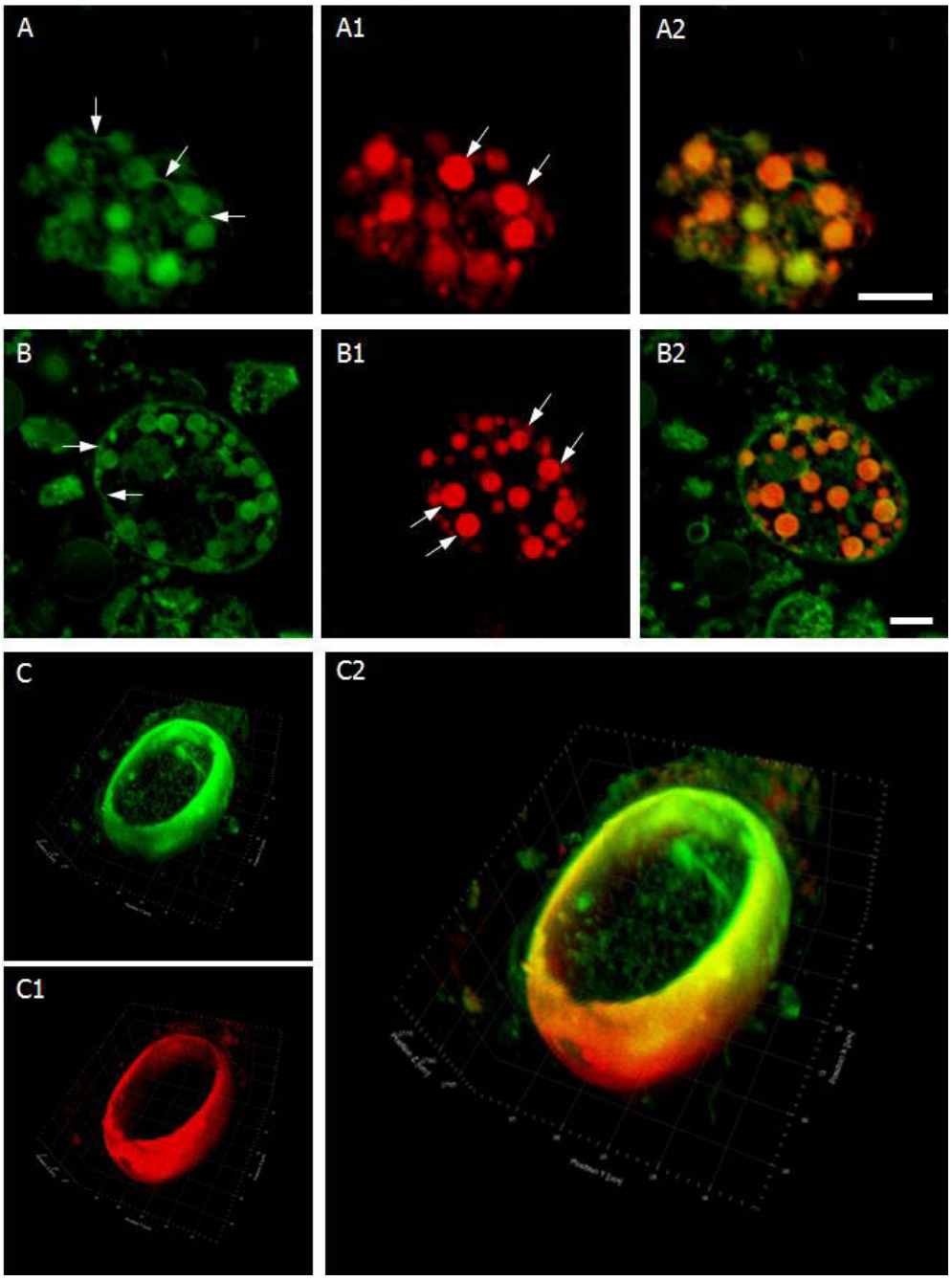

Figure 19: **Subcellular distribution of actin and spatial organisation of type 1 WFBs by confocal microscopy.** Isolated macrogametocytes were incubated with F-actin marker phalloidin conjugated to Oregon Green 514 (green) and Evan blue (red) to highlight type 1 WFBs. Cells were then analysed by confocal microscopy. Arrows in A, B and C indicate actin (green), while arrows in A1 and B1 indicate WFB1s and the outer oocyst wall in C1 (red). A2, B2, C2 are overlays. Note the co-localisation of F-actin (C1) and the type 1 wall forming body-derived material (A2) in the WFB1s and the oocyst wall (C2). Scale bars represent 5 µm. (C2) 3D projection image of the actin (green) and outer oocyst wall (red), which was reconstructed from 30 confocal z-stacks. Actin forms a 3D scaffold, which was stained with phalloidin (green). Quadrants in the volume indicate 5 µm.

We next analysed whether or not the actin cytoskeleton may be involved in the transport of WFBs. Freshly harvested sexual stages were incubated in the presence of cytochalasin D or colchicine, respectively over a period of 1 h. The samples were then processed for confocal microscopy using Oregon Green 514-phalloidin and Evans blue dye. Drug treated parasites showed a reduction in the intensity of Evans blue staining (Figure 20, "WFB1s" column), as well as reduced or abolished actin labelling of the cytosolic filaments (Figure 20, "actin" column). In addition, the drug-treated parasites displayed abnormal cell shapes with the Evans blue positive material found to be dispersed in the cytosol (Figure 20, "WFB1s" column). Only a few oocysts were detected.

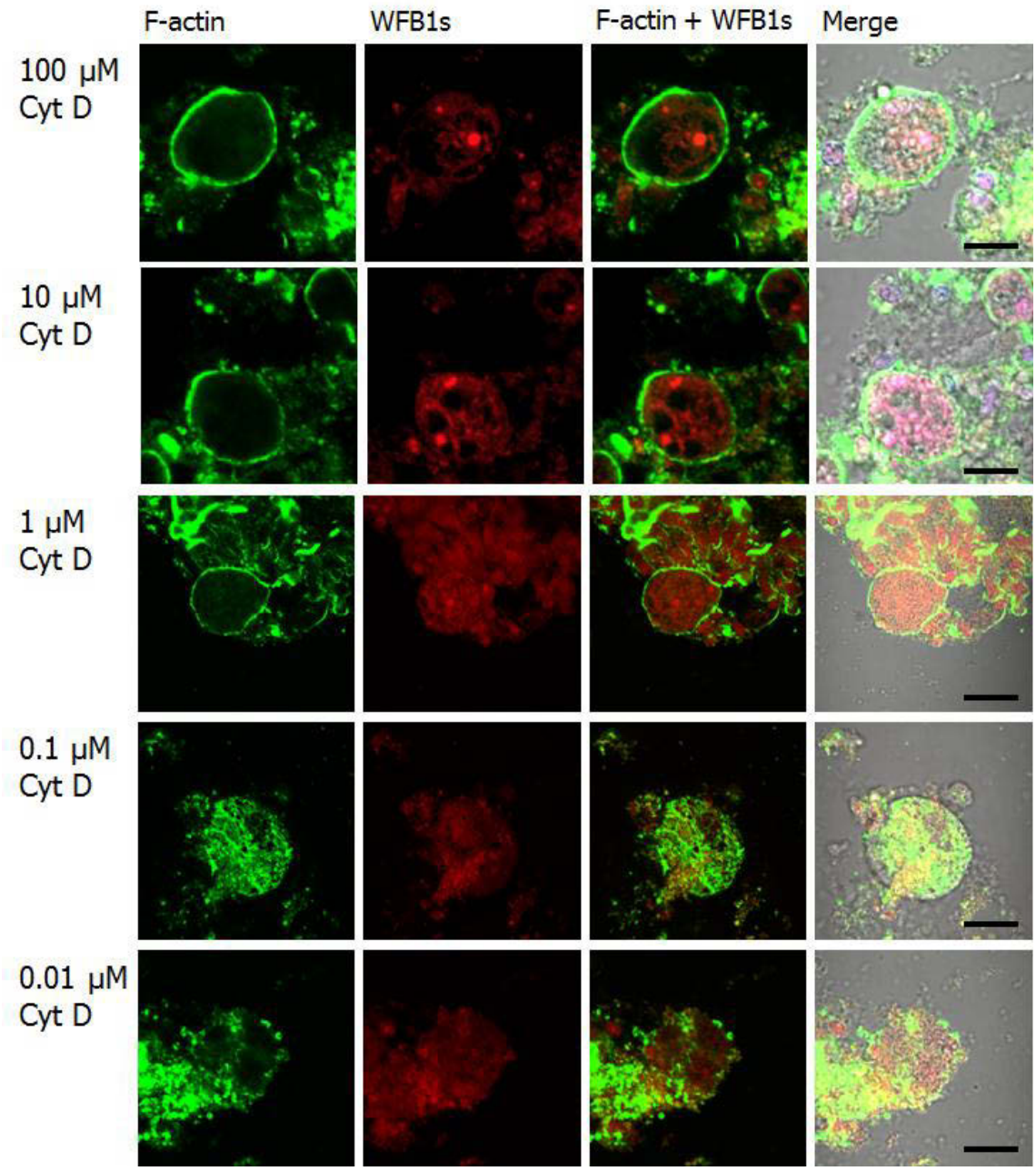

Figure 20: Effects of cytochalasin D on subcellular distribution of actin. Fresh parasites were incubated in the presence of cytochalasin D (0.01, 0.1, 1, 10, 100 µM) for 45 min. Following washing, the F-actin distribution was visualised with phalloidin conjugated to Oregon Green 514 (green) and WFB1s using the Evans blue (red) (columns indicated). Overlays of green fluorescence and transmission detection are displayed to the right. Note the distortion of the gametocytes shapes, the disruption (0.01 and 0.1 µM Cyt D) and the absence (1, 10, 100 µM Cyt D) of actin filaments in the cytosol, as well as the dispersion of the WFB1 material (red) in the cytosol of drug treated cells. Scale bars 10 µm.

4.3.7 Label-free quantitative proteomics reveals differentially abundant proteins in the extracted WFBs

A shotgun proteomics approach using LC-MS/MS was employed to identify molecules with a potential role in vesicle and protein trafficking. Purified *E. maxima* macrogametocytes were lysed, processed and filtered to produce a final filtrate that was highly enriched with wall forming bodies as described Chapter 3. The extract was tested by Western blotting and IFA using antibodies to the known WFB proteins, EmGam 56 and EmGam 82, which as expected were found to be highly enriched in this fraction.

As a negative control for our extraction procedure, uninfected enterocytes purified from control, untreated chickens were processed using the same method employed to extract gametocyte WFBs isolated from infected chickens. The final filtrate produced from uninfected enterocytes was analysed by SDS-PAGE and silver staining (Figure 21, A), where we found that we were unable to detect any host protein bands (Figure 21, A, lane 3).

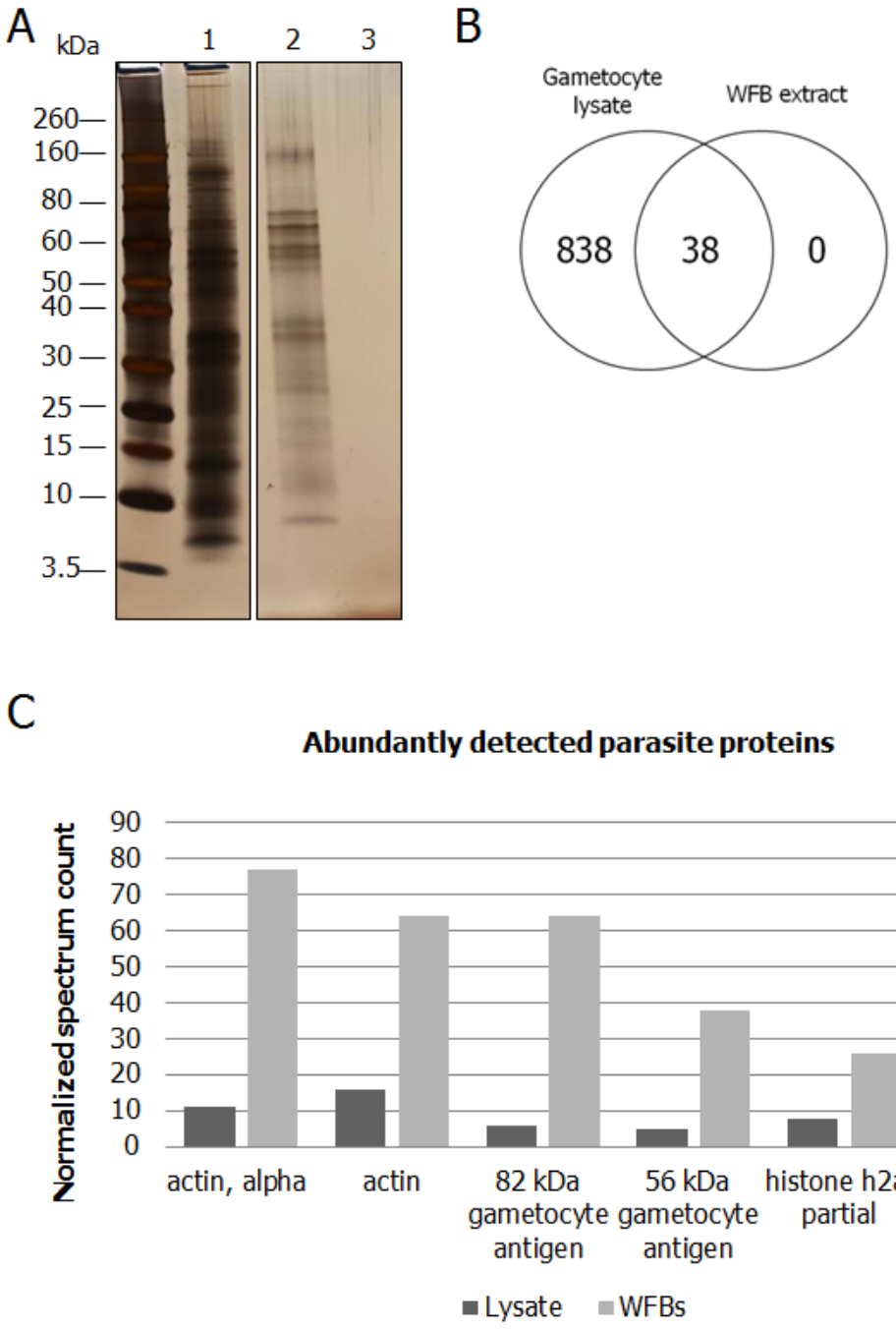

Figure 21: Identification of proteins in the WFBs extracted from *E. maxima* macrogametocytes. (A) Silver stained 4-12% SDS-PAGE Bis-Tris gel showing the protein content of fractionated un-infected enterocytes. Lane 1, the lysate of disrupted un-infected enterocytes. Lane 2, the flowthrough. Lane 3 is the retaintate, which in fractionated gametocytes results in accumulation of the parasite WFBs. Note the absence of proteins in the retaintate. kDa, protein marker. (B) Venn diagram comparing the distribution of total proteins detected in the gametocyte lysate versus the WFB extract. Numbers represent the number of proteins that are either shared between the two samples (overlapping areas) or that are detected in single sample. (C) Comparison of spectrum counts assigned to each parasite specific protein detected in the gametocyte lysate versus the WFB extract.

To identify parasite specific proteins in the WFB-rich extract, multiple protein databases were used for peptide matching. First, peptides generated from mass spectrometry were matched against all *Eimeria-specific* and other available protein sequences in the NCBI database (including several closely related parasitic protozoan parasites), yielding 838 protein identifications in the gametocyte lysate and 38 in the WFB extract (Figure 21, B). After the removal of redundancies and additional blast searches, 18 proteins out of the initial 38 were found to either be enriched or depleted in the WFB rich fraction as determined by spectral counting when compared to the gametocyte lysate (Table 1 lists all 18 proteins). Seven of these proteins were predicted to be parasite derived and the remaining eleven were predicted to originate from the chicken host enterocytes in contrast to the results seen by gel analysis. Of the seven parasite proteins identified in the WFB extract, 6 were found to be highly enriched and abundant in comparison to the gametocyte lysate (Figure 21, C). Based on spectral counting there was a 7.4 and 10.0 fold enrichment of the two WFB gametocyte glycoprotein antigens, EmGam 56 and EmGam 82, respectively (Table 2). Also highly abundant and enriched in the WFB extract was actin (Figure 21, C), which showed a 7.0-fold increase in the WFB proteome similar to that seen for EmGam 56 (Table 2). Unexpectedly, two additional parasite proteins, histone H2a and elongation factor 1-alpha (Figure 21, C), were also highly abundant and enriched in the WFB dataset and showed a 3.1 and 4.1-fold increase in concentration respectively (Table 2).

Table 1. List of non-redundant proteins identified in the *Eimeria maxima* WFBs-rich fraction.

Accession	Protein description	Mr	Mascot score	Matches[a]	Sequences[b]	emPAI[c]
Predicted parasite proteins						
XP_002369663.1	Actin	42 kDa	722	23(6)	18(5)	0.99
EPR56714.1	Alpha actin	42 kDa	544	16(6)	13(4)	0.84
gi|38565038	82 kDa gametocyte antigen	66 kDa	451	11(5)	9(5)	0.71
XP_672153.1	Histone H2a	27 kDa	286	8(2)	7(2)	0.41
gi|38565038	56 kDa gametocyte antigen	53 kDa	281	7(3)	7(3)	0.35
XP_002697543.1	Translation elongation factor 1-alpha	50 kDa	104	3(0)	3(0)	0.05
XP_004830556.1	Tubulin alpha-1 chain	49 kDa	55	2(0)	2(0)	0.06
Predicted host proteins						
NP_990263.1	Keratin type II cytoskeletal cochleal	54 kDa	920	24(10)	21(9)	1.17
NP_990605.1	Myosin-11	230 kDa	351	8(1)	8(1)	0.07
XP_003207675.1	Desmin-like	52 kDa	336	9(2)	9(2)	0.2
XP_003208007.1	Voltage-dependent anion-selective channel protein 2-like	30 kDa	108	2(1)	2(1)	0.23
XP_005063062.1	Pancreatic alpha-amylase-like, partial	57 kDa	80	2(1)	2(1)	0.06
650770B	Fibrinogen alpha chain-like	49 kDa	71	1(1)	1(1)	0.07
XP_004634344.1	Heterogeneous nuclear ribonucleoprotein A1-like	34 kDa	69	1(1)	1(1)	0.10
XP_003786336.1	Peptide YY	4 kDa	68	2(0)	2(0)	2.65
NP_990598.1	Nucleophosmin	10 kDa	57	1(1)	1(1)	0.32
XP_003257910.1	Fibrinogen beta chain isoform 2	12 kDa	56	1(1)	1(1)	0.27
gi|326492520	Predicted protein	54 kDa	55	1(1)	1(1)	0.06

[a]Number of matching peptides

[b]Number of proteins matching the same set of peptides

[c]The Exponentially Modified Protein Abundance Index (emPAI), which is an approximate, label-free, relative quantitation of the proteins in a mixture based on protein coverage by the peptide matches in a database search result.

Mass spectrometry analysis showed that the overall number of chicken proteins identified was reduced significantly in the WFB extract (Figure 22, A). Eight of these host proteins were found to either increase or decrease in concentration in the WFB extract. Spectral counting showed that the fold enrichment of transcription regulators (nucleophosmin and histone 1), structural proteins (keratin and desmin) and transport proteins (voltage-dependent anion-selective channel protein and putative solute carrier protein) varied from 2.5 to 8.2-fold (Figure 22, B and Table 2). In contrast, host protein myosin had a significant 3 to 4-fold decrease in the WFB dataset, showing that only a specific subset of host proteins were enriched in the extracted WFBs.

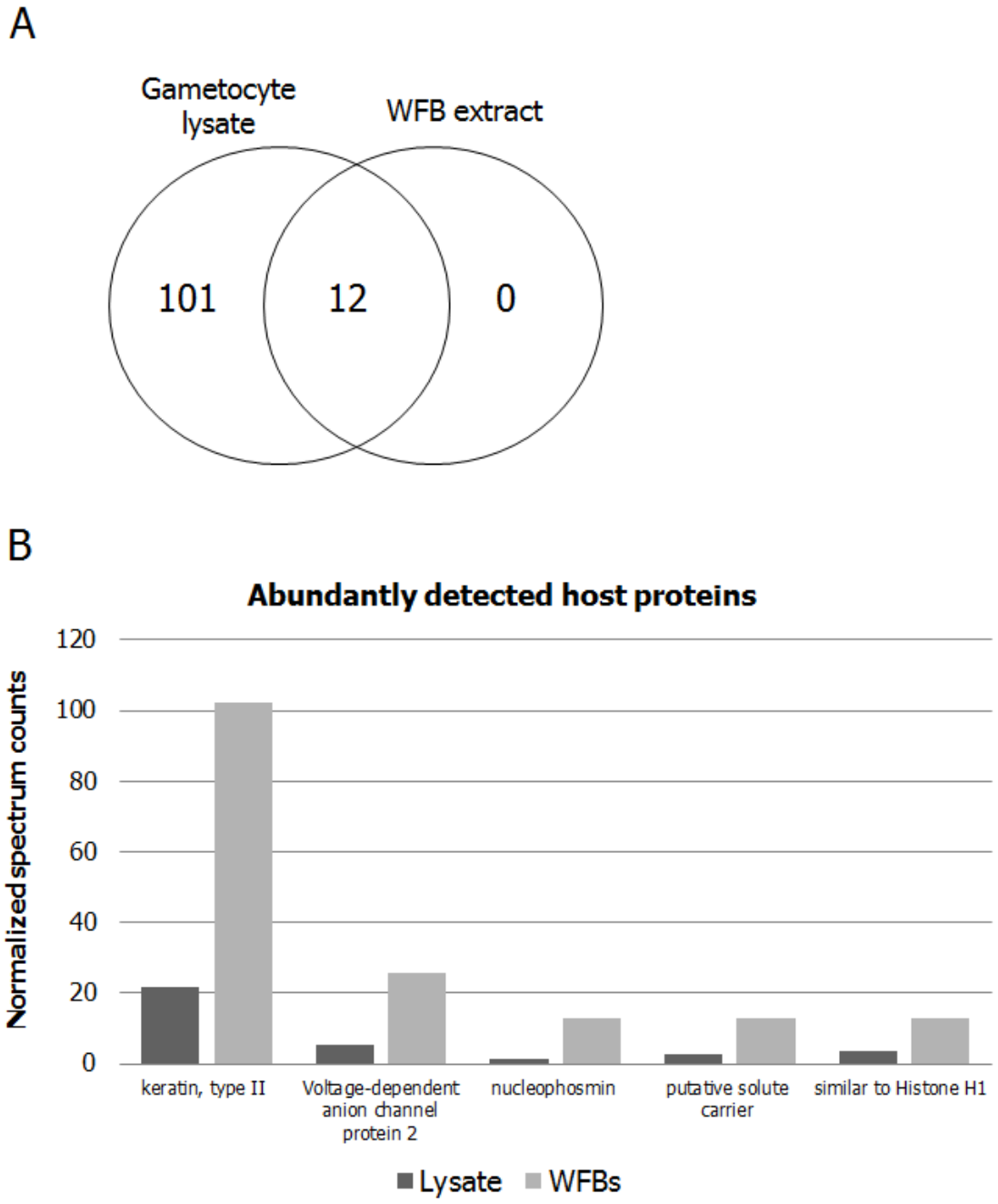

Figure 22: Identification of predicted host chicken proteins in the WFB extract. (A) Venn diagram depicting the distribution of host proteins detected in the gametocyte lysate versus the WFB extract. Numbers represent the number of proteins that are either shared between the two samples (overlapping areas) or that are detected in single sample. (B) Comparison of spectrum counts assigned to each host protein detected in the gametocyte lysate versus the WFB extract.

Table 2. LC-MS/MS spectral counts of abundantly detected proteins in the *Eimeria maxima* WFB-rich fraction.

			Isolated WFBs		**Gametocyte lysate**		
Accession	**Protein description**	**Mr**	**Sequence coverage**	**Spectral count[a]**	**Sequence coverage**	**Spectral count[a]**	**Fold enrichment[b]**
Predicted parasite proteins							
EPR56714.1	Actin, alpha	42 kDa	17%	77	37%	11	7.0
ABD64377.1	Actin	42 kDa	18%	64	43%	16	4.1
gi|38565038	82 kDa gametocyte antigen	66 kDa	11%	64	28%	6	10.0
gi|25989587	56 kDa gametocyte antigen	53 kDa	6.1%	38	25%	5	7.4
XP_672153.1	Histone H2a, partial	22 kDa	6.9%	26	28%	8	3.1
CAA11847.1	Elongation factor 1- alpha	50 kDa	6.3%	13	11%	3	4.1
Predicted host proteins							
gi|45384378	Keratin, type II cytoskeletal cochleal	54 kDa	23%	102	67%	22	4.7
gi|11134020	Voltage-dependent anion-selective channel protein 2	30 kDa	16%	26 26	44%	5	4.9
gi|2959450	Desmin	52 kDa	6.5%		35%	10	2.5
gi|45383996	Nucleophosmin	33 kDa	9.9%	13	20%	2	8.2
gi|197127557	Putative solute carrier family 25 member 6 variant 1	33 kDa	3.4%	13	17%	3	4.9
gi|50729210	Similar to Histone H1	22 kDa	6.9%	13	28%	4	3.5
gi|3915778	Myosin heavy chain 11	229 kDa	0.91%	13	37%	36	0.4
gi|45382693	Myosin-9	227 kDa	1.1%	13	40%	45	0.3

List of all abundantly detected proteins identified in the WFB extract. Proteins are sorted according to highest spectral counts (abundance) with fold-enrichments shown in the last column.

[a]Normalized abundance intensities of a given protein in WFBs or the gametocyte lysate.

[b]Fold-enrichment is the ratio between the average of spectral counts detected for a given protein in the WFB proteome versus the average spectral counts detected for the same protein in the gametocyte lysate

In order to try and identify additional WFB specific proteins, a search was performed using closely related and publically available *E. tenella* database of predicted proteins along with the host *Gallus gallus* and *Homo sapiens* protein databases. Over 70 WFB proteins were found to be parasite specific as listed in Table 3. Apart from the expected EmGam 56 glycoprotein, the list of *Eimeria* specific proteins included those involved with stabilization of cytoskeleton (actin, alpha depolymerising factor, alpha and beta tubulin, Ras family domain-containing protein), vesicular trafficking (dynein cytoplasmic and heavy chain proteins, myosin heavy chain and myosin light chain kinase, 14-3-3 protein) and membrane docking (ankyrin repeat protein with transmembrane domains, Plekstrin homology domain-containing protein, calmodulin, Receptor for activated C kinase) (Table 3). Also identified were two proteins with presumed roles in processing of the gametocyte antigen, EmGam 56, during oocyst wall formation (eimepsin 2 and subtilisin) (Table 3), as well as a number of additional proteins involved in translation, protein folding and carbohydrate metabolism (Table 4).

Table 3. List of *Eimeria* specific proteins detected in the *Eimeria maxima* WFBs-rich fraction.

Accession	Description[a]	Biological process[b]
Oocyst proteins/enzymes		
ETH_00007315	56 kDa gametocyte antigen	oocyst wall formation
ETH_00020205	Eimepsin 2, partial	oocyst wall formation
ETH_00023365	Subtilisin-like	proteolysis, oocyst wall formation
Cytoskeletal		
ETH_00020315	Actin depolymerizing factor	actin filament depolymerization
ETH_00009555	Actin	mediators of internal cell motility
ETH_00010000	Ankyrin repeat protein, signal peptide	microtubule organisation, ancors proteins to membranes
ETH_00002520	Beta tubulin	microtubule-based process
ETH_00032320	Calmodulin, putative	cytoplasmic and organellar calcium sensor
ETH_00021280	Cytoplasmic dynein intermediate chain	transports cargo by "walking" along microtubules
ETH_00004415	Dynein heavy chain	motility of vesicles and organelles along microtubules
ETH_00029760	Myosin heavy chain	actin ATP-dependent motor, moves cargo vesicles
ETH_00015345	Myosin light chain kinase	regulates movement of vesicles along actin fibres
ETH_00028380	Ras family domain-containing protein	Regulates signalling pathways and actin cytoskeletal integrity
ETH_00033310	Tubulin alpha chain	microtubule-based process
ETH_00028620	Plekstrin homology domain-containing protein	lipid binding specificity, regulation of cell-matrix adhesion
Transport		
ETH_00007980	14-3-3 protein	cellular membrane organisation, protein targeting
ETH_00021075	Facilitative glucose transporter	carbohydrate transport, transport
ETH_00008600	Fructose-1,6-bisphosphate aldolase	carbohydrate transport, transport
ETH_00008120	Plant ubiquilin	selects ubiquitin-conjugates for destruction
ETH_00010940	Ubiquitin / ribosomal protein CEP52 fusion protein	selects ubiquitin-conjugates for destruction

ETH_00005270	ATP synthase alpha chain	hydrogen ion transport
ETH_00026650	Receptor for activated C kinase, RACK protein	regulation of protein localization

List of all *Eimeria* specific proteins identified in the WFB-rich fraction according to *E. tenella* database housed within ToxoDB.org (v8.2)
Only proteins with a minimum of 2 unique peptides, a peptide -10logP ≥ 22.5 and a FDR (peptide spectrum matches) equal to 2.0% were included in the list
[a]Identity of proteins assigned by *E. tenella* database housed within ToxoDB.org (v8.2)
[b]Biological function assigned based on Swissprot.org and Uniprot.org

Table 4. List of *Eimeria* specific proteins detected in the *Eimeria maxima* WFBs-rich fraction.

Enzymes		
ETH_00020140	Deoxyxylulose 5-phosphate synthase, partial	1-deoxy-D-xylulose 5-phosphate biosynthetic process
ETH_00008865	Glyceraldehyde-3-phosphate dehydrogenase	carbohydrate metabolism, glycolysis
ETH_00039380	Phosphoglycerate mutase, related	carbohydrate metabolism, spermatogenesis
ETH_00011175	Proteasome subunit alpha type 4 subunit	protease, host-virus interaction
Signal transduction		
ETH_00011145	Pyruvate kinase	carbohydrate metabolism
ETH_00015140	Phosphoglycerate kinase	carbohydrate metabolism
ETH_00006810	DnaJ domain-containing protein, putative	response to heat, protein folding
Transcription and translation		
ETH_00012285	Cell division cycle protein related	cell cycle, transcription, mRNA processing
ETH_00025480	mRNA capping enzyme	mRNA processing, host-pathogen interaction
ETH_00007055	Bromodomain-containing protein	chromosome segregation
ETH_00017420	Prohibitin	inhibits DNA synthesis
ETH_00024795	40S ribosomal protein S11	translation initiation, elongation and termination
ETH_00036875	40S ribosomal protein S13	translation initiation, elongation and termination
ETH_00004575	40S ribosomal protein s14	translation initiation, elongation and termination
ETH_00012530	40S ribosomal protein S18	translation initiation, elongation and termination
ETH_00024835	40S ribosomal protein S2	translation initiation, elongation and termination
ETH_00032325	40s ribosomal protein S20	translation initiation, elongation and termination
ETH_00016415	40S ribosomal protein S21	translation initiation, elongation and termination
ETH_00022265	40S ribosomal protein S28	translation initiation, elongation and termination
ETH_00024855	40S ribosomal protein S3	translation initiation, elongation and termination
ETH_00009830	40S ribosomal protein S8	translation initiation, elongation and termination

ETH_00013610	40S ribosomal protein S9	translation initiation, elongation and termination
ETH_00002815	60S ribosomal protein L10	translation initiation, elongation and termination
ETH_00009250	60S ribosomal protein L12	translation initiation, elongation and termination
ETH_00026515	60S ribosomal protein L13	translation initiation, elongation and termination
ETH_00024285	60S ribosomal protein L23 H80	translation initiation, elongation and termination
ETH_00031600	60S ribosomal protein L24	translation initiation, elongation and termination
ETH_00012265	60S ribosomal protein L9	translation initiation, elongation and termination
ETH_00020700	Ribosomal protein L11	translation initiation, elongation and termination
ETH_00018650	Ribosomal protein L15	translation initiation, elongation and termination
ETH_00019820	Ribosomal protein L32	translation initiation, elongation and termination
ETH_00001185	Ribosomal protein S23	translation initiation, elongation and termination
ETH_00016635	Histone H2A	centrosome duplication, nucleosome assembly
ETH_00028290	Histone H2B_ related	centrosome duplication, nucleosome assembly
ETH_00016640	Histone H3	centrosome duplication, nucleosome assembly
ETH_00028080	Histone H4	centrosome duplication, nucleosome assembly
ETH_00018735	Translation initiation factor eif-2b epsilon subunit, possible	protein biosynthesis
ETH_00021645	GTP-binding nuclear protein	ribosome biogenesis
ETH_00010290	Elongation factor alpha	transcription, transcription regulation
ETH_00028310	Eukaryotic translation initiator factor 4A	host-virus interaction, protein biosynthesis
ETH_00008605	Polyadenylate-binding protein	nonsense-mediated mRNA decay, mRNA processing, mRNA splicing
ETH_00007715	Proliferating cell nuclear antigen 1	DNA damage, repair, replication
ETH_00001495	R1 protein	DNA damage, repair, replication
ETH_00007155	RNA pseudouridine synthase domain containing protein	alternative splicing, polymorphism
ETH_00018150	RNA recognition motif-containing protein	DNA recombination and repair

ETH_00009730	Purine nucleoside phosphorylase	purine metabolism
Unclassified		
ETH_00029250	Penicillin amidase domain-containing protein	hydrolase activity in linear amides
ETH_00016590	*Eimeria*-specific protein [*Eimeria* maxima]	unknown
ETH_00002460	Immune mapped protein 1	a new vaccine candidate, IMP-1, inhibition of cell invasion
ETH_00010065	Zinc finger (CCCH type) protein	apoptotic process,
ETH_00005075	Gbp1p protein	unknown

List of all *Eimeria* specific proteins identified in the WFB-rich fraction according to *E. tenella* database housed within ToxoDB.org (v8.2)
Only proteins with a minimum of 2 unique peptides, a peptide -10logP ≥ 22.5 and a FDR (peptide spectrum matches) equal to 2.0% were included in the list
[a]Identity of proteins assigned by *E. tenella* database housed within ToxoDB.org (v8.2)
[b]Biological function assigned based on Swissprot.org and Uniprot.org

4.4 Discussion

The findings reported here using a variety of microscopic and biochemical methods have shown that the sexual stages of *E. maxima* can internalize exogenous material across parasite membranes. This is based on results found using a variety of methods including scanning electron microscopy where we observed that the surface of all of the freshly isolated, unfixed macrogametocytes and early oocysts contained invaginations and pores. Our results are in agreement with previously published findings using TEM to study the surface membrane of *E. maxima* macrogametocytes (Mehlhorn, 1971). In addition, using time lapse microscopy and confocal microscopy on isolated gametocytes, we observed the internalisation of particles from the external milieu into the parasite cytoplasm. Using markers for actin and type 1 WFBs, we characterised for the first time the spatial distribution of actin before and after treatment with inhibitors, indicating that endocytosis was the predominant route of nanoparticle entry into gametocytes *in vitro*. These results taken together indicate that both isolated gametocytes and early stage oocysts of *E. maxima* are viable *in vitro* and are capable of the active uptake of external particles via endocytosis.

Our studies showed that sexual stage parasites were able to uptake both 40 and 100 nm beads and internalised them *in vitro,* however, their subcellular distribution after internalisation was found to be size dependent. We observed that the smaller 40 nm beads were distributed within small cytosolic granules reaching 0.5 - 1.5 µm in diameter, whereas the 100 nm beads accumulated within the large type 1 WFBs. These results suggest that there are different endocytotic pathways used by the parasite dependent upon the size of the particle. In addition, it appeared that the type 1 WFBs have the ability to specifically attract and bind exogenous material.

We found that in *E. maxima* macrogametocytes and oocysts, the transport of WFBs to the periphery of the parasite and subsequent oocyst wall formation was dependent upon having intact actin and tubulin filaments. This conclusion was based on the finding that gametocytes treated with actin and tubulin inhibitors showed dispersion of the WFBs in the cytoplasm as well as deformed and incomplete oocyst walls in both gametocytes and oocysts. We used IFA to further elucidate the role of actin in the transport of WFB

organelles to the periphery of the cell. We found that actin formed a filamentous network in the cytosol of the macrogametocytes, and linked the type 1 WFBs together to appear as "beads on a chain". In addition, there were also shorter actin filaments observed on the parasite's cell surface, which were found to co-localise with the early oocyst wall. Thus, we concluded that actin is a very crucial molecule involved in WFB formation, transport and oocyst wall formation.

To try and identify other molecules involved in WFB transport and oocyst wall formation, we enriched for the wall forming bodies isolated from macrogametocytes using a previously published method (Frölich et al., 2013). We then used a label-free quantitative shotgun approach to identify the extracted parasite specific peptides. The initial screening was performed using a large number of eukaryotic as well as parasite-specific predicted protein databases. However, only a relatively small number of parasite proteins were identified. As a second screening step, proteins predicted from a first draft genome sequence of a closely related *Eimeria* species, *E. tenella*, together with the host chicken genome was incorporated into the workflow in order to identity additional parasite specific proteins. Apart from the expected WFB-specific proteins, EmGam 56 and EmGam82, we detected a number of other parasite specific proteins. These included major components of the cytoskeleton (actin and tubulin), as well as regulators of cell shape and actin reorganization (dynein, ankyrin, calmodulin, Pleckstrin homology domain-containing protein and 14-3-3 transport protein, etc.), which are all involved in the transport of intracellular vesicles and cargo along microfilaments and microtubules (Miki et al., 2005; Thompson and Langford, 2002; van den Heuvel and Dekker, 2007). Together with the actin localisation and drug inhibition studies, these results indicate that both actin and tubulin play an important role in the transport of WFBs during sexual stage development and oocyst wall formation.

Our data also revealed the presence of two parasite specific proteases, eimepsin and subtilisin, which are proteolytic enzymes known to play an important role in host cell invasion, remodelling and egress in Apicomplexa (Li et al., 2012). These two proteases were identified in gametocyte specific gene expression studies using *E. tenella* (Katrib et al., 2012) where they were found to be strongly upregulated in the sexual stages of development. Their co-purification with the WFBs has led us to also predict that they are directly involved in protein processing and wall formation in *E. maxima*. Further

studies on the subcellular location of these proteases by IFA are needed in order to confirm this finding.

We found that SDS-PAGE and silver staining failed to detect host protein in material extracted from the un-infected enterocytes. In addition, in our previous studies comparing proteins extracted from host cells to those from gametocytes or enriched WFBs (Frölich et al., 2013), little or no host contamination was found. In contrast, by mass spectrometry and spectral counting we detected a few chicken proteins in the macrogametocyte WFB extract isolated from infected enterocytes that were relatively abundant. Of these, six were highly enriched in the WFB extract (nucleophosmin, putative solute carrier protein, voltage gated channel protein, keratin, desmin, similar to Histone H1 protein), while host myosin proteins were found to be depleted in the WFB extract. Our results indicated that there is a specific enrichment and depletion of these host proteins in the WFBs of macrogametocytes. In support of this conclusion, our results using fluorescent nano beads showed that the parasite does internalize material from the external milieu ending up in the type 1 WFBs. Thus, it is not unexpected to find host proteins associated with the WFBs. Further studies on the mechanisms and specificity of endocytosis during sexual stage development are required to further elucidate this specific enrichment of host proteins into the WFBs and its importance in sexual stage development in *Eimeria*.

4.5 Conclusions

We have shown that *E. maxima* macrogametocytes and oocysts isolated from infected chickens, are capable of the uptake of exogenous molecules via endocytosis, and that this internalisation process depends upon the integrity and dynamics of the parasite cell membrane. Using *in vitro* culture techniques in combination with SEM, we have measured the size of micropores observed at the surface of sexual stage parasites. In addition, using time-lapse live cell and confocal microscopy, we observed parasite membrane dynamics and characterized the endocytotic pathways using fluorescently-labelled nano beads. Our results showed that actin and tubulin play an important role in endocytosis as well as in the transport of WFBs to the parasite periphery ending in the incorporation of the WFB cargo into the oocyst wall. Indeed, the finding that actin and tubulin inhibitors induced WFB dispersion and cell deformities provided evidence for

this. Our proteomic analysis showed that *E. maxima* WFBs contain proteins of both parasite and host origin, that are specifically enriched in these organelles. Therefore, our findings contribute to the overall understanding of the sexual stage development and have also identified some potential targets that can be used for new drug development in the future.

UNIVERSITY OF TECHNOLOGY, SYDNEY

Chapter 5

Paper IV: In vivo targeting of Eimeria maxima sexual stages with antibodies raised against Wall Forming Bodies

Declaration

I declare that the following publication included in this thesis in lieu of a chapter meets the following:

- More than 50% of the content in the following publication included in this chapter has been planned, executed and prepared for publication by me
- The work presented here has been peer-reviewed and accepted for publication
- I have obtained approval to include the publication in this thesis from the Publisher
- The initial draft of the work has been written by me and any subsequent changes in response to co-authors and editors reviews was performed by me
- The publication is not subject to any obligations or contractual agreements with a third party that would constrain its inclusion in the thesis.

Publication title: *In vivo* localisation of antibodies raised against Eimeria maxima Wall Forming Bodies during sexual intracellular development

Authors: Sonja Frölich, Annisha Shahparee, Valerie C. Wasinger, Michael Wallach

Candidate's contribution (%): above 50 %

Journal name: Parasitology

Volume/ page numbers: in press

Status: under review (manuscript number: PAR-2014-0054.R2)

I declare that the publication above meets the requirements to be included in the thesis

Candidate's name: Candidate's signature: Date (dd/mm/yy):

5.1 Brief Introduction:

Eimeria is a member of the protozoan parasitic phylum Apicomplexa, which includes parasites which pose major health threats to humans and domestic animals globally. Coccidiosis is one of these important diseases caused by several different species of the genus *Eimeria*, and is responsible for significant losses of revenue in the chicken industry of about 2 billion dollars per annum. Like other apicomplexans, the *Eimeria* parasite undergoes a complex life cycle (i.e. sporogony, merogony, gamogony) in the epithelial cells lining the intestinal mucosa of infected host. The parasite is transmitted by environmentally stable oocysts, which develop as a result of sexual reproduction, whereby male gametes (micro-) fertilize the female (macro-) gametocytes.

We and others have studied the antibody response to *Eimeria* sexual stage parasites and showed that chickens exposed to a live *Eimeria* infection secrete highly protective anti-gametocyte antibodies that can be transferred via passive or maternal immunization to young offspring chicks (Wallach, 1997; Wallach, 2010; Wallach et al., 1992; Wallach et al., 1990; Wallach et al., 1995a; Wallach et al., 1995b; Wallach et al., 1989). These antibodies act to markedly reduce parasite development and oocyst shedding thus preventing the transmission of the disease (i.e. transmission blocking immunity). Indeed, this principle has been used in the development of a subunit vaccine against coccidiosis, CoxAbic. Over the years research has been carried out on the molecular basis for the immunity induced by this vaccine, however, no direct evidence was provided showing that the induced anti-gametocyte antibodies are capable of reaching the parasites developing in the intestinal epithelial cells *in vivo*.

In order to evaluate the ability of anti-gametocyte IgG to reach *E. maxima* macrogametocytes *in vivo,* chickens were immunized with *E. maxima* purified WFB antigens and 1 week later were challenged with *E. maxima* oocysts. After 6 days, sexual stage parasites were released from the infected chicken and were incubated with secondary antibody conjugated to FITC in order to localise the serum antibodies by 3-D confocal microscopy. Results presented here show that WFB antigens induced the production of high-titer serum IgG, which have the ability to reach *in situ* gametocytes

in the intestinal lumen and permeate the enterocyte/parasite membranes in order to bind to the cytoplasmic Type 1 and Type 2 WFBs.

5.2 Materials and Methods:

5.2.1 Animals and parasites

The Houghton strain of *E. maxima* used throughout these experiments was originally provided by Martin Shirley (Institute for Animal Health, Compton, Newbury, Berkshire, United Kingdom). The oocysts were periodically propagated in 3-7 week old light breed Australorp chickens (Barter and Sons Hatchery, Luddenham, Australia) using established methods (Wagenbach et al., 1966). Oocysts were harvested from the faeces, sporulated *in vitro* at 30°C in an incubator and isolated by salt floatation and bleach treatment (2%, Milton solution). Gametocytes were isolated at 134 h postinfection and purified from infected chicken intestines by techniques published previously (Wallach et al., 1989), and stored as aliquots at -80°C until required.

5.2.2 Preparation of wall forming body antigens

To prepare antigen for immunization experiments, wall forming bodies (WFBs) of *E. maxima* macrogametocytes were extracted essentially as described previously (Frölich et al., 2013) with a minor modification. Briefly, the clean freeze-thawed gametocytes (6 x 10^6 cells) were extracted with 0.1% saponin in TNEP (10 mM Tris-HCl, pH 7.4, 50 mM NaCl, 2 mM EDTA) for 20 min at room temperature and spun at 1,000xg for 5 min. The resulting pellet was washed three times in TNEP by centrifugation at 3,000xg for 2 min, and the supernatant discarded. The pellet was resuspended in TNEP and mechanically dispersed by ultrasonication (Vibra Cell Sonicator) using a 2-mm microtip and a wave amplitude of 2.5W, 3 times for 10-s with intervals with cooling on ice between each burst. The sexual stage parasites were checked for complete lysis based on microscopy. The sonicate was then centrifuged at 15 000xg for 10 min and the pellet

was re-suspended in 1% sodium-dodecyl-sulphate (w/v) and the mixture was centrifuged at 15,000 g for 10 min. The resulting wall forming body rich extract was then concentrated on a 1,000 kDa cut-off filter (MWCO, VivaSpin) and washed three times in TNEP by centrifugation (4,000 g for 20min). Protein concentration was measured using the bicinchronic protein assay kit (Pierce) with bovine serum albumin (BSA) as the standard prior to storing at -20˚C for use in immunisation experiments (see below).

5.2.3 Immunization, challenge with oocysts and collection of mucosal scrapes

The flow chart describing steps involved in the immunization regime is shown below. Chickens kept coccidia free were allowed unlimited time to feed. Immunisation of chickens with purified WFBs antigens was carried out as follows. At three weeks of age, the chickens were immunised intramuscularly once a week with either 50 µg of WFB-rich fraction (WFB-immunized group), or sham-immunized (adjuvant-immunized group) with PBS in Freud's adjuvant (Sigma), or were left unimmunized (un-immunized group). The chickens were injected intramuscularly with 0.5 ml emulsion into their breast muscle. The final boost was administered one week prior to challenge. Reactivity of sera from all groups were screen by Western blotting and indirect immunofluorescence analysis.

At seven weeks of age, the chickens were challenged with 50,000 sporulated *E. maxima* oocysts per os and infected small intestines were removed 134 h post infection. Following extensive washing with ice cold PBS, the intestines were slit open lengthwise and a 1 cm^2 piece was cut from around the diverticulum. The exposed mucosa was then gently scraped using a glass cover slip and scrapings collected into an eppendorf tube. The scrapings were resuspended in TNEP buffer (10 mM Tris-HCl, pH 7.4, 50 mM NaCl, 2 mM EDTA) and mixed by brief vortexing. The quality of harvested parasites was tested by Evans blue staining using methods published previously (Ferguson et al., 2003). Secreted IgG was analysed by incubating suspended scrapings with FITC conjugated rabbit anti-chicken IgG $(Fab`)_2$ antibody (Jacksons research laboratories) diluted to 1:500. Following one hour incubation at 4°C in dark, samples were washed three times in PBS by centrifugation at 800 g for 5 mins, pipetted onto a slide coated

with 0.1% poly-L-Lysine and mounted using Vectashield® (Vector Laboratories, Burlingame, CA, USA) prior to confocal microscopy.

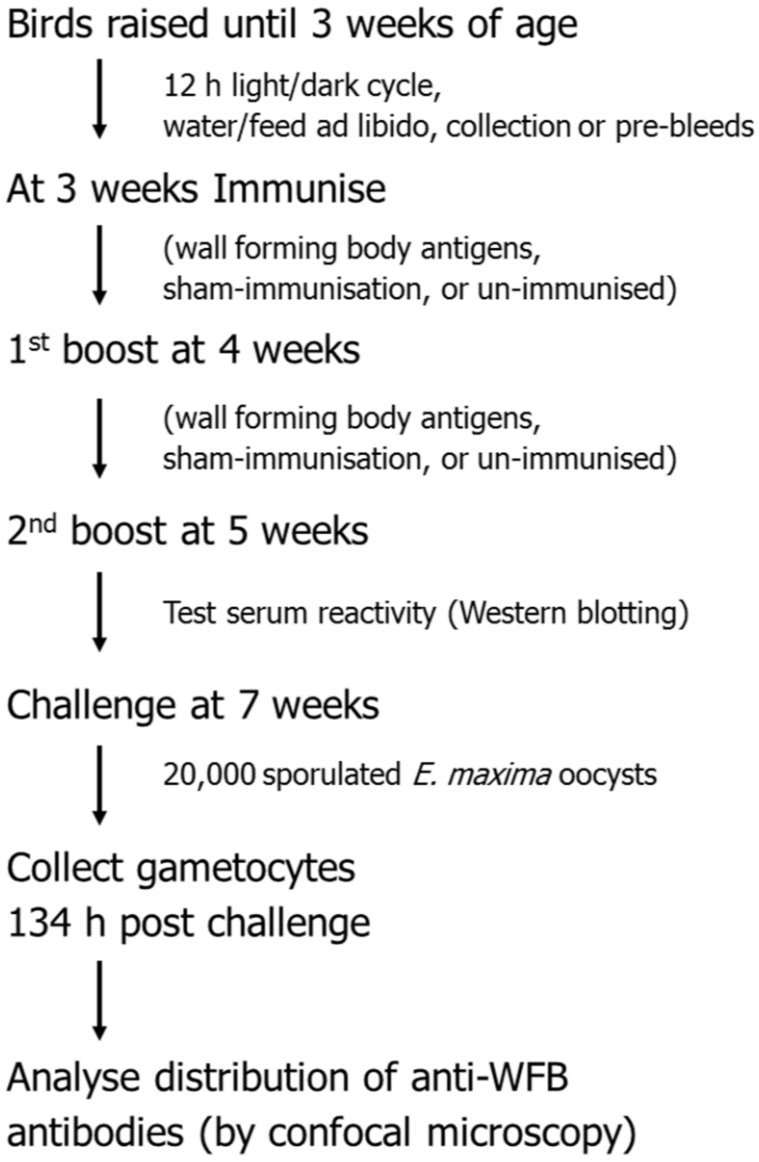

Flow chart of the experimental protocol for immunization.

5.2.4 Indirect immunofluorescence analysis

To evaluate specificity of the extracted WFB antigens, isolated gametocytes were fixed for 5 min at room temperature with either ice-cold methanol (95% v/v), or ice-cold acetone (95% v/v), permeabilized in 0.1% Tween20/PBS and non-specific binding was blocked with either normal mouse or chicken serum (1:500 dilution) for 1 h, at room temperature. The harvested gametocytes were then incubated with a panel of antibodies, including: mouse anti-APGA antibody (1:200 dilution) generated to a fraction of macrogametocyte proteins enriched for gam56 and gam82, amongst other molecules (Fried et al., 1992); mouse monoclonal anti-WFB2 1E11-11 antibody (1:200 dilution) raised against *E. maxima* gametocyte glycoprotein gam56, or chicken anti-WFB polyclonal antibodies generated to a fraction enriched for *E. maxima* macrogametocyte WFBs (1:500 dilution). Incubations were carried out for 1 hour at room temperature in dark. Following washes with PBS, primary antibodies were detected with Alexa Fluor 549 – conjugated goat anti-mouse IgM (1:500 dilution, Invitrogen, Australia), or with FITC conjugated rabbit anti-chicken IgG (Fab`)$_2$ antibody (1:500 dilution, Jacksons research laboratories). As a control for nonspecific binding, primary antibody was either omitted or substituted with the normal mouse or chicken sera (pre-bleed, 1:500) or the sera collected from birds immunized with adjuvant (1:500).

5.2.5 Confocal microscopy

Localisation of bound antibodies was visualized with an inverted Nikon A1 laser scanning confocal microscope equipped with 60X and 100 X oil objective lens (Plan Apo NA 1.4 aperture) MadCity ultra-fast piezo Z-drive, galvano scanners and Perfect Focus System^{TM} for continuous maintainance of focus. Stained cells were examined with a green (488/500-550 nm), red (561/570-620 nm) and far red (637/662-737 nm) lasers. To acquire three-dimensional volumes, ranging from 25 to 91-z serial optical sections were collected with a step size of 0.25 µm, using NIS Elements software (Nikon). The images were processed in NIS-Elements Viewer software, Advanced Version (Nikon, Melville, NY, USA). The laser intensity, photomultiplier tube gains (PMT-HV), and photomultiplier offset (PMT-offset) levels were kept constant during

the image acquisition. Raw images were reconstructed and rendered in 3D using IMARIS v.7 software (Bitplane Scientific, Zurich, Swizerland).

5.2.6 SDS PAGE and Western blotting

For identification of immunogenic WFB antigens, proteins from gametocyte lysate were separated by size as described previously (Frölich et al., 2013). Laemmli sample buffer containing β-mercaptoethanol and 10% sodium-dodecyl-sulphate was added prior to boiling for 10 min at 95°C. Samples were then centrifuged at 12 000xg for 5 min, at room temperature to remove insoluble and aggregated matter prior to SDS–PAGE on NuPAGE® Novex 4–12% Bis-Tris gradient gels (Invitrogen). Total protein (4 µg) loaded per lane was determined by bicinchoninic protein assay (Pierce). The proteins were then visualized by staining with Coomassie or, alternatively, transferred to polyvinylidene difluoride (PVDF, Pall Corporation) membranes and incubated with mouse anti-1E11–11 monoclonal antibody (1:500), mouse anti-APGA (1:500), chicken anti-WFB antibody (1:2000) or normal mouse or chicken serum (1:500). PVDF membranes were then incubated with alkaline-phosphatase conjugated rabbit anti-mouse IgM or anti-chicken IgG (1:1000; Sigma) and developed with 5-bromo-4-chloro-3-indolyl-phosphate/nitro blue tetrazolium (SIGMA *FAST* ™ BCI/NBT, Sigma) according to the manufacturer's instructions.

5.2.7 In-gel and in-solution trypsin digestion

The bands corresponding to the 43-45 kDa region of the gel were excised and subjected to in-gel trypsin digestion prior to mass spectrometry using published methods (Bogema et al., 2011). Briefly, the excised gel pieces were reduced and alkylated with 5 mM tributylphosphine and 20 mM acrylamide for 90 min at room temperature. The gel pieces were then digested with 12.5 ng μl^{-1} sequencing grade trypsin (Promega) at 37°C overnight and the resulting peptides were solubilized with 2% formic acid (v/v). Each digestion was carried out in triplicates, and the generated peptides purified with C18

reveres-phase minicolumn filled in a micropipette tip, ZipTip C18 (Millipore, USA) according to the manufacturer's manual.

For quantitative label-free LC-MS/MS, a total of 100 µg of protein aliquots were precipitated using acetone precipitation, and the dried pellet was stored at -80°C. The frozen pellet was resuspended in 8M urea/100 mM NH_4HCO_3, reduced with 5 mM TCEP for 30 min and alkylated with 40 mM iodacetamide at room temperature in the dark. Protein samples were diluted five times with 50 mM NH_4HCO_3 to reduce urea concentration to 1.6 M. Ten micrograms of trypsin (Promega) was added to the proteins sample (protein ratio 50:1), and digestion was carried out at 37°C overnight prior to mass spectrometry followed by label-free quantification..

5.2.7 Mass spectrometry and label-free quantification

LC-MS/MS analysis of digested and purified *E. maxima* lysates was performed at the Bioanalytical Mass Spectrometry Facility, The University of New South Wales (Sydney) on an LTQ-Orbitrap Velos (Thermo Fisher Scientific, Massachusetts, USA). Each sample was reconstituted in 10 µL of 0.1% formic acid and separated by nano-LC using an Ultimate 3000 HPLC and autosampler (Dionex, Amsterdam, Netherlands). Sample was divided into three technical replicates. A total of 0.2 µl was injected into a micro C_{18} precolumn (500 µm × 2 mm, Michrom Bioresources, Auburn, CA, USA) with Buffer A (98% H_2O, 2% CH_3CN, 0.1% TFA) at 10 µl min^{-1}. After a 4 min wash the pre-column was switched (Valco 10 port valve, Dionex) into line with a fritless nano column (75 µm i.d × 11 cm) containing reverse phase C18 media (5 µm, 200 Å Magic, Michrom Bioresources). Peptides were eluted using a linear gradient of Buffer A (98% H_2O, 2% CH_3CN, 0.1% TFA) to Buffer B (98% CH_3CN, 2% H_2O, 0.1% formic acid) at 250 nl min^{-1} over 70min. High voltage (2000 V) was applied to low volume (Upchurch Scientific, Oak Harbor, WA, USA) and the column tip positioned approx. 0.5 cm from the heated capillary (*T*=280°C) of an Orbitrap Velos (Thermo Electron, Bremen, Germany) mass spectrometer. Positive ions were generated by electrospray and the Orbitrap operated in data-dependent acquisition mode. A survey scan *m/z* 350–1750 was acquired in the Orbitrap (Resolution=30,000 at *m/z* 400, with an accumulation target value of 1 e^6 ions). Up to the 10 most abundant ions (>5,000 counts) with charge

states 2+ to 4+ were sequentially isolated and fragmented within the linear ion trap using collisionally induced dissociation with an activation q=0.25 and activation time of 30 ms at a target value of 30,000 ions. The *m/z* ratios selected for MS/MS were dynamically excluded for 30 s.

After converting the acquired raw files to the profile mzML format, the files were imported into Scaffold 4 (version 4.2.0, Proteome Software Inc., OR) for label-free quantification. Data in mgf format was searched using Mascot (Matrix Science, London, UK) against all entries in NCBI database (24_8_12, containing 19,941,864 entries for all species). The search criteria were set as follows: full tryptic specificity; 3 missed cleavages were allowed; oxidation (M) as variable modification. The mass tolerance was set to 4 ppm for precursor ions and 0.6 Da for fragment ions. The peptide false discovery rate (FDR) was set to 1.8% on the peptide level, 2 minimum peptides.

5.2.8 Database searching and protein identification

To identify proteins specific to *E. maxima*, which lacks an annotated genome sequence, *Eimeria tenella* protein database (housed within www.ToxoDB.org, version 8.2) was searched using Peaks studio (v6.0, Bioinformatics Solutions Inc.). The genome of Houghton strain *E. tenella* was annotated by the Parasite Genomics Group at the Wellcome Trust Sanger Institute using Workflow-based Automatic Genome Annotation (WAGA) and has been provided prepublication. To identify host proteins and common contaminants, the parasite database was supplemented with complete *Gallus gallus* database and a contaminant database from NCBI. The parameters for the search were as follows; the modifications propionamide on cysteine residues, methionine oxidation and deamidation of aspargine and glutamate were considered as a variable modification and three was used as the maximum missed tryptic cleavage sites. The precursor ions tolerance was set to ± 4.0 ppm and ± 0.60 Da for fragment ions. Proteins matched to unidentified or hypothetical *Eimeria* proteins were identified by searching the peptide sequences using BLASTP algorithm (www.blast.ncbi.nlm.nih.gov) for short, nearly exact matches. If there were multiple possibilities for peptide ID, the top scoring hit was selected. Theoretical pI (isoelectric oint) and Mw (molecular weight) were calculated using Compute pI/Mw tool housed within ExPASY Bioinformatics Resource Portal

(www.expasy.org). Amino acid sequence alignments were carried out using a ClustalW program (http://www.ebi.ac.uk/Tools/msa/clustalw2/).

5.3 Results

5.3.1 Polyclonal anti-WFB antibody localizes to the intracellular WFBs and the oocyst wall

We purified gametocyte WFBs as described in Materials & Methods, emulsified them in Freund's adjuvant and used 50 μg of protein to immunize naïve chickens for the production of polyclonal antibodies (pAbs). The resulting sera were tested by IFA on *E. maxima* purified gametocytes to study the subcellular localisation of the WFBs. In addition, the sera were tested by Western blotting using purified gametocyte lysate to analyse the molecular weights and band intensity of the antigens that were recognized in comparison with control anti-affinity purified gametocyte antigen (APGA) serum. A monoclonal antibody to the 56 kDa gametocyte protein (1E11-11) was used as a positive control for detection of the Type 2 WFBs, while sham immunized and untreated chicken sera were used as negative controls.

As can be seen in Figure 23 Aa, the anti-WFB pAb was found to intensely stain Type 1 (arrows) and Type 2 (double arrows) WFBs as well as the oocyst wall (arrowheads). Antisera raised against APGA and a monoclonal antibody to the 56 kDa WFB1 protein (1E11-11) used for comparison stained type 1 and type 2 WFBs of *E. maxima* macrogametocytes (Figures 23 A,b and 2A,c). Negative control sera gave very low levels of staining and there was no reactivity detected in enterocytes collected from the intestinal mucosa of uninfected birds (not shown).

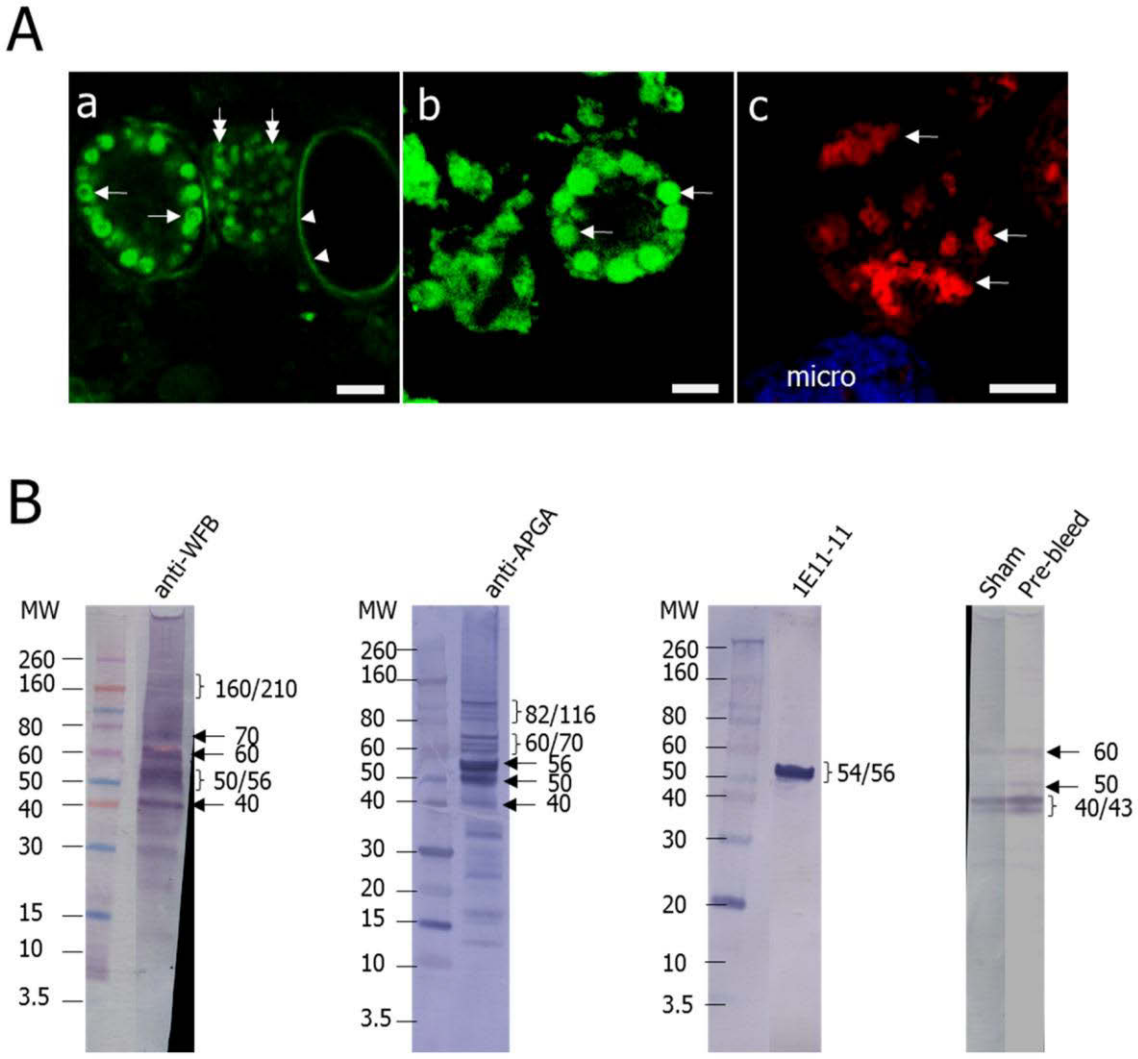

Figure 23: Immuno-labelling (A) and Western blot analysis (B) of sexual stage parasites probed with anti-WFB sera. (Aa) Confocal micrographs of harvested macrogametocytes probed with chicken anti-WFB polyclonal antibodies generated to a fraction enriched for *E. maxima* macrogametocyte WFBs (1:2000), mouse anti-APGA antibody (1:200 dilution) generated to a fraction of macrogametocyte proteins enriched for gam56 and gam82, amongst other molecules (Wallach et al., 1989), or mouse monoclonal 1E11-11 antibody (1:200 dilution) raised against *E. maxima* gametocyte glycoprotein gam56 (Fried et al., 1992). Primary antibodies were detected with Alexa Fluor 549 – conjugated goat anti-mouse IgM (1:500 dilution), or with FITC conjugated rabbit anti-chicken IgG $(Fab`)_2$ antibody (1:500 dilution). (Aa) Shows isolated gametocytes at various stages of maturation with stained large type 1 WFBs (arrows), type 2 WFBs (double arrows) and oocyst wall (arrowheads). Note the ring-like appearance of type 1 WFBs. (Ab) Shows mature macrogametocyte labelled with anti-APGA antibody. Note the staining of the luminal content of the WFB1s (arrows). (Ac) Shows early macrogametocyte with donut-shaped type 2 WFBs clustered in the cytoplasm (arrows). Microgametocyte is highlighted in blue stained with DAPI. Scale bar, 5 µm. (B) An immunoblot probed with anti-WFB polyclonal antibody (anti-WFB lane), anti-APGA antibody (anti-APGA lane) and 1E11-11 monoclonal antibody (1E11-11 lane). Note the presence of a prominent 54/56 protein band when all three antibodies

are used. Note the presence of 40/45, 50 and 60 kDa band detected non-specifically in negative controls (sham and pre-bleed lanes). A total of 5 µg of protein was loaded per lane. The position and molecular weight (in kDa) of protein standards are indicated on the left.

In comparing the antisera raised against the WFB preparation to anti-APGA, we observed some differences in the labelling of the parasites. While anti-APGA strongly detected antigens found within the lumen of the Type 1 WFBs (Figure 23 A, b), in several cases the anti-WFB predominantly stained the membrane surrounding the WFB1s producing a large ring with a central luminal hole (Figure 23 A, a, arrows). As expected, the control anti-56kDa monoclonal antibody exclusively stained donut-shaped structures clustered within the cytoplasm of an early macrogametocyte (Figure 23 A, c, arrows).

Western blot analysis of *E. maxima* gametocyte lysates showed that all three antibodies detected a prominent band of 54/56 kDa (Figure 23 B), while only the polyclonal anti-APGA and WFB showed an additional band at 50 kDa. Multiple smaller weak bands migrating between 40 and 10 kDa were also detected with both anti-APGA and anti-WFB polyclonal antibodies. Using anti-APGA, bands were also detected at 60, 70, 82 and 116 kDa with some weaker bands in between. The 60 and 70 kDa bands were also seen with the anti-WFB antibody, although not very distinctly. The polyclonal anti-WFB detected additional high molecular weight bands at 160 and 210 kDa, which were difficult to detect with anti-APGA, indicating that there are substantial differences in the recognition pattern of these two types of sera. As expected the monoclonal 1E11-11 antibody, strongly reacted with a doublet protein with a molecular weight of 54/56 kDa. Finally, there were two bands migrating at approximately 40/45 kDa along with 2 weak bands at 50 and 60 kDa when control sera were used (Figure 23 B, pre-bleed and sham sera lanes).

5.3.2 Identification of the 40/45 kDa protein band found using control sera by mass spectrometry

The bands corresponding to the 40/45 kDa region of the gel, digested the proteins with trypsin, and analysed the tryptic peptides by mass spectrometry. A number of proteins were identified (Table 5) among them the *Eimeria* immunoglobulin heavy chain binding protein (BiP) of 701 amino acids, with a predicted molecular mass of 74 kDa. 16% sequence coverage with 8 unique peptides were identified for this particular protein. Interestingly, all of the proteins that were identified are molecular chaperones associated with the endoplasmic reticulum (ER), which play a role in the transport of proteins destined for oligomerization, folding or degradation.

Table 5. List of proteins identified in the excised region of the SDS-PAGE gel corresponding to 43 kDa

[a]Accession	[a]Coverage (%)	Peptide number	Molecular weight	[b]Description	[c]Biological function
ETH_00007385 on Supercontig_38:118443-121468(+)	6	4	82,499	Heat shock protein 90	Prevention of steroid receptor binding to DNA
ETH_00005065 on Supercontig_0:627388-631208(-)	4	3	62,236	Sec61 alpha subunit isoform 1 transport protein	Protein translocation across the endoplasmic reticulum (ER)
ETH_00025545 on Supercontig_128:32283-35281(+)	8	4	73,789	Immunoglobulin heavy chain binding protein (BiP)	Immunoglobulin assembly, class II antigen processing, highly antigenic protein of pathogens
ETH_00000210 on Supercontig_342:4870-7083(-)	13	8	79,893	Heat shock protein 70	Protein folding and degardation, assembly into oligomeric complexes, translocation of polypeptides
ETH_00006810 on Supercontig_65:71979-75109(+)	5	2	48,084	DnaJ domain-containing protein	Also known as Hsp 40, regulator of ATPase activity of Hsp 70
ETH_00021780 on Supercontig_108:2787-23411(-)	1	4	53,6074	Ubuquitin C-terminal hydrolase of the cysteine proteinase fold	Cysteine protease, degradation of proteins via proteosome or lysosome, protein-protein interactions, cellular localisation

List of all *Eimeria* specific proteins identified in the excised 43 kDa band according to *E. tenella* database housed within ToxoDB.org (v8.2).
Only proteins with a minimum of 2 unique peptides, a peptide -10logP ≥ 15 and a peptide FDR equal to 1.9% were included in the list.
[a]The percentage of all the amino acids in the protein sequence that were detected in the sample
[b]Identity of proteins assigned by *E. tenella* database housed within ToxoDB.org (v8.2),
[c]Biological function assigned based on Swissprot.org and Uniprot.org

In order to determine whether the identified BiP protein is a chicken contaminant, the sequence was analysed by clustalw alignment with the sequence of the chicken BiP (Figure 24 A). We found that there were significant differences in the sequences and therefore concluded that the BiP we identified is indeed parasite specific. Furthermore, the BiP protein was also detected by label-free quantitative shotgun proteomic analysis of the whole gametocyte lysate. According to spectral counting, the *Eimeria* BiP in the lysate was very highly represented and found to be similar in abundance to that of the highly abundant 56 kDa gametocyte antigen (Table 6).

The full protein coverage map for the identified peptide sequence and the quality of the spectra are shown in Figure 24 B and C. As can be seen, the 8 identified peptides fall in a region that predicts a 47 kDa protein. No peptides were found in the regions at the amino terminal or carboxy terminal ends suggesting that they were not present in the protein extracted from the 45 kDa band.

Table 6. LC-MS/MS spectral counts of abundantly detected proteins in the *Eimeria maxima* whole gametocyte lysate

Identified Proteins	**Accession Number**	**Molecular weight**	**[a]Total spectrum count**	**[b]Coverage (%)**
82 kDa gametocyte antigen	gi|38565038	66 kDa	23	35.0
56 kDa gametocyte antigen	gi|25989587	53 kDa	12	25.0
beta-tubulin	gi|21542248 (+1)	50 kDa	11	27.0
alpha tubulin	gi|1045052 (+1)	50 kDa	9	27.0
immunoglobulin heavy chain binding protein	gi|1037176	77 kDa	9	16.0
actin	gi|357017703	57 kDa	7	0.0
230 kDa gametocyte antigen	gi|1372954	48 kDa	3	8.7

List of all *Eimeria* specific proteins identified in the gametocyte lysate according to all entries in NCBI database
Only proteins with a minimum of 2 unique peptides, a peptide -10logP ≥ 15 and a peptide FDR equal to 0.4% were included in the list.
Proteins are sorted according to highest spectral counts (abundance).
[a]The total number of spectra associated to a single protein group, including those shared with other proteins.
[b]The percentage of all the amino acids in the protein sequence that were detected in the sample.

A

```
Etenella        LDLNKLWYLFGLSASKHTQPGDPSARPHVLYTMGVGFHGAAALPFCFFLLSLFSHYPHAV 60
Emaxima         ------------------------------------------------------------
Gallus          ------------------------------------MRHLLLALLLLG-------GA 14

Etenella        RGDDTEGDGKVKDVVIGIDLGTTYSCVGVYRQGRVDIIPNDQGNRITPSYVSFA-EDERK 119
Emaxima         ------------------------------------------------------------
Gallus          RADDEEKKEDVG-TVVGIDLGTTYSCVGVFKNGRVEIIANDQGNRITPSYVAFTPEGERL 73

Etenella        IGEAAKNEAAINPTNTIFDVKRLIGRRFNEKEVQRDKELLPYEIINKDGKPYIRVMVKG- 178
Emaxima         ------------------------------------------------------------
Gallus          IGDAAKNQLTSNPENTVFDAKRLIGRTWNDPSVQQDIKYLPFKVVEKKAKPHIQVDVGGG 133

Etenella        QPKELAPEEVSAMVLGKMKEVAESYLGKEVKNAVVTVPAYFNDAQRQATKDAGAIAGLNV 238
Emaxima         ----------------------------------------------------AIAGLNV 7
Gallus          QTKTFAPEEISAMVLTKMKETAEAYLGKKVTHAVVTVPAYFNDAQRQATKDAGTIAGLNV 193
                                                                    :******

Etenella        IRIINEPTAAAIAYGLDKKD-EKTILVYDLGGGTFDVSVLVIDNGVFEVHATSGDTHLGG 297
Emaxima         IRIINEPTAAAIAYGIDKKD-EKTILVYDLGGGTFDVSVLVIDNGVFEVHATSGDTHLGG 66
Gallus          MRIINEPTAAAIAYGLDKREGEKNILVFDLGGGTFDVSLLTIDNGVFEVVATNGDTHLGG 253
                :***************:**:: **.***:**********:*.******** **.*******

Etenella        EDFDQRVMDHFLKIIQKKYNKDLRKDKSALQRLRREVERAKRALSSSHQVTVEVEGLVDG 357
Emaxima         EDFDQRVMDHFLKIIQKKFGKDLRKDKSGLQRLRREVERAKRALSSSHQVTVEVEGLVDG 126
Gallus          EDFDQRVMEHFIKLYKKKTGKDVRKDNRAVQKLRREVEKAKRALSSQHQARIEIESFFEG 313
                ********:**:*: :** .**:***: .:*:******:*******.**. :*:*.:.:*

Etenella        EDFSETLTRAKFEELNADLFQKTLKPVKQVLEDADLKKSQIDEIVLVGGSTRIPKIQQLI 417
Emaxima         EDFSETLTRAKFEELNADLFQKTLKPVKQVLEDADLKKSQIDEIVLVGGSTRIPKIQQLI 186
Gallus          EDFSETLTRAKFEELNMDLFRSTMKPVQKVLEDSDLKKSDIDEIVLVGGSTRIPKIQQLV 373
                *************** ***:.*:***::****:*****:******************:

Etenella        KEFFNGKEPNRGINPDEAVAYGAAVQAGILSGE-GTQDMVLLDVTPLTLGIETAGGVMAK 476
Emaxima         KEFFNGKEPNRGINPDEAVAYGAAVQAGILSGE-GTQDMVLLDVTPLTLGIETAGGVMAK 245
Gallus          KEFFNGKEPSRGINPDEAVAYGAAVQAGVLSGDQDTGDLVLLDVCPLTLGIETVGGVMTK 433
                *********.******************:***: .* *:***** ********.****:*

Etenella        VINKNTVIPTKKTQTFSTYSDNQSAVLIQVYEGERPMTKNNHLLGKFELTGIPPAPRGVP 536
Emaxima         VINKNTVIPTKKTQTFSTYSDNQSAVLIQVYEGERPMTKNNHLLGKFELTGIPPAPRGVP 305
Gallus          LIPRNTVVPTKKSQIFSTASDNQPTVTIKVYEGERPLTKDNHLLGTFDLTGIPPAPRGVP 493
                :* :***:****:* *** ****.:* *:*******:**:*****.*:************

Etenella        QIDVTFDVDRNGILNVSAVDKGTGKSEKITITNDKGRLTPDEIERMIQEAERFADEDRKT 596
Emaxima         QIDVTFDVDRNGILNVSAVDKGTGKSEKITITNDKGRLTPDEIEG--------------- 350
Gallus          QIEVTFEIDVNGILRVTAEDKGTGNKNKITITNDQNRLTPEEIERMVNDAEKFAEEDKKL 553
                **:***::* ****.*:* *****:.:*******:.****:***

Etenella        KERVDARNALEGYLHSMRSTVEDKDKLADKIEDDDKKTIMDKITEANEWLVANPEADGEE 656
Emaxima         ------------------------------------------------------------
Gallus          KERIDARNELESYAYSLKNQIGDKEKLGGKLSSEDKETIEKAVEEKIEWLESHQDADIED 613

Etenella        LRDKLKDVESVCNPIISKVYGQTGAPSDSGATSTSDDDYSSHDEL 701
Emaxima         ---------------------------------------------
Gallus          FKSKKKELEEVVQPIVSKLYGSAGPPP------TGEEEAAEKDEL 652
```

B

gi|1037176 (100%), 77,394.2 Da
immunoglobulin heavy chain binding protein [Eimeria tenella]
8 exclusive unique peptides, 9 exclusive unique spectra, 9 total spectra, 109/701 amino acids (16% coverage)

LDLNKLWYLF GLSASKHTQP GDPSARPHVL YTMGVGFHGA AALPFCFFLL
SLFSHYPHAV RGDDTEGDGK VKDVVIGIDL GTTYSCVGVY RQGRVDIIPN
DQGNRITPSY VSFAEDERKI GEAAKNEAAI NPTNTIFDVK RLIGRRFNEK
EVQRDKELLP YEIINKDGKP YIRVMVKGQP KELAPEEVSA MVLGKMKEVA
ESYLGKEVKN AVVTVPAYFN DAQRQATKDA GAIAGLNVIR IINEPTAAAI
AYGLDKKDEK TILVYDLGGG TFDVSVLVID NGVFEVHATS GDTHLGGEDF
DQRVMDHFLK IIQKKYNKDL RKDKSALQRL RREVERAKRA LSSSHQVTVE
VEGLVDGEDF SETLTRAKFE ELNADLFQKT LKPVKQVLED ADLKKSQIDE
IVLVGGSTRI PKIQQLIKEF FNGKEPNRGI NPDEAVAYGA AVQAGILSGE
GTQDMVLLDV TPLTLGIETA GGVMAKVINK NTVIPTKKTQ TFSTYSDNQS
AVLIQVYEGE RPMTKNNHLL GKFELTGIPP APRGVPQIDV TFDVDRNGIL
NVSAVDKGTG KSEKITITND KGRLTPDEIE RMIQEAERFA DEDRKTKERV
DARNALEGYL HSMRSTVEDK DKLADKIEDD DKKTIMDKIT EANEWLVANP
EADGEELRDK LKDVESVCNP IISKVYGQTG APSDSGATST SDDDYSSHDE
L

C

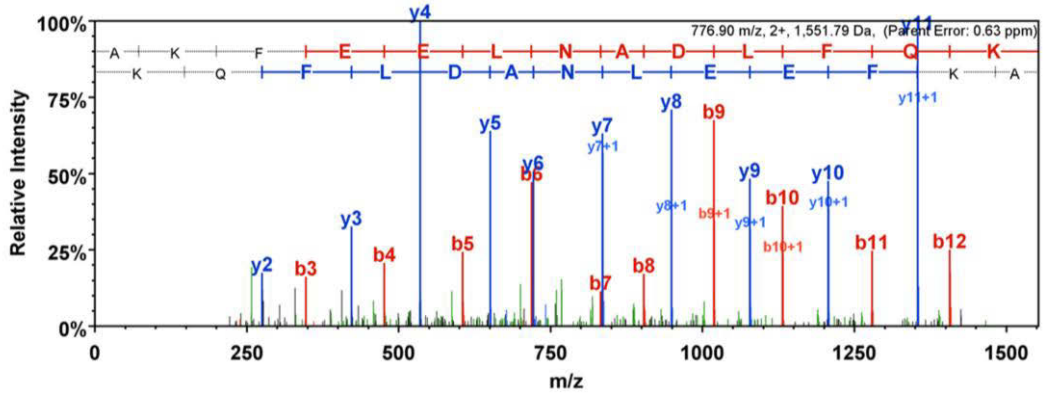

Figure 24: Identification of *Eimeria* immunoglobulin heavy chain binding protein (BiP) by mass spectrometry. (A) Comparison of the amino acid sequences of BiP homologs from E. tenella (Q24928), *E. maxima* (Q2489) and chicken (Q90593). Alignment of amino acid sequences was carried out using ClustalW program. Conserved amino acids are marked with an asterisk, conservation of strongly similar properties is highlighted with a colon and conservation between groups of weakly similar properties is marked with a period. Small and hydrophobic residues (red), acidic (blue), basic (magenta), hydroxyl sulfhydryl amine G (green). (B) The full protein coverage map for identified peptide sequence. Matching peptides are outlined in yellow. (C) Spectrum view.

5.3.3 Determining the quality of gametocytes used in *in situ* experiments

As a control for our *in situ* experiment, immunized and control chickens (used to produce the sera described in the experiments above) were challenged with 20,000 sporulated *E. maxima* oocysts. They were sacrificed at 134 hours post-infection and the intestines were removed, carefully washed and very gently scraped to release gametocytes without damaging the microvasculature, which were fixed and stained with Evans blue. The gametocytes were then analysed by 3D confocal microscopy to observe the cell geometry and three-dimensional shape of the WFB1s at various developmental stages. The perspectives chosen for analysis were from the top (x, y, z axis, Figure 25 A, B, C), the side view (x or y axis, Figure 25 A1, B1, B2) and corresponding single 2D focal slices (Figure 25 A2, B2, C2). Figure 24A shows a mature macrogametocyte with a total of 37 concentrically arranged type 1 WFBs, which varied in size from 0.3 – 3 μm in diameter (Figure 25 A and B). The focal slice of the macrogametocyte showed the WFB1s linked to one another via membrane projections (Figure 25 A2, arrows). These membranous projections interconnected WFB1s into structures resembling beads on a chain.

The 3D confocal image in Figure 24B shows an example of an early oocyst in which WFB 1 fusion and wall formation has commenced. The top view enabled visualization of the WFB1s fusion taking place at the surface of the parasite (Figure 25 B and B1, arrows). The focal slice enabled visualisation of the luminal content of the organelle which appeared uniformly distributed throughout (Figure 25 B2, arrows). Using 3D confocal microscopy to view all planes, the oocyst outer wall exhibited homogeneous staining (Figure 25 C1-2), consistent with its appearance in 2D (Figure 25 C2, arrows). The 3D digital reconstructions enabled visualization of the entire outer oocyst wall matrix.

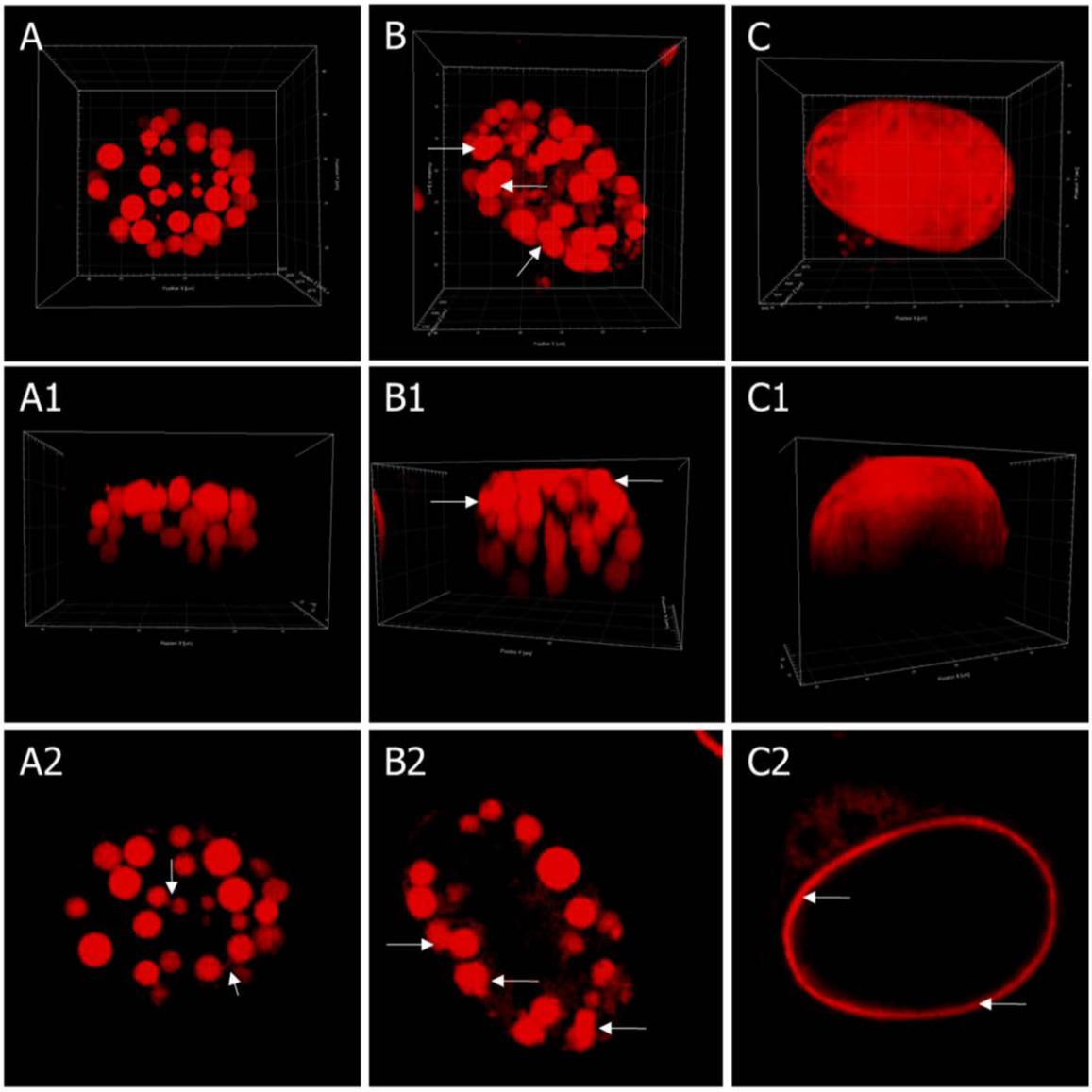

Figure 25: Three-dimensional confocal microscopy images of macrogametocytes harvested 134 hours post infection. Harvested sexual stage parasites stained with Evans blue dye (red), highlighting the large type 1 WFBs and the outer oocyst wall. (A-A1) 3D reconstruction of a mature macrogametocyte showing numerous type 1 WFBs of different size occupying the entire cytoplasm of the cell. (A2) A single focal slice of a cell shown in A1. Note the membrane projections connecting WFB1s making them appear as beads on a chain (arrows). (B-B1) 3D reconstruction of an ovoid macrogametocyte at early stages of oocyst wall formation with large type 1 WFBs fusing at the cell surface (arrows). (B2) A single focal slice of a cell shown in B1. Note the fused WFB1s (arrows). (C-C1) 3D reconstruction of a fully formed oocyst showing Evans blue positive outer oocyst wall. (C2) A single focal slice of a cell shown in C. Note the presence of a single layer around the oocyst. A, A1, B, B1, C, C1 represent 3D volumetric view with blending effect. A1, B1, C1 show side views for each cell (x and y planes are indicated). Quadrants in each box represent 5 μm.

5.3.4 Spatial distribution of endogenous IgG antibodies at different stages of oocyst biogenesis

We used the WFB immunized chickens to determine if the resulting serum antibodies have the ability to reach *Eimeria maxima* gametocytes *in vivo* to bind to the intracellular antigens. Immediately after sacrificing the chickens, the intestines were very gently scraped and the bound IgG was visualized by incubating the gametocytes with FITC-conjugated anti-chicken $(Fab')_2$ IgG secondary antibody. Figure 26 shows low magnification confocal micrographs of gametocytes from WFB immunized, sham-immunized and non-immunized control birds. While strong labelling could be observed in gametocytes harvested from birds immunized with WFB antigens (Figure 26, A1-3), very weak staining was detected in gametocytes collected from non and sham-immunized birds (Figure 26, B1-3, C1-3). This strong difference in fluorescence intensity shows that the serum IgG antibodies were able to reach the gametocyte, permeate the cellular membranes and bind to the cytoplasmic type 1 and type 2 WFBs.

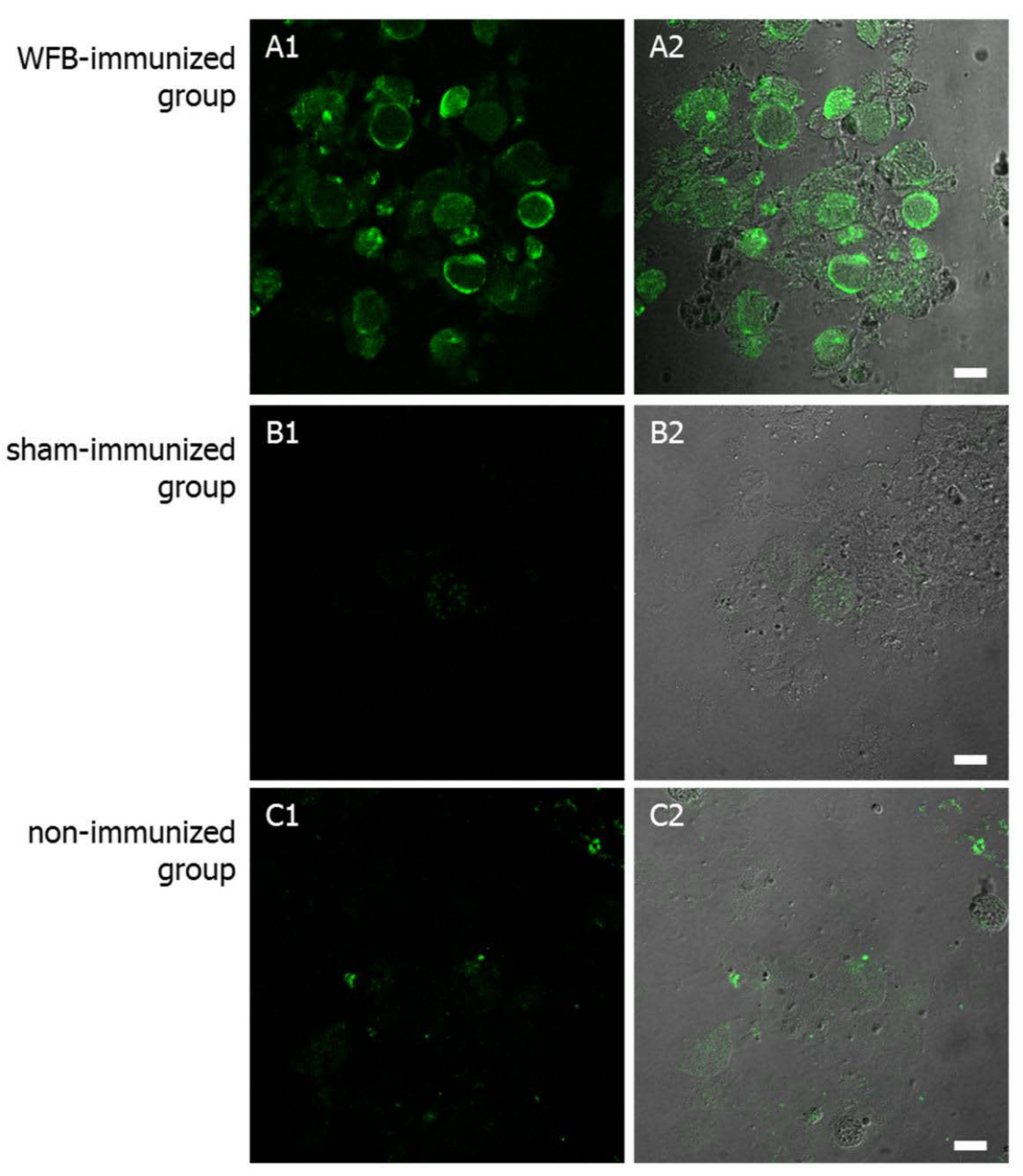

Figure 26: Distribution of fluorescence signals in macrogametocytes harvested from immunized (A1-3) and sham- (B1-3) or non-immunized (C1-3) birds. Low magnification (40 X) of sexual stage parasites extracted from all groups were washed and immediately incubated with the FITC conjugated anti-chicken IgG (Fab) secondary antibody. Fluorescence signals indicative of secondary antibody binding to the target antigen were analysed using confocal microscopy keeping fluorescence intensities and gains constant. (A1-2) Show macrogametocytes isolated from the chickens immunized with the purified WFB antigens in which strongly fluorescing parasites can be observed. Note the weak fluorescence signals in sham-immunized (B1-3) and non-immunized (C1-2) birds. Scale bar, 20 µm.

2D and 3D high resolution confocal microscopy were used to observe the subcellular localisation of the antibodies. Analysing single focal planes of the cells, we were able to visualize binding of the IgG to both the parasite's surface and the intracellular compartments. Figure 26 A-B shows that the large type 1 WFBs were strongly stained giving a crescent-shaped appearance (Figure 27 A-B, arrows). Also strongly stained were small granules approximately 0.7-1.5 µm in diameter (WFB2s) which condensed near the surface of the parasite (Figure 27 B-B1, arrows). In parasites which were at the start of oocyst wall formation, the IgG was found bound to the exocytosed WFB1s (Figure 27 C, arrows). The IgG was also found to bind to the inner oocyst wall of formed oocysts (Figure 27 D-D1, arrows).

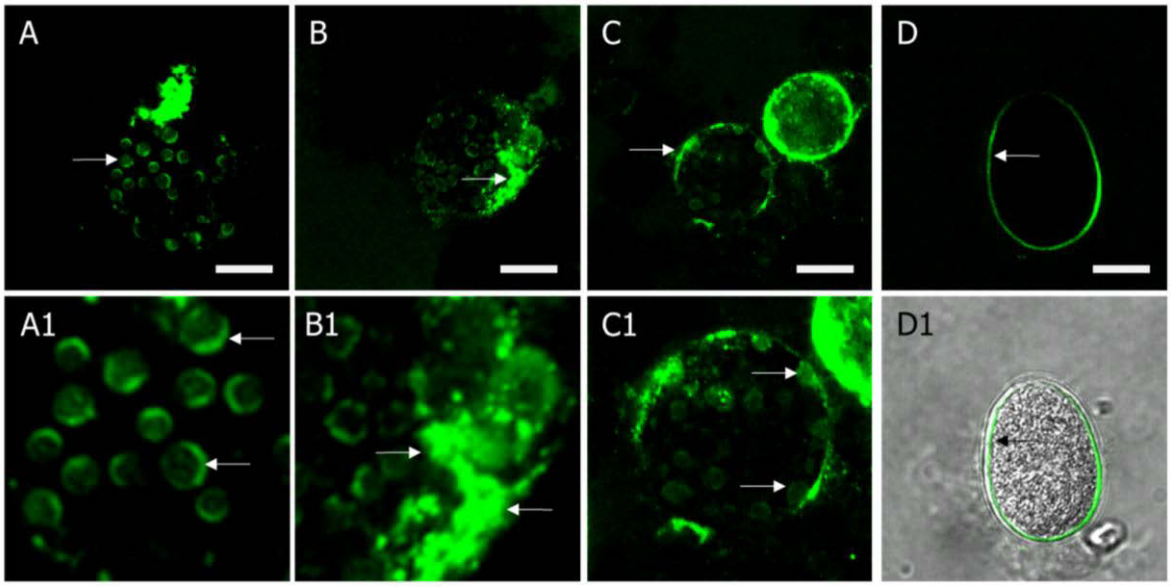

Figure 27: Localisation of secreted IgG in macrogametocytes harvested from birds immunized with purified WFB antigens. Sexual stage parasites extracted from WFB-immunized birds were washed and immediately incubated with the FITC conjugated anti-chicken IgG (Fab) secondary antibody. Fluorescence signals indicative of secondary antibody binding to the target antigen were analysed using confocal microscopy. (A) Shows a late stage macrogametocytes in which fluorescing type 1 WFBs can be observed inside the parasites. (A1) Insert shows a close-up of the crescent-shaped type 1 WFB organelles (arrows). (B-B1) Shows a macrogametocyte with fluorescing type 2 WFBs clustered at the parasite's surface (arrows). (C) Shows zygotes at different points of oocyst wall secretion. (D-D1) Show an oocyst with fluorescing inner oocyst wall (arrows). Scale bar, 5 µm.

We next processed the z-stack images of gametocytes in order to obtain a 3D reconstruction as shown in Figure 28. Digital 3D reconstruction of macrogametocytes (Figure 28 A1) showed that the anti WFB pAbs were not uniformly distributed inside the WFB1s and instead showed a punctate staining of the organelle lumen (Figure 28 A2). Furthermore, the close-up of the region depicted in A1 showed fluorescently labelled IgG embedded into the membrane coating the type 1 WFBs (Figure 28 A3 and A4). In digital reconstructions of the fully formed oocyst (Figure 28 B1-4), the IgG is associated with the surface of the oocysts, which now appeared embedded in the surface matrix forming a scaffold (Figure 28, B4).

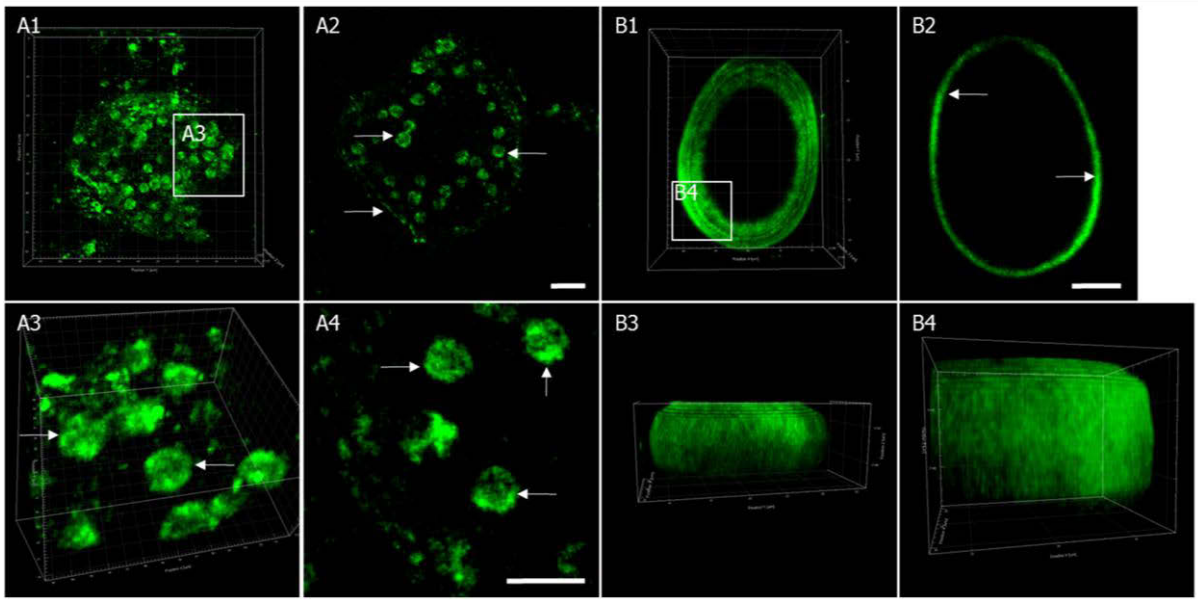

Figure 28: Spatial distribution of endogenous IgG at different stage of oocyst biogenesis. Following harvest from WFB-immunized birds, sexual stage parasites were washed extensively and incubated immediately with the FITC conjugated anti-chicken IgG (Fab) secondary antibody. The localisation and distribution of fluorescence was analysed by confocal microscopy. (A1) 3D reconstruction of a mature macrogametocyte showing positive labelling of the cell surface and the large type 1 WFBs occupying the cytoplasm of the cell. (A2) shows a single focal slice of a cell shown in A1. (A3) Shows a close-up of a region depicted in A1 with numerous positively stained type 1 WFBs (arrows). (A4) shows a focal slice of vesicles shown in A3. Note the punctate staining of the the WFB1s (arrows). (B1) 3D reconstruction of an oocyst showing positive labelling of the inner oocyst wall. (B2) Shows a focal slice of the oocyst shown in B1. (B3) Side view of the inner oocyst wall scaffold. (B4) Shows a close-up of a region depicted in B1 with clearly visible inner oocyst wall "scaffolding" pattern. Images in A1, A3, B1, B3, B4 represent 3D volumetric view with blending effect. Quadrants in A1, B1, B3 and B4 represent 5 µm, quadrants in A3 show 1 µm.

5.4 Discussion

The results of the present study have shown that purified wall forming bodies isolated from *E. maxima* gametocytes using a high concentration of the denaturing detergent SDS, were still highly immunogenic in chickens. Antibodies produced against these organelles were found to localise specifically to the Type 1 and 2 WFBs as well as the oocyst wall in isolated macrogametocytes and early stage oocysts as expected. Chickens immunized with WFBs were challenged with *E. maxima* oocysts and then sacrificed at 134 hours post infection to localise the anti WFB antibodies produced in situ. Using 2D confocal fluorescence microscopy and 3D computer reconstruction, we found that the anti-WFB antibodies were able to reach the gametocytes located in the intestinal mucosa and bind to the internal Type 1 and 2 WFB organelles. These results help elucidate the means by which antibodies produced against gametocyte antigens can provide protection against challenge *Eimeria* infections.

The geometry and three-dimensional shape of the WFB1s was studied at different stages of oocyst biogenesis using a 3D confocal microscope to visualize oocyst wall secretion in both lateral and axial planes. Micrographs showed the expected concentrically arranged WFB1s of different sizes in the mature macrogametocytes. During the early stages of oocyst wall development, we observed the secretion of the contents of the WFB1s which was characteristic of vesicles undergoing exocytosis. Evans blue showed that the WFB1s fused prior to liberating their luminal content at the surface of the developing oocyst.

We incubated gametocytes extracted from immunized and control chickens with FITC-conjugated secondary antibody only to detect anti-WFB antibodies produced *in situ*. Both low magnification and high resolution confocal micrographs, showed strong labelling of the surface as well as the internal WFB type 1 and 2 organelles. These results show that the serum IgG antibodies were able to reach the gametocyte in the intestinal mucosa, permeate the cellular membranes and bind to the cytoplasmic type 1 and type 2 WFBs. In a recent study we had also shown that even relatively large 100 nm nanoparticles are able to transverse membranes and reach the intracellular WFB1s where they accumulate. Thus, we postulate that via endocytosis, antibodies to the WFBs are taken into the gametocytes and are able to bind to the internal organelles.

Interestingly, we found by IFA that WFB1s labelled with the anti-WFB antibodies *in situ* gave a crescent shaped appearance (Figure 26 A-B). There are a few possible explanations for this result. Firstly, the specific antigens recognized by these antibodies may have a polar distribution over the surface of the organelle *in situ*. Secondly, antibody uptake into the gametocytes may be occurring from only 1 side of the parasite and they thereby accumulate in one portion of the organelle. Further work is required to elucidate this phenomenon.

In our previous studies, we used antibodies raised against affinity purified gametocyte antigens (APGA) to study the subcellular localisation of these antigens. In the present study, we compared antibodies raised against purified WFBs to those produced against APGA. We found that although the two types of antisera gave similar results there were some noted differences. By IFA we found that the anti WFBs predominantly stained the surface of the WFB1s whereas the anti APGA stained the whole organelle. This result is similar to that we found previously using a monoclonal antibody raised against a WFB1 protein (Frölich et al., 2013). We therefore concluded that the antibodies produced by vaccination with WFBs are mainly directed against the proteins found on the surface of the WFB1s and not in the lipid core. By Western blot analysis we found a difference in the banding pattern whereby the anti WFB sera produced more intense bands in the 160-210 kDa ranges as compared to the anti APGA antisera.

The results described above may be explained by the differences in the extraction methods. While preparation of affinity purified gametocyte antigens (APGA) relies on the use of non-ionic, non-denaturing detergent (Pugatsch et al., 1989; Wallach et al., 1989), the extraction of WFBs relies heavily on the use of high concentrations (1% w/v) of strong anionic surfactant sodium-dodecyl-sulphate (SDS) (Frölich et al., 2013). SDS surfactant is a strong protein denaturant able to disrupt non-covalent bonds within and between proteins. It addition it is commonly used to remove lipids from experimental samples (Samso et al., 1995). Given that the type 1 WFBs are a lipid-rich organelle with a protein-rich membrane coat (Frölich et al., 2013), it is very likely that the SDS denatured and/or removed some of the antigens recognized by the anti-APGA, hence, the difference in IFA and in the recognition pattern of proteins between these two types of anti-sera.

We had previously found that the gametocyte surface bound to any Ig it was brought in contact with and that normal IgG bound to a 43 kDa gametocyte band (Pugatsch et al., 1989; Wallach et al., 1989). It was therefore postulated that the 43 kDa band is an Fc receptor that plays a role in host immune evasion. To attempt to identify this protein, we employed a mass spectrometry based approach to analyse the bands detected in isolated WFBs non-specifically using normal chicken serum. Apart from a number of *Eimeria* specific endoplasmic reticulum (ER) associated molecular chaperone proteins (Hsp 90, 70, 40, Sec61, ubiquitin C-terminal hydrolase) we identified an immunoglobulin heavy chain binding protein (BiP), which was found to be highly abundant in the WFBs as well as the gametocyte lysate. We therefore predicted that this is the Fc receptor we had identified in our previous work.

The finding that BiP migrated at 40/45 kDa is in contrast to a recent report which had shown that a BiP homolog in sporozoites of *Eimeria tenella* exists as a single antigen of 70 kDa (Dunn et al., 1996). Using bioinformatics tools to predict the molecular weight of the identified BiP peptides, we found that in *E. maxima* gametocytes BiP exists as a shorter fragment of 47 kDa, suggesting that in sexual stages the BiP may exist in a processed form. In immunity, the major role of Hsp 70 cognate, BiP, is its participation in the assembly of immunoglobulins in the ER. BiP binds to the Ig heavy chain within the ER until association with the Ig light chain occurs, thus prevents premature self-assembly of the two Ig heavy chains (Kaufmann, 1990; Zhang et al., 2012). In addition, it plays a role in class II antigen processing. Although further work is needed to elucidate this possibility further, the findings reported here implicate BiP as a virulence factor. The BiP may be an important survival strategy by which *Eimeria* parasites avoid destruction by the host's immune system.

Finally, digital reconstructions of the fully formed oocysts showed an intriguing "scaffolding" pattern, showing incorporation of the processed WFB proteins into the inner oocyst wall. A similar scaffolding pattern was reported previously in the inner layer of the oocyst wall of E. tenella (Bushkin et al., 2012), which, in addition to tyrosine rich proteins, was found to be composed of fibrils of beta-1, 3-glucan that form a trabecular scaffold. Therefore, it is plausible that the WFB antigens were also incorporated into the wall in a similar pattern to that of the glucan scaffold.

5.4.1 Conclusions

Based on these results it was concluded that immunization with WFB rich extract induces a large production of antibodies which have the ability to reach the parasite *in situ*, and bind to the WFBs. We postulate that via this process antibodies block the development of *Eimeria maxima in vivo*. These findings broaden our understanding of the avian intestinal immunity and mucosal immune response and may have implications for design of new generation of anti-coccidial vaccines.

Chapter Six

Final summary and future work

6.1 Summary and conclusions

This study had five aims. **The first aim was to characterize the subcellular localisation and spatial organization of WFBs at various stages of sexual development in isolated macrogametocytes using wide-fieled and fluorescent microscopy.** *Eimeria* is a cyst-forming intracellular parasite that causes the economically important disease, coccidiosis, in intensely reared broiler chickens worldwide. The ability of the *Eimeria* parasite to replicate very rapidly and to synthesize an impenetrable, highly resistant oocyst wall, allows it to build up to very large numbers in the litter of broiler flocks. The molecular machinery involved in the assembly of the oocyst wall is housed in the two types of wall forming bodies (WFB1 and WFB2) of the sexual stage parasites (macrogametocytes). The aim here was to expand our understanding of the fundamental mechanisms involved in oocyst wall formation by characterising the morphological changes involved in oocyst wall assembly during oocyst biogenesis. Isolated macrogametocytes were stained using cytochemical techniques, and morphological changes of the developing zygote characterised by bright-field and 3D confocal microscopy. Additionally, the macrogametocytes harvested from the infected chicken intestine were analysed by immune-fluorescent microscopy using a panel of antibodies specific to two types of WFBs. Data indicates that the gametocyte preparation contains all stages of sexual development. In addition, it was demonstrated that harvested gametocytes are viable and intact and contain numerous WFBs. This was the first study in which isolated gametocytes were used to characterise the morphological changes involved in wall formation. In addition, the development of an *in vitro* system for maintaining gametocytes viable was reported for the first time, which was then used for biochemical and proteomic analyses to decipher the mechanisms involved in the building of the oocyst wall and nutrient uptake.

The second aim was to characterize molecular mechanisms of outer oocyst wall formation. Successful transmission of the Apicomplexan parasites depends on their ability to synthesize and store the material required to form the bi-layered oocyst in

specialised organelles, called wall forming bodies (WFBs), during gametocytogenesis. However, the precise molecular and biochemical differences between the two types of WFBs and the two layers of the oocyst wall are so far unknown. In order to address this issue, we used *Eimeria maxima* as a model cyst-forming apicomplexan and 3D confocal and wide-field fluorescent microscopy to analyse the presence of lipids and/or glycoproteins within the WFBs of developing macrogametocytes and the two layers of the oocyst wall. Microscopic analyses revealed that *E. maxima* is selective in compartmentalizing neutral lipids to the type 1, and glycoproteins to the type 2 wall forming bodies during gametocytogenesis. Furthermore, using Nile red stain we were able to visualise both neutral lipids and glycoproteins during outer and inner oocyst wall formation. Thus, we proposed a model of outer oocyst wall formation and suggest that neutral lipids found in the WFB1s are translocated to the parasite's surface where they deposit their cargo via exocytosis. The released molecules insert between the parasite's surface membranes and walls for incorporation into the neutral lipid rich outer oocyst wall. These findings are in agreement with the role lipids have in membrane synthesis in related parasites, *Toxoplasma* and *Plasmodium spp*., and confirm previous findings that neutral lipids play a role in oocyst wall formation. The neutral lipids (i.e. waxes) surrounding the forming oocysts may provide protection from the HCl and other acids in the gut prior to excretion.

The third aim was to develop a method for the isolation of gametocyte WFBs in order to analyse their molecular make up. Having demonstrated that the isolated macrogametocytes are intact and contain numerous wall forming bodies, the gametocyte WFBs were enriched by subcellular fractionation and fractions containing these organelles were analysed by microscopy, western blot and immunofluorescence microscopy. The results obtained using H&E and Nile red staining, as well as IFA using monoclonal antibodies specific to type 1 and 2 WFBs, showed that the extraction procedure used in this study led to the isolation and enrichment of the WFB organelles and the proteins associated with them. The WFB extract was then prepared for label-free shotgun proteomic analysis to identify and quantify proteins in the WFBs rich extract. Despite the lack of *E. maxima* predicted protein databases, we identified the expected WFB resident proteins, the 56, 82 and 230 kDa gametocyte antigens.

Moreover, MS analysis of the isolated WFBs showed that actin was highly abundant and enriched in this fraction. In addition, two enzymes, subtilisin and eimepsin, with predicted roles in processing of tyrosine-rich gametocyte antigens to form the oocyst wall (ref) were also identified, making it an appropriate and effective method for analysis of this sample.

The fourth aim was to gain insight into the nature and mechanism of nutrient acquisition in developing *E. maxima* macrogametocytes *in vitro.* Previously, it was shown that the process of oocyst wall formation in *Eimeria maxima* is analogous to the sclerotization of insect cuticles and involves protein-tyrosine crosslinks. Moreover, we and others have provided evidence for a structural role for lipids in the oocyst wall that makes them resistant to environmental stress. However, exactly how the parasite assembles these molecules into an impervious oocyst wall while maintaining the ability to acquire nutrients needed for development into an infectious cyst form remains an open question. Therefore, we harvested and maintained viable *E. maxima* gametocytes *in vitro* for several hours to study the mechanisms of nutrient intake by visualising the structure and dynamics of the parasite surface membrane. We have shown that *E. maxima* macrogametocytes and oocysts isolated from infected chickens, are capable of the uptake of exogenous molecules via endocytosis, and that this internalisation process depends upon the integrity and dynamics of the parasite cell membrane. Using *in vitro* culture techniques in combination with SEM, we have measured the size of micropores observed at the surface of sexual stage parasites. In addition, using time-lapse live cell and confocal microscopy, we observed parasite membrane dynamics and characterized the endocytotic pathways using fluorescent nano beads. Our results indicate that actin and tubulin play an important role in endocytosis as well as in the transport of WFBs to the parasite periphery ending in the incorporation of the WFB cargo into the oocyst wall. Indeed, the finding that actin and tubulin inhibitors induced WFB dispersion and cell deformities further supports this contention. Our proteomic analysis showed that *E. maxima* WFBs contain proteins of both parasite and host origin, that are specifically enriched in these organelles.

The fifth aim was to determine if anti-gametocyte antibodies have the ability to gain access to the intracellular parasite *in vivo*. In order to evaluate the ability of anti-gametocyte IgG to reach *E. maxima* macrogametocytes *in vivo,* chickens were immunized with *E. maxima* purified WFB antigens and 1 week later were challenged with *E. maxima* oocysts. After 6 days, sexual stage parasites were released from the infected chicken and were incubated with secondary antibody conjugated to FITC in order to localise the serum antibodies by 3-D confocal microscopy. This has been carried out in order to localise the antibody produced by immunisation. Results indicate that WFB antigens induced the production of high-titer serum IgG, which have the ability to reach *in situ* gametocytes in the intestinal lumen and permeate the enterocyte/parasite membranes in order to bind to the cytoplasmic Type 1 and Type 2 WFBs.

In summary, using a variety of microscopic and biochemical assays we have shown that freshly harvested gametocytes are viable and contain numerous intact WFBs. In addition, we demonstrated that the WFBs extracted from the gametocyte stages are intact and functionally preserved. We describe for the first time the biochemical difference between the two types of WFBs, report the proteome of these organelles and show the presence of novel proteins and enzymes involved in oocyst wall formation. Therefore, our findings contribute to the overall understanding of the sexual stage development and have also identified some potential targets that can be used for new drug development in the future.

6.2 Future work

More work is needed to complete the protein characterization work presented here. This includes the immunolocalisation of the two enzymes, subtilisin and eimepsin, to confirm they are localised to the WFBs and involved in oocyst wall formation. More extensive immunolocalisation studies including other molecular motors and signalling pathways involved in intracellular trafficking and uptake of solutes may enhance our understanding of the functions of these proteins in development of *Eimeria* oocysts.

Unfortunately, as the *Eimeria maxima* predicted genome and protein databases were not available when proteomic analysis of the isolated WFBs was carried out, we were relying on heterologous species *E. tenella*, the production of anti-peptide antibodies was not feasible, reducing the chances of identifying additional molecules with potential role in oocyst wall formation and uptake of exogenous material.

There are also many other proteins of interest that were identified in the gametocytes which were not investigated in this thesis. These include proteins with known roles in active and receptor-mediated cellular transport, including ion channels and pumps as well as proteins involved in receptor-mediated endocytosis (clathrin and calveolin). Biochemical assays and DNA probes targeting pathways mediated by these membrane transporters will provide a better understanding of these proteins in oocyst development. In addition, there also remains a long list of proteins with unknown or unassigned function. Continued efforts in sequencing and annotating *Eimeria* and other coccidian databases will provide further insights into the function of the unknown proteins reported in this thesis.

Considering that the previously characterized gametocyte 56 and 82 kDa antigens of *E. maxima* have proven to be effective vaccine candidates, it is possible that other proteins involved in oocyst biogenesis would also make effective targets. As most of the intracellular trafficking and endocytosis-related proteins identified here are conserved across the Apicomplexa, they have the potential for investigation as novel drug or vaccine targets in other cyst-forming parasites, such as Neospora, Toxoplasma, Cryptosporidium and Plasmodium, parasites that have a strong impact on economies worldwide.

Bibliography

Aguilar-Delfin, I., Wettstein, P.J., Persing, D.H., 2003, Resistance to acute babesiosis is associated with interleukin-12- and gamma interferon-mediated responses and requires macrophages and natural killer cells. Infection and Immunity 71, 2002-2008.

Akiba, M., Saeki, H., Ishii, T., Yamamoto, S., Ueda, K., 1991, Immunological changes in Babesia rodhanini infected BALB/C mice after treatment with anti-babesial drug, diminazene diaceturate. Journal of Veterinary Medical Science 53, 371-377.

Al-Khedery, B., Allred, D.R., 2006, Antigenic variation in Babesia bovis occurs through segmental gene conversion of the ves multigene family, within a bidirectional locus of active transcription. Molecular Microbiology 59, 402-414.

Allen, P.C., Danforth, H.D., Augustine, P.C., 1998, Dietary modulation of avian coccidiosis. International Journal for Parasitology 28, 1131-1140.

Allen, P.C., Lydon, J., Danforth, H.D., 1997, Effects of components of Artemisia annua on coccidia infections in chickens. Poultry Science 76, 1156-1163.

Allred, D.R., 1998, Antigenic variation in Babesia bovis: how similar is it to that in Plasmodium falciparum? Annals of Tropical Medicine and Parasitology 92, 461-472.

Aly, A.S.I., Matuschewski, K., 2005, A malarial cysteine protease is necessary for Plasmodium sporozoite egress from oocysts. Journal of Experimental Medicine 202, 225-230.

Artavanis-Tsakonas, K., Riley, E.M., 2002, Innate immune response to malaria: Rapid induction of IFN-gamma from human NK cells by live Plasmodium falciparum-infected erythrocytes. Journal of Immunology 169, 2956-2963.

Artavanis-Tsakonas, K., Tongren, J.E., Riley, E.M., 2003, The war between the malaria parasite and the immune system: immunity, immunoregulation and immunopathology. Clinical and Experimental Immunology 133, 145-152.

Ashburner, M., Ball, C.A., Blake, J.A., Botstein, D., Butler, H., Cherry, J.M., Davis, A.P., Dolinski, K., Dwight, S.S., Eppig, J.T., Harris, M.A., Hill, D.P., Issel-Tarver, L., Kasarskis, A., Lewis, S., Matese, J.C., Richardson, J.E., Ringwald, M., Rubin, G.M., Sherlock, G., Gene Ontology, C., 2000, Gene Ontology: tool for the unification of biology. Nature Genetics 25, 25-29.

Belli, S.I., Lee, M., Thebo, P., Wallach, M.G., Schwartsburd, B., Smith, N.C., 2002a, Biochemical characterisation of the 56 and 82 kDa immunodominant gametocyte antigens from *Eimeria maxima*. International Journal for Parasitology 32, 805-816.

Belli, S.I., Mai, K., Skene, C.D., Gleeson, M.T., Witcombe, D.M., Katrib, M., Finger, A., Wallach, M.G., Smith, N.C., 2004, Characterisation of the antigenic and immunogenic properties of bacterially expressed, sexual stage antigens of the coccidian parasite, *Eimeria maxima*. Vaccine 22, 4316-4325.

Belli, S.I., Smith, N.C., Ferguson, D.J.P., 2006, The coccidian oocyst: a tough nut to crack! Trends in Parasitology 22, 416-423.

Belli, S.I., Wallach, M.G., Luxford, C., Davies, M.J., Smith, N.C., 2003a, Roles of tyrosine-rich precursor glycoproteins and dityrosine- and 3,4-dihydroxyphenylalanine-mediated protein cross-linking in development of the oocyst wall in the coccidian parasite *Eimeria maxima*. Eukaryotic Cell 2, 456-464.

Belli, S.I., Wallach, M.G., Smith, N.C., 2003b, Cloning and characterization of the 82 kDa tyrosine-rich sexual stage glycoprotein, GAM82, and its role in oocyst wall formation in the apicomplexan parasite, *Eimeria maxima*. Gene 307, 201-212.

Belli, S.I., Witcombe, D., Wallach, M.G., Smith, N.C., 2002b, Functional genomics of gam56: characterisation of the role of a 56 kilodalton sexual stage antigen in oocyst wall formation in *Eimeria maxima*. International Journal for Parasitology 32, 1727-1737.

Belli, S.L., Walker, R.A., Flowers, S.A., 2005, Global protein expression analysis in apicomplexan parasites: Current status. Proteomics 5, 918-924.

Bhopale, G.M., 2003, Development of a vaccine for toxoplasmosis: current status. Microbes and Infection 5, 457-462.

Blake, D.P., Alias, H., Billington, K.J., Clark, E.L., Mat-Isa, M.-N., Mohamad, A.-F.-H., Mohd-Amin, M.-R., Tay, Y.-L., Smith, A.L., Tomley, F.M., Wan, K.-L., 2012, EmaxDB: Availability of a first draft genome sequence for the apicomplexan Eimeria maxima. Molecular and Biochemical Parasitology 184, 48-51.

Blake, D.P., Billington, K.J., Copestake, S.L., Oakes, R.D., Quail, M.A., Wan, K.-L., Shirley, M.W., Smith, A.L., 2011, Genetic Mapping Identifies Novel Highly Protective Antigens for an Apicomplexan Parasite. Plos Pathogens 7.

Blake, D.P., Smith, A.L., Shirley, M.W., 2004, Parasite genetics and the immune host: a novel strategy in the search for a vaccine against Eimeria spp. British poultry science 45 Suppl 1, S16-17.

Brinkmann, V., Remington, J.S., Sharma, S.D., 1993, Vaccination of mice with the protective F3G3 antigen of Toxoplasma gondii activates CD4+ but not CD8+ T

cells and induces Toxoplasma specific IgG atibody. Molecular Immunology 30, 353-358.

Broen, K., Brustoski, K., Engelmann, I., Luty, A.J.F., 2007, Placental Plasmodium falciparum infection: Causes and consequences of in utero sensitization to parasite antigens. Molecular and Biochemical Parasitology 151, 1-8.

Berlin, O.G.W., Peter, J.B., Gagne, C., Conteas, C.N., Ash, L.R., 1998, Autofluorescence and the detection of Cyclospora oocysts. Emerging Infectious Diseases 4, 127-128.

Bogema, D.R., Scott, N.E., Padula, M.P., Tacchi, J.L., Raymond, B.B.A., Jenkins, C., Cordwell, S.J., Minion, F.C., Walker, M.J., Djordjevic, S.P., 2011, Sequence TTKF down arrow QE Defines the Site of Proteolytic Cleavage in Mhp683 Protein, a Novel Glycosaminoglycan and Cilium Adhesin of Mycoplasma hyopneumoniae. Journal of Biological Chemistry 286, 41217-41229.

Bushkin, G.G., Motari, E., Carpentieri, A., Dubey, J.P., Costello, C.E., Robbins, P.W., Samuelson, J., 2013, Evidence for a structural role for Acid-fast lipids in oocyst walls of cryptosporidium, toxoplasma, and eimeria. mBio 4.

Bushkin, G.G., Motari, E., Magnelli, P., Gubbels, M.-J., Dubey, J.P., Miska, K.B., Bullitt, E., Costello, C.E., Robbins, P.W., Samuelson, J., 2012, beta-1,3-Glucan, Which Can Be Targeted by Drugs, Forms a Trabecular Scaffold in the Oocyst Walls of Toxoplasma and Eimeria. Mbio 3.

Chen, X.M., Gores, G.J., Paya, C.V., LaRusso, N.F., 1999, Cryptosporidium parvum induces apoptosis in biliary epithelia by a Fas/Fas ligand-dependent mechanism. American Journal of Physiology-Gastrointestinal and Liver Physiology 40, G599-G608.

Chen, X.M., Levine, S.A., Splinter, P.L., Tietz, P.S., Ganong, A.L., Jobin, C., Gores, G.J., Paya, C.V., LaRusso, N.F., 2001, Cryptosporidium parvum activates nuclear factor kappa B in biliary epithelia preventing epithelial cell apoptosis. Gastroenterology 120, 1774-1783.

Clark, I.A., Allison, A.C., 1974a, Babesia microti and Plasmodium berghei yoelii infcetions in nude mice. Nature 252, 328-329.

Clark, I.A., Allison, A.C., 1974b, Babesia microti and Plasmodium berghei yoelii infections in nude mice. Nature 252, 328-329.

Coombs, G.H., Muller, S., 2002, Recent advances in the search for new anti-coccidial drugs. International Journal for Parasitology 32, 497-508.

Cowman, A.F., Crabb, B.S., 2006, Invasion of red blood cells by malaria parasites. Cell 124, 755-766.

Danforth, H.D., 1983, Use of monoclonal antibodies directed against *Eimeria tenella* sporozoites to determine stage specificity and *in vitro* effect on parasite penetration and development. American Journal of Veterinary Research 44, 1722-1727.

de Graaf, D.C., Spano, F., Petry, F., Sagodira, S., Bonnin, A., 1999, Speculation on whether a vaccine against cryptosporidiosis is a reality or fantasy. International Journal for Parasitology 29, 1289-1306.

de Waal, D.T., Combrink, M.P., 2006, Live vaccines against bovine babesiosis. Veterinary Parasitology 138, 88-96.

del Cacho, E., Gallego, M., Francesch, M., Quilez, J., Sanchez-Acedo, C., 2010, Effect of artemisinin on oocyst wall formation and sporulation during Eimeria tenella infection. Parasitology International 59, 506-511.

Dent, A.E., Bergmann-Leitner, E.S., Wilson, D.W., Tisch, D.J., Kimmel, R., Vulule, J., Sumba, P.O., Beeson, J.G., Angov, E., Moormann, A.M., Kazura, J.W., 2008, Antibody-Mediated Growth Inhibition of Plasmodium falciparum: Relationship to Age and Protection from Parasitemia in Kenyan Children and Adults. Plos One 3.

Dent, A.E., Chelimo, K., Sumba, P.O., Spring, M.D., Crabb, B.S., Moormann, A.M., Tisch, D.J., Kazura, J.W., 2009, Temporal stability of naturally acquired immunity to Merozoite Surface Protein-1 in Kenyan Adults. Malaria Journal 8.

Dent, A.E., King, C.L., Malhotra, I., Crabb, B.S., Kazura, J.W., 2005, Impact of prenatal exposure to malaria antigens on levels of MSP-1(19) invasion-inhibitory antibodies during infancy. American Journal of Tropical Medicine and Hygiene 73, 866.

Dobbelaere, D., Heussler, V., 1999, Transformation of leukocytes by Theileria parva and T-annulata. Annual Review of Microbiology 53, 1-11.

Dobbelaere, D.A.E., Rottenberg, S., 2003, Theileria-induced leukocyte transformation. Current Opinion in Microbiology 6, 377-382.

Doolan, D.L., Dobano, C., Baird, J.K., 2009, Acquired Immunity to Malaria. Clinical Microbiology Reviews 22, 13-36.

Daugschies, A., Bialek, R., Joachim, A., Mundt, H.C., 2001, Autofluorescence microscopy for the detection of nematode eggs and protozoa, in particular Isospora suis, in swine faeces. Parasitology Research 87, 409-412.

Dunn, P.P.J., Bumstead, J.M., Tomley, F.M., 1996, Primary structure of a BiP homologue in Eimeria spp. Parasitology Research 82, 566-568.

Elliott, S.R., Payne, P.D., Duffy, M.F., Byrne, T.J., Tham, W.H., Rogerson, S.J., Brown, G.V., Eisen, D.P., 2007, Antibody recognition of heterologous variant surface antigens after a single Plasmodium falciparum infection in previously naive adults. American Journal of Tropical Medicine and Hygiene 76, 860-864.

Entzeroth, R., Mattig, F.R., Werner-Meier, R., 1998, Structure and function of the parasitophorous vacuole in Eimeria species. International Journal for Parasitology 28, 1015-1018.

Eschenbacher, K.H., Eggli, P., Wallach, M., Braun, R., 1996, Characterization of a 14 kDa oocyst wall protein of *Eimeria tenella* and *Eimeria acervulina*. Parasitology 112, 169-176.

Fowler, S.D., Greenspan, P., 1985, Application of Nile red, a fluorescent hydrophobic probe, for the detection of neutral lipid deposits in tissue sections - comparison with Oil red O. Journal of Histochemistry & Cytochemistry 33, 833-836.

Fritz, H.M., Bowyer, P.W., Bogyo, M., Conrad, P.A., Boothroyd, J.C., 2012a, Proteomic Analysis of Fractionated Toxoplasma Oocysts Reveals Clues to Their Environmental Resistance. Plos One 7.

Fritz, H.M., Buchholz, K.R., Chen, X., Durbin-Johnson, B., Rocke, D.M., Conrad, P.A., Boothroyd, J.C., 2012b, Transcriptomic Analysis of Toxoplasma Development Reveals Many Novel Functions and Structures Specific to Sporozoites and Oocysts. Plos One 7.

Frölich, S., Johnson, M., Robinson, M., Entzeroth, R., Wallach, M., 2013, The spatial organization and extraction of the wall-forming bodies of Eimeria maxima. Parasitology 140, 876-887.

Frölich, S., Entzeroth, R., Wallach, M., 2012, Comparison of protective immune responses to apicomplexan parasites. Journal of Parasitology Research 2012, 852591-852591.

Ferguson, D.J.P., 2002, Toxoplasma gondii and sex: essential or optional extra? Trends in Parasitology 18, 355-359.

Ferguson, D.J.P., Birchandersen, A., Hutchison, W.M., Siim, J.C., 1977a, Ultrastructural studies on endogenous development of Eimeria brunetti. 3. Macrogametogony and macrogamete. Acta Pathologica Et Microbiologica Scandinavica Section B-Microbiology 85, 78-88.

Ferguson, D.J.P., Birchandersen, A., Hutchison, W.M., Siim, J.C., 1977b, Ultrastructural studies on endogenous development of *Eimeria brunetti.* Fomration and structure of oocyst wall. Acta Pathologica Et Microbiologica Scandinavica Section B-Microbiology 85, 201-211.

Ferguson, D.J.P., Birchandersen, A., Hutchison, W.M., Siim, J.C., 1977c, Ultrastructural studies on endogenous development of *Eimeria brunetti*. Microgametogony and microgamete. Acta Pathologica Et Microbiologica Scandinavica Section B-Microbiology 85, 67-77.

Ferguson, D.J.P., Birchandersen, A., Hutchison, W.M., Siim, J.C., 1978a, Light and electron-microscopy on sporulation of oocysts of *Eimeria brunetti*.1. Development of zygote and formation of sporoblasts. Acta Pathologica Et Microbiologica Scandinavica Section B-Microbiology 86, 1-11.

Ferguson, D.J.P., Belli, S.I., Smith, N.C., Wallach, M.G., 2003, The development of the macrogamete and oocyst wall in *Eimeria maxima*: immuno-light and electron microscopy. International Journal for Parasitology 33, 1329-1340.

Ferguson, D.J.P., Birchandersen, A., Hutchison, W.M., Siim, J.C., 1977, Ultrastructural studies on endogenous development of *Eimeria brunetti.* Fomration and structure of oocyst wall. Acta Pathologica Et Microbiologica Scandinavica Section B-Microbiology 85, 201-211.

Ferguson, D.J.P., Hutchison, W.M., Siim, J.C., 1975, Ultrastructural development of macrogamete and formation of oocyst wall of *Toxoplasma gondii*. Acta Pathologica Et Microbiologica Scandinavica Section B-Microbiology 83, 491-505.

Ferguson, D.J.P., Sahoo, N., Pinches, R.A., Bumstead, J.M., Tomley, F.M., Gubbels, M.J., 2008, MORN1 has a conserved role in asexual and sexual development across the Apicomplexa. Eukaryotic Cell 7, 698-711.

Fried, M., Mencher, D., Sarshalom, O., Wallach, M., 1992, Developmental gene-expression of 230-kilodalton macrogamete-specific protein of the avian coccidial parasite, *Eimeria maxima*. Molecular and Biochemical Parasitology 51, 251-262.

Graves, P., Gelband, H., 2003, Vaccines for preventing malaria. Cochrane Database Syst Rev, CD000129.

Graves, P., Gelband, H., 2006a, Vaccines for preventing malaria (blood-stage). Cochrane Database Syst Rev, CD006199.

Graves, P., Gelband, H., 2006b, Vaccines for preventing malaria (pre-erythrocytic). Cochrane Database Syst Rev, CD006198.

Graves, P., Gelband, H., 2006c, Vaccines for preventing malaria (SPf66). Cochrane Database Syst Rev, CD005966.

Green, D.R., 2000, Apoptotic pathways: Paper wraps stone blunts scissors. Cell 102, 1-4.

Guerra, C.A., Snow, R.W., Hay, S.I., 2006, Mapping the global extent of malaria in 2005. Trends in Parasitology 22, 353-358.

Guevara-Patino, J.A., Holder, A.A., McBride, J.S., Blackman, M.J., 1997, Antibodies that inhibit malaria merozoite surface protein-1 processing and erythrocyte invasion are blocked by naturally acquired human antibodies. Journal of Experimental Medicine 186, 1689-1699.

Greenspan, P., Fowler, S.D., 1985, Spectrofluorometric studies of lipid probe, Nile red. Journal of Lipid Research 26, 781-789.

Greenspan, P., Mayer, E.P., Fowler, S.D., 1984, Use of Nile red in fluorescence microscopy and flow cytometer analysis of intracellular lipid loading. Journal of Cell Biology 99, A58-A58.

Greenspan, P., Mayer, E.P., Fowler, S.D., 1985, Nile red- a selective fluorescent stain for intracellular lipid droplets. Journal of Cell Biology 100, 965-973.

Katrib, M., Ikin, R.J., Brossier, F., Robinson, M., Slapetova, I., Sharman, P.A., Walker, R.A., Belli, S.I., Tomley, F.M., Smith, N.C., 2012, Stage-specific expression of protease genes in the apicomplexan parasite, Eimeria tenella. Bmc Genomics 13.

Hammond, D.M. 1973. Life cycles and development of of coccidia. In the Coccidia. *Eimeria, Isospora, Toxoplasma* and *Related Genera.* In In the Coccidia. *Eimeria,*

Isospora, Toxoplasma and *Related Genera*, P.L., H.D.M.a.L., ed. (University Park Press), pp. 45-79.

Hogh, B., 1996, Clinical and parasitological studies on immunity to Plasmodium falciparum malaria in children. Scand J Infect Dis Suppl 102, 1-53.

Hommel, M., David, P.H., Oligino, L.D., 1983, Surface alterations of erythrocytes in Plasmodium falciparum malaria - antigenic variation, antigenic diversity and the role of the spleen. Journal of Experimental Medicine 157, 1137-1148.

Huff, C.G., Marchbank, D.F., 1955, Changes in infectiousness of malarial gametocytes. I. Patterns of oocyst production in seven host-parasite combinations. Exptl Parasitol 4, 256-270.

Huff, C.G., Marchbank, D.F., Shiroishi, T., 1958, Changes in infectiousness of malarial gametocytes. II. Analysis of the possible causative factors. Exptl Parasitol 7, 399-417.

Hui, G., Hashimoto, C., 2007, Plasmodium falciparum anti-MSP1-19 antibodies induced by MSP1-42 and MSP1-19 based vaccines differed in specificity and parasite growth inhibition in terms of recognition of conserved versus variant epitopes. Vaccine 25, 948-956.

Igarashi, I., Suzuki, R., Waki, S., Tagawa, Y., Seng, S., Tum, S., Omata, Y., Saito, A., Nagasawa, H., Iwakura, Y., Suzuki, N., Mikami, T., Toyoda, Y., 1999, Roles of CD4+ T cells and gamma interferon in protective immunity against Babesia microti infection in mice. Infection and Immunity 67, 4143-4148.

Igarashi, I., Waki, S., Ito, M., Omata, Y., Saito, A., Suzuki, N., 1994, Role of CD4+ T cells in the control of primary infection with Babesia microti in mice. Journal of Protozoology Research 4, 164-171.

Janouskovec, J., Horak, A., Obornik, M., Lukes, J., Keeling, P.J., 2010, A common red algal origin of the apicomplexan, dinoflagellate, and heterokont plastids. Proceedings of the National Academy of Sciences of the United States of America 107, 10949-10954.

Jeffery, G.M., 1966, Epidemiological significance of repeated infections with homologous and hetereologous strains and species of Plasmodium. Bulletin of the World Health Organization 35, 873-&.

Jenkins, M., Kerr, D., Fayer, R., Wall, R., 1995, Serum and colostrum antibody responses induced by jet-injection of sheep with DNA encoding a Cryptosporidium parvum antigen. Vaccine 13, 1658-1664.

Jenkins, M.C., 2004, Present and future control of cryptosporidiosis in humans and animals. Expert Rev Vaccines 3, 669-671.

Kaufmann, S.H.E., 1990, Heat-shock proteins and the immune response. Immunology Today 11, 129-136.

Kaslow, D.C., Bathurst, I.C., Isaacs, S.N., Keister, D.B., Moss, B., Barr, P.J., 1992, Induction of *Plasmodium falciparum* transmission-blocking antibodies by recombinant PFS25. Memorias Do Instituto Oswaldo Cruz 87, 175-177.

Kassim, O.O., Ako-Anai, K.A., Torimiro, S.E., Hollowell, G.P., Okoye, V.C., Martin, S.K., 2000, Inhibitory factors in breastmilk, maternal and infant sera against in vitro growth of Plasmodium falciparum malaria parasite. Journal of Tropical Pediatrics 46, 92-96.

Kauth, C.W., Epp, C., Bujard, H., Lutz, R., 2003, The merozoite surface protein 1 complex of human malaria parasite Plasmodium falciparum - Interactions and arrangements of subunits. Journal of Biological Chemistry 278, 22257-22264.

Kinyanjui, S.M., Mwangi, T., Bull, P.C., Newbold, C.I., Marsh, K., 2004, Protection against clinical malaria by heterologous immunoglobulin G antibodies against malaria-infected erythrocyte variant surface antigens requires interaction with asymptomatic infections. Journal of Infectious Diseases 190, 1527-1533.

Krucken, J., Hosse, R.J., Mouafo, A.N., Entzeroth, R., Bierbaum, S., Marinovski, P., Hain, K., Greif, G., Wunderlich, F., 2008, Excystation of *Eimeria tenella* sporozoites impaired by antibody recognizing gametocyte/oocyst antigens GAM22 and GAM56. Eukaryotic Cell 7, 202-211.

Keller, A., Nesvizhskii, A.I., Kolker, E., Aebersold, R., 2002, Empirical statistical model to estimate the accuracy of peptide identifications made by MS/MS and database search. Analytical Chemistry 74, 5383-5392.

Kuenzi, P., Schneider, P., Dobbelaere, D.A.E., 2003, Theileria parva-transformed T cells show enhanced resistance to Fas/Fas ligand-induced apoptosis. Journal of Immunology 171, 1224-1231.

Lacroix-Lamande, S., Mancassola, R., Naciri, M., Laurent, F., 2002, Role of gamma interferon in chemokine expression in the ileum of mice and in a murine intestinal epithelial cell line after Cryptosporidium parvum infection. Infection and Immunity 70, 2090-2099.

Lang, C., Algner, M., Beinert, N., Gross, U., Luder, G.K., 2006, Diverse mechanisms employed by Toxoplasma gondii to inhibit IFN-gamma-induced major histocompatibility complex class II gene expression. Microbes and Infection 8, 1994-2005.

Laurent, F., Eckmann, L., Savidge, T., Naciri, M., Kagnoff, M.F., 1998, Cryptosporidium parvum infection of human intestinal epithelial cells induces the polarized secretion of C-X-C chemokines and prostaglandin E-2 and F-2 alpha production. Faseb Journal 12, 2105.

Laurent, F., McCole, D., Eckmann, L., Kagnoff, M.F., 1999, Pathogenesis of Cryptosporidium parvum infection. Microbes and Infection 1, 141-148.

Leiriao, P., Albuquerque, S.S., Corso, S., van Gemert, G.J., Sauerwein, R.W., Rodriguez, A., Giordano, S., Mota, M.M., 2005, HGF/MET signalling protects Plasmodium-infected host cells from apoptosis. Cellular Microbiology 7, 603-609.

Lillehoj, H.S., Trout, J.M., 1994, CD8+ T cell coccidia infections. Parasitology Today 10, 10-14.

Lillehoj, H.S., Trout, J.M., 1996, Avian gut-associated lymphoid tissues and intestinal immune responses to Eimeria parasites. Clinical Microbiology Reviews 9, 349-357.

Lee, D.L., Millard, B.J., 1971, Structure and development of macrogamete and oocyst of *Eimeia acervulina*. Parasitology 62, 31-42.

Li, H., Child, M.A., Bogyo, M., 2012, Proteases as regulators of pathogenesis: Examples from the Apicomplexa. Biochimica Et Biophysica Acta-Proteins and Proteomics 1824, 177-185.

Lindquist, H.D.A., Bennett, J.W., Hester, J.D., Ware, M.W., Dubey, J.P., Everson, W.V., 2003, Autofluorescence of Toxoplasma gondii and related coccidian oocysts. J. Parasitol. 89, 865-867.

Mai, K., Smith, N.C., Feng, Z.-P., Katrib, M., Slapeta, J., Slapetova, I., Wallach, M.G., Luxford, C., Davies, M.J., Zhang, X., Norton, R.S., Belli, S.I., 2011, Peroxidase catalysed cross-linking of an intrinsically unstructured protein via dityrosine bonds in the oocyst wall of the apicomplexan parasite, Eimeria maxima. International Journal for Parasitology 41, 1157-1164.

Mahoney, D.F., 1967, Bovine Babesiosis - passive immunization of calves against Babesia argetina with special reference to role of complement fixing antibodies. Experimental Parasitology 20, 119-125.

Mai, K., Sharman, P.A., Walker, R.A., Katrib, M., De Souza, D., McConville, M.J., Wallach, M.G., Belli, S.I., Ferguson, D.J.P., Smith, N.C., 2009, Oocyst wall formation and composition in coccidian parasites. Memorias Do Instituto Oswaldo Cruz 104, 280-288.

Marsh, K., Snow, R.W., 1997, Host-parasite interaction and morbidity in malaria endemic areas. Philosophical Transactions of the Royal Society of London Series B-Biological Sciences 352, 1385-1394.

Matsubara, J., Koura, M., Kamiyama, T., 1993, Infection of immunodeficient mice with a mouse adapted substrain of the gray strain of Babesia microti. J. Parasitol. 79, 783-786.

McFadden, G.I., van Dooren, G.G., 2004, Evolution: Red algal genome affirms a common origin of all plastids. Current Biology 14, R514-R516.

Meeusen, E., Lloyd, S., Soulsby, E.J.L., 1984a, Babesia microti in mice - adoptive transfer of immunity with serum and cells. Australian Journal of Experimental Biology and Medical Science 62, 551-566.

Meeusen, E., Lloyd, S., Soulsby, E.J.L., 1984b, Babesia microti in mice - adoptive trnsfer of immunity with serum and cells. Australian Journal of Experimental Biology and Medical Science 62, 551-566.

Mehlhorn, E.S.a.H., 1971, Fine strucutre of macrogametes and oocysts of coccidia and related organisms. Zeitschrift Fur Parasitenkunde 37, 1-43.

Mineo, J.R., McLeod, R., Mack, D., Smith, J., Khan, I.A., Ely, K.H., Kasper, L.H., 1993, Antibodies to Toxoplasma gondii major surface protein (SAG-1, P-30) inhibit infection of host cells and are produced in murine intestine after peroral infection. Journal of Immunology 150, 3951-3964.

Miura, K., Keister, D.B., Muratova, O.V., Sattabongkot, J., Long, C.A., Saul, A., 2007, Transmission-blocking activity induced by malaria vaccine candidates Pfs25/Pvs25 is a direct and predictable function of antibody titer. Malaria Journal 6.

Molestina, R.E., Payne, T.M., Coppens, I., Sinai, A.P., 2003, Activation of NF-kappa B by Toxoplasmal gondii correlates with increased expression of antiapoptotic genes and localization of phosphorylated I kappa B to the parasitophorous vacuole membrane. Journal of Cell Science 116, 4359-4371.

Moreira, C.K., Templeton, T.J., Lavazec, C., Hayward, R.E., Hobbs, C.V., Kroeze, H., Janse, C.J., Waters, A.P., Sinnis, P., Coppi, A., 2008, The Plasmodium TRAP/MIC2 family member, TRAP-Like Protein (TLP), is involved in tissue traversal by sporozoites. Cellular Microbiology 10, 1505-1516.

Morgan, R.E., Evans, K.M., Patterson, S., Catti, F., Ward, G.E., Westwood, N.J., 2007, Targeting invasion and egress: From tools to drugs? Current Drug Targets 8, 61-74.

Mehlhorn, H., 1974, Electron-microscopic studies in developmental stages of *Eimeria maxima*. Fine-structure of schizonts and merozoites. Acta Veterinaria Academiae Scientiarum Hungaricae 24, 383-401.

Mehlhorn, H. 1988. Parasitology in Focus. In Springer, Mehlhorn, H., ed. (Germany).

Mouafo, A.N., Weck-Heimann, A., Dubremetz, J.F., Entzeroth, R., 2002, Monoclonal antibodies specific for the two types of wall-forming bodies of *Emeria tenella* macrogametes (Coccidia, Apicomplexa). Parasitology Research 88, 217-224.

Mehlhorn, H., 1972, Fine structural study on developmental stages of *Eimeria maxima* parasitic in common fowl. Differentiation of microgametes with special reference to nculear divisions. Zeitschrift Fur Parasitenkunde-Parasitology Research 40, 243-260.

Mencher, D., Pugatsch, T., Wallach, M., 1989, Antigenic properties of *Eimeria maxima* gametocytes. Cell free translation and detection with recovered chicken serum. Experimental Parasitology 68, 40-48.

Miki, H., Okada, Y., Hirokawa, N., 2005, Analysis of the kinesin superfamily: insights into structure and function. Trends in Cell Biology 15, 467-476.

Mouafo, A.N., Weck-Heimann, A., Dubremetz, J.F., Entzeroth, R., 2002, Monoclonal antibodies specific for the two types of wall-forming bodies of *Emeria tenella* macrogametes (Coccidia, Apicomplexa). Parasitology Research 88, 217-224.

Nesvizhskii, A.I., Keller, A., Kolker, E., Aebersold, R., 2003, A statistical model for identifying proteins by tandem mass spectrometry. Analytical Chemistry 75, 4646-4658.

Nelson, M.M., Jones, A.R., Carmen, J.C., Sinai, A.P., Burchmore, R., Wastling, J.A., 2008, Modulation of the host cell proteome by the intracellular apicomplexan parasite Toxoplasma gondii. Infection and Immunity 76, 828-844.

Oconnor, R.M., Lane, T.J., Stroup, S.E., Allred, D.R., 1997, Characterization of a variant erythrocyte surface antigen (VESA1) expressed by Babesia bovis during antigenic variation. Molecular and Biochemical Parasitology 89, 259-270.

Page A.P., J.I.L. 2007. The cuticle, the *C. elegans* research community. In WormBook, ed., Moerman, J.M.K.a.D.G., ed. (St Albans, UK: CABI), pp. 8-11.

Payne, T.M., Molestina, R.E., Sinai, A.P., 2003, Inhibition of caspase activation and a requirement for NF-kappa B function in the Toxoplasma gondii-mediated blockade of host apoptosis. Journal of Cell Science 116, 4345-4358.

Pittilo, R.M., Ball, S.J., 1979, Fine structure of the developing macrogamete and oocyst wall formation in *Eimeria maxima*. Parasitology 79, R34-R34.

Precigout, E., Valentin, A., Carcy, B., Gorenflot, A., Nakamura, K.I., Aikawa, M., Schrevel, J., 1993, Babesia divergens characterization of a 17 kDa merozoite membrane protein. Experimental Parasitology 77, 425-434.

Pugatsch, T., Mencher, D., Wallach, M., 1989, *Eimeria maxima*: isolation of gametocytes and their immunogenicity in mice, rabbits and chickens. Experimental Parasitology 68, 127-134.

Pittilo, R.M., Ball, S.J., 1979a, Fine structure of developing macrogamete of *Eimeria maxima*. Parasitology 79, 259-271.

Pittilo, R.M., Ball, S.J., 1979b, Fine structure of the developing macrogamete and oocyst wall formation in *Eimeria maxima*. Parasitology 79, R34-R34.

Pittilo, R.M., Ball, S.J., 1980, The ultrastructural development of the oocyst wall of *Eimeria maxima*. Parasitology 81, 115-124.

Pittilo, R.M., Ball, S.J., 1985, Ultrastructural observations on the sporogony of *Eimeria maxima*. International Journal for Parasitology 15, 617-620.

Pittilo, R.M., Ball, S.J., Joyner, L.P., Norton, C.C., 1981, Ultrastructural changes in the macrogamete and early oocyst of *Eimeria maxima* resulting from drug treatment. Parasitology 83, 285-293.

Pittenger, M.F., Mackay, A.M., Beck, S.C., Jaiswal, R.K., Douglas, R., Mosca, J.D., Moorman, M.A., Simonetti, D.W., Craig, S., Marshak, D.R., 1999, Multilineage potential of adult human mesenchymal stem cells. Science 284, 143-147.

Paoletti, A.C., Washburn, M.P., 2006, Quantitation in proteomic experiments utilizing mass spectrometry. Biotechnology & genetic engineering reviews 22, 1-19.

Ryley, J.F., Long, P.L., Millard, B.J., 1972, Further studies on life-cycle of *Eimeria brunetti* levine 1942. Zeitschrift Fur Parasitenkunde 40, 35-52.

Rose, M.E., 1971, Immunity to coccidiosis: protective effect of transferred serum in *Eimeria maxima* infections. Parasitology 62, 11-27.

Rose, M.E., 1972, Immunity to coccidiosis: maternal transfer in *Eimeria maxima* infections. Parasitology 65, 273-293.

Rose, M.E., 1987, Immunity to *Eimeria* infections. Veterinary Immunology and Immunopathology 17, 333-343.

Rose, M.E., Hesketh, P., 1976, Immunity to coccidiosis: stages of life cycle of *Eimeria maxima* which induce, and are affected by, responce of host. Parasitology 73, 25-37.

Rose, M.E., Hesketh, P., Grencis, R.K., Bancroft, A.J., 2000, Vaccination against coccidiosis: host strain-dependent evocation of protective and suppressive subsets of murine lymphocytes. Parasite Immunology 22, 161-172.

Samso, M., Daban, J.R., Hansen, S., Jones, G.R., 1995, Evidence for sodium dodecyl sulphate/ protein complexes adopting necklace structure. European Journal of Biochemistry 232, 818-824.

Sato, S., 2011, The apicomplexan plastid and its evolution. Cellular and Molecular Life Sciences 68, 1285-1296.

Sharma, S.D., Araujo, F.G., Remington, J.S., 1984, Toxoplasma antigen isolated by affinity chromatography with monoclonal antibody protects mice against lethal infection with Toxoplasma gondii. Journal of Immunology 133, 2818-2820.

Shiels, B., Langsley, G., Weir, W., Pain, A., McKellar, S., Dobbelaere, D., 2006, Alteration of host cell phenotype by Theileria annulata and Theileria parva: mining for manipulators in the parasite genomes. International Journal for Parasitology 36, 9-21.

Shirley, M.W., Smith, A.L., Tomley, F.M., 2005, The biology of avian *Eimeria* with an emphasis on their control by vaccination, In: Advances in Parasitology, Vol 60. Elsevier Academic Press Inc, San Diego, pp. 285-330.

Sinai, A.P., Payne, T.M., Carmen, J.C., Hardi, L., Watson, S.J., Molestina, R.E., 2004, Mechanisms underlying the manipulation of host apoptotic pathways by Toxoplasma gondii. International Journal for Parasitology 34, 381-391.

Sinai, A.P., Webster, P., Joiner, K.A., 1997, Association of host cell endoplasmic reticulum and mitochondria with the Toxoplasma gondii parasitophorous vacuole membrane: a high affinity interaction. Journal of Cell Science 110, 2117-2128.

Smith, J.D., Chitnis, C.E., Craig, A.G., Roberts, D.J., Hudsontaylor, D.E., Peterson, D.S., Pinches, R., Newbold, C.I., Miller, L.H., 1995, Switches in expression of Plasmodium falciparum VAR genes correlate with changes in antigenic and cytoadherent phenotypes of infested erythrocytes. Cell 82, 101-110.

Smith, N.C., Wallach, M., Miller, C.M.D., Braun, R., Eckert, J., 1994a, Maternal transmission of immunity to *Eimeria maxima*: western blot analysis of protective antibodies induced by infection. Infection and Immunity 62, 4811-4817.

Smith, N.C., Wallach, M., Miller, C.M.D., Morgenstern, R., Braun, R., Eckert, J., 1994b, Maternal transmission of immunity to *Eimeria maxima* enzyme linked immunosorbent assay analysis of protective antibodies induced by infection. Infection and Immunity 62, 1348-1357.

Smith, N.C., Wallach, M., Petracca, M., Braun, R., Eckert, J., 1994c, Maternal transfer of antibodies induced by infection with *Eimeria maxima* partially protects chickens against challenge with *Eimeria tenella*. Parasitology 109, 551-557.

Smith, T.G., Walliker, D., Ranford-Cartwright, L.C., 2002, Sexual differentiation and sex determination in the Apicomplexa. Trends in Parasitology 18, 315-323.

Stepek, G., McCormack, G., Page, A.P., 2010, The kunitz domain protein BLI-5 plays a functionally conserved role in cuticle formation in a diverse range of nematodes. Molecular and Biochemical Parasitology 169, 1-11.

Stotish, R.L., Wang, C.C., Meyenhofer, M., 1978, Structure and composition of the oocyst wall of *Eimeria tenella*. J. Parasitol. 64, 1074-1081.

Soldati, D., Foth, B.J., Cowman, A.F., 2004, Molecular and functional aspects of parasite invasion. Trends in Parasitology 20, 567-574.

Sturm, A., Amino, R., van de Sand, C., Regen, T., Retzlaff, S., Rennenberg, A., Krueger, A., Pollok, J.M., Menard, R., Heussler, V.T., 2006, Manipulation of host hepatocytes by the malaria parasite for delivery into liver sinusoids. Science 313, 1287-1290.

Sturm, A., Heussler, V., 2007, Live and let die: manipulation of host hepatocytes by exoerythrocytic Plasmodium parasites. Medical Microbiology and Immunology 196, 127-133.

Su, X.Z., Heatwole, V.M., Wertheimer, S.P., Guinet, F., Herrfeldt, J.A., Peterson, D.S., Ravetch, J.A., Wellems, T.E., 1995, The large diverse gene faily VAR encodes proteins involved in cytoadherence and antigenic variation of Plasmodium falciparum infected erythrocytes. Cell 82, 89-100.

Templeton, T.J., 2007, Whole-genome natural histories of apicomplexan surface proteins. Trends in Parasitology 23, 205-212.

Thacker, C., Rose, A.M., 2000, A look at the Caenorhabditis elegans Kex2/subtilisin-like proprotein convertase family. Bioessays 22, 545-553.

Thacker, C., Srayko, M., Rose, A.M., 2000, Mutational analysis of bli-4/kpc-4 reveals critical residues required for proprotein convertase function in *C. elegans*. Gene 252, 15-25.

Thompson, R.F., Langford, G.M., 2002, Myosin superfamily evolutionary history. Anatomical Record 268, 276-289.

Tomley, F., 1997, Techniques for isolation and characterization of apical organelles from *Eimeria tenella* sporozoites. Methods-a Companion to Methods in Enzymology 13, 171-176.

Tomley, F.M., Shirley, M.W., 2009, Livestock infectious diseases and zoonoses. Philosophical Transactions of the Royal Society B-Biological Sciences 364, 2637-2642.

Trout, J.M., Lillehoj, H.S., 1993, Evidence of a role for intestinal CD8+ lymphocytes and macrophages in transport of Eimeria acervulina sporozoites J. Parasitol. 79, 790-792.

Trout, J.M., Lillehoj, H.S., 1995, Eimeria acervulina infection evidence for the involvement of CD8+ T lymphocytes in sporozoites transport and host protection. Poultry Science 74, 1117-1125.

Trout, J.M., Lillehoj, H.S., 1996, T lymphocyte roles during Eimeria acervulina and Eimeria tenella infections. Veterinary Immunology and Immunopathology 53, 163-172.

van den Heuvel, M.G.L., Dekker, C., 2007, Motor proteins at work for nanotechnology. Science 317, 333-336.

Waite, J.H., 1995, Precursors of quinone tanning DOPA-containing proteins, In: Redox-Active Amino Acids in Biology. pp. 1-20.

Wallach, M., Smith, N.C., Braun, R., Eckert, J., 1995, Potential control of chicken coccidiosis by maternal immunization. Parasitology Today 11, 262-265.

Wallach, M., Smith, N.C., Braun, R., Eckert, J., 1995a, Potential control of chicken coccidiosis by maternal immunization. Parasitology Today 11, 262-265.

Wallach, M.G., Mencher, D., Yarus, S., Pillemer, G., Halabi, A., Pugatsch, T., 1989, *Eimeria maxima*: identification of gametocyte protein antigens. Experimental Parasitology 68, 49-56.

Wallach, M., Pillemer, G., Yarus, S., Halabi, A., Pugatsch, T., Mencher, D., 1990, Passive immunization of chickens aganst *Eimeria maxima* infection with a monoclonal antibody developed against a gametocyte antigen. Infection and Immunity 58, 557-562.

Wallach, M., Smith, N.C., Braun, R., Eckert, J., 1995a, Potential control of chicken coccidiosis by maternal immunization. Parasitology Today 11, 262-265.

Wallach, M., 1997, The importance of transmission-blocking immunity in the control of infections by apicomplexan parasites. International Journal for Parasitology 27, 1159-1167.

Wallach, M., 2010, Role of antibody in immunity and control of chicken coccidiosis. Trends Parasitol 26, 382-387.

Wallach, M., Halabi, A., Pillemer, G., Sarshalom, O., Mencher, D., Gilad, M., Bendheim, U., Danforth, H.D., Augustine, P.C., 1992, Maternal immunization with

gametocyte antigens as a means of providing protective immunity against *Eimeria maxima* in chickens. Infection and Immunity 60, 2036-2039.

Wallach, M., Smith, N.C., Miller, C.M.D., Eckert, J., Rose, M.E., 1994, *Eimeria maxima*: elisa and western-blot analyses of protective sera. Parasite Immunology 16, 377-383.

Wallach, M., Smith, N.C., Petracca, M., Miller, C.M.D., Eckert, J., Braun, R., 1995, *Eimeria maxima* gametocyte antigens: potential use in a subunit maternal vaccine against coccidiosis in chickens. Vaccine 13, 347-354.

Wallach, M.G., Ashash, U., Michael, A., Smith, N.C., 2008, Field Application of a Subunit Vaccine against an Enteric Protozoan Disease. Plos One 3.

Wallach, M.G., Mencher, D., Yarus, S., Pillemer, G., Halabi, A., Pugatsch, T., 1989, *Eimeria maxima*: identification of gametocyte protein antigens. Experimental Parasitology 68, 49-56.

West, S.A., Smith, T.G., Read, A.F., 2000, Sex allocation and population structure in apicomplexan (protozoa) parasites. Proceedings of the Royal Society of London Series B-Biological Sciences 267, 257-263.

Walliker, D., 1991, Malaria parasites randomly interbred or clonal populations. Parasitology Today 7, 232-235.

West, S.A., Reece, S.E., Read, A.F., 2003, Toxoplasma gondii, sex and premature rejection. Trends in Parasitology 19, 155-157.

West, S.A., Smith, T.G., Read, A.F., 2000, Sex allocation and population structure in apicomplexan (protozoa) parasites. Proceedings of the Royal Society of London Series B-Biological Sciences 267, 257-263.

Williams, R.B., 2002, Fifty years of anticoccidial vaccines for poultry (1952-2002). Avian Diseases 46, 775-802.

Williamson, K.C., Criscio, M.D., Kaslow, D.C., 1993, Cloning and expression of the gene for *Plasmodium falciparum* transmission-blocking target antigen, PFS230. Molecular and Biochemical Parasitology 58, 355-358.

Witcombe, D.A., Belli, S.I., Wallach, M.G., Smith, N.C., 2003, Molecular characterisation of EmTFP250: a novel member of the TRAP protein family in Eimeria maxima. International Journal for Parasitology 33, 691-702.

Witcombe, D.M., Ferguson, D.J.P., Belli, S.I., Wallach, M.G., Smith, N.C., 2004, Eimeria maxima TRAP family protein EmTFP250: subcellular localisation and induction of immune responses by immunisation with a recombinant C-terminal derivative. International Journal for Parasitology 34, 861-872.

WHO, 2012, World Health Report. Geneva: World Health Organization.

Zhang, L., Ma, L., Liu, R., Zhang, Y., Zhang, S., Hu, C., Song, M., Cai, J., Wang, M., 2012, Eimeria tenella heat shock protein 70 enhances protection of recombinant microneme protein MIC2 subunit antigen vaccination against E. tenella challenge. Veterinary Parasitology 188, 239-246.